

Ground Cloud Dispersion Measurements During The Titan IV Mission #K15 (5 December 1995) at Vandenberg Air Force Base

Volume 1—Test Overview and Data Summary

10 February 1997

DTIC QUALITY INSPECTED 2

Assembled by

Environmental Systems Directorate
Systems Engineering
Space Launch Operations

Prepared for

Launch Programs
SPACE AND MISSILE SYSTEMS CENTER
AIR FORCE MATERIEL COMMAND
2430 E. El Segundo Boulevard
Los Angeles Air Force Base, CA 90245

Space Systems Group

APPROVED FOR PUBLIC RELEASE;
DISTRIBUTION UNLIMITED

19970409 076

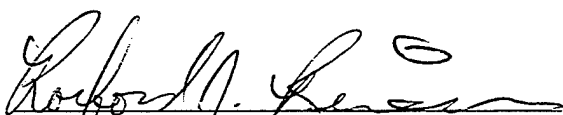


**THE AEROSPACE
CORPORATION**
El Segundo, California

This report was submitted by The Aerospace Corporation, El Segundo, CA 90245-4691, under Contract No. F04701-93-C-0094 with the Space and Missile Systems Center, 2430 E. El Segundo Blvd., Los Angeles Air Force Base, CA 90245. It was reviewed and approved for The Aerospace Corporation by N. F. Dowling Systems Director, Environmental Systems, Systems Engineering Directorate.

This report has been reviewed by the Public Affairs Office (PAS) and is releasable to the National Technical Information Service (NTIS). At NTIS, it will be available to the general public, including foreign nationals.

This technical report has been reviewed and is approved for publication. Publication of this report does not constitute Air Force approval of the report's findings or conclusions. It is published only for the exchange and stimulation of ideas.

A handwritten signature in black ink, appearing to read "Robert M. Reiners", is written over a horizontal line.

R. Reiners, Maj, USAF
SMC/CLN

REPORT DOCUMENTATION PAGE			Form Approved OMB No. 0704-0188	
Public reporting burden for this collection of information is estimated to average 1 hour per response, including the time for reviewing instructions, searching existing data sources, gathering and maintaining the data needed, and completing and reviewing the collection of information. Send comments regarding this burden estimate or any other aspect of this collection of information, including suggestions for reducing this burden to Washington Headquarters Services, Directorate for Information Operations and Reports, 1215 Jefferson Davis Highway, Suite 1204, Arlington, VA 22202-4302, and to the Office of Management and Budget, Paperwork Reduction Project (0704-0188), Washington, DC 20503.				
1. AGENCY USE ONLY (Leave blank)		2. REPORT DATE 10 February 1997		3. REPORT TYPE AND DATES COVERED
4. TITLE AND SUBTITLE Ground Cloud Dispersion Measurements During The Titan IV Mission #K15 (5 December 1995) at Vandenberg Air Force Base — Vol. 1 Test Overview and Data Summary			5. FUNDING NUMBERS F04701-93-C-0094	
6. AUTHOR(S) Environmental Systems Directorate				
7. PERFORMING ORGANIZATION NAME(S) AND ADDRESS(ES) The Aerospace Corporation Technology Operations El Segundo, CA 90245-4691			8. PERFORMING ORGANIZATION REPORT NUMBER TR-97(1410)-3	
9. SPONSORING/MONITORING AGENCY NAME(S) AND ADDRESS(ES) Space and Missile Systems Center Air Force Materiel Command 2430 E. El Segundo Boulevard Los Angeles Air Force Base, CA 90245			10. SPONSORING/MONITORING AGENCY REPORT NUMBER SMC-TR-97-05	
11. SUPPLEMENTARY NOTES				
12a. DISTRIBUTION/AVAILABILITY STATEMENT Approved for public release; distribution unlimited			12b. DISTRIBUTION CODE	
13. ABSTRACT (Maximum 200 words) Launch plume imagery, airborne and ground-level HCl measurement results, and meteorological data measured during the launch of a Titan IV vehicle at Vandenberg Air Force Base on 5 December 1995 (mission K-15) are presented. These data is used to determine the accuracy of the Rocket Exhaust Effluent Diffusion Model (REEDM). The imagery showed the separation into ground cloud and launch column segments, with the ground cloud stabilization height occurring 28% higher than predicted by REEDM. It also moved in a direction 24° more clockwise than predicted by REEDM, and 21% faster, but in good agreement with that calculated for the rawinsonde T-15 minute data. Of 34 dosimeters placed along the projected plume path, all but three provided usable data, ranging from 13 to 340 ppm min dosages. Aircraft data during cloud fly-throughs were obtained using both the Geomet and Spectral Science instruments.				
14. SUBJECT TERMS Toxic launch cloud, Toxic hazard corridors, Atmospheric dispersion models, Launch cloud development and dispersion, Launch cloud imagery, HCl monitoring			15. NUMBER OF PAGES 51	
			16. PRICE CODE	
17. SECURITY CLASSIFICATION OF REPORT UNCLASSIFIED	18. SECURITY CLASSIFICATION OF THIS PAGE UNCLASSIFIED	19. SECURITY CLASSIFICATION OF ABSTRACT UNCLASSIFIED	20. LIMITATION OF ABSTRACT	

Preface

The Air Force Space and Missile Systems Center's Launch Programs Office (SMC/CL) is sponsoring the Atmospheric Dispersion Model Validation Program (MVP). This program is collecting launch cloud dispersion data that will be used to determine the accuracy of atmospheric dispersion models, such as REEDM, in predicting toxic hazard corridors at the launch ranges. This report presents launch cloud dispersion and meteorological measurements performed during the #K15 Titan IV launch at Vandenberg AFB on 5 December 1995.

An MVP Integrated Product Team (IPT) led by Capt. Brian Laine (SMC/CLNM) is directing the MVP effort. Dr. Bart Lundblad of The Aerospace Corporation's Environmental Systems Directorate (ESD) is the MVP technical manager. This report was prepared by Mr. Norm Keegan (ESD) and Dr. Lundblad from materials contributed by personnel participating in the #K15 launch cloud dispersion measurements.

Visible and infrared imagery measurements were made of the launch cloud by Dr. Robert Abernathy, Ms. Karen Foster, Mr. Bob Klingberg, Mr. Tom Knudtson, and Dr. George Scherer of The Aerospace Corporation's Environmental Monitoring and Technology Department (EMTD). Mr. Jim Kephart of Aerospace's Western Range Directorate coordinated site selection and logistical support with Range organizations. Ms. Foster digitized the imagery data for analysis by Dr. Abernathy. The description of the cloud imagery results was prepared by Dr. Abernathy.

The aircraft-based HCl measurement effort was managed by Mr. Marv Becker and Mr. Pete Mazur of SRS Technologies. The Piper Seminole sampling aircraft was owned and operated by the Florida Institute of Technology. The aircraft was outfitted with a Geomet HCl detector that was modified and calibrated for airborne sampling by Mr. Paul Yocom of the NASA Toxic Vapor Detection/Contamination Monitoring Laboratory. Ms. Jeanne Hawkins of the 45th Medical Group Bioenvironmental Engineering Services (45 AMDS/SGPB) was on-board the aircraft during the sampling measurements to monitor Geomet performance and cockpit contamination. The on-board data logger and GPS system was provided and installed by Mr. Shane Beard of NOAA's Environmental Research Laboratories. The Spectral Sciences infrared HCl detector was installed and managed by Dr. Steve Richtsmeier of Spectral Sciences, Inc. The raw aircraft sampling data was processed and analyzed by Drs. Abernathy and Richtsmeier.

The ground-level HCl measurement effort was managed by Lt. Col. Kent Stringham of the 30th Medical Group Bioenvironmental Engineering Services organization (30 AMDS/SGPB). The HCl dosimeters were provided by and later analyzed by the NASA Toxic Vapor Detection/Contamination Monitoring Laboratory.

The meteorological data displayed in this report was provided by Mr. Steve Sambol of the VAFB Weather Squadron (30WS/DOS). The REEDM launch cloud dispersion prediction was provided by Mr. Darryl Dargitz of the VAFB Range Safety Office (30 SW/SEY).

The #K15 mission was the fifth Titan IV launch for which usable launch cloud dispersion data was collected by MVP. The previous missions were #K7, #K23, #K19, and #K21. It was the second Titan IV launch to employ an aircraft to collect HCl dispersion data. The previous airborne sampling activity was following the #K23 launch.

Contents

1.	Introduction	1
2.	Imagery of the Titan IV #K15 Ground Cloud.....	3
2.1	Background.....	3
2.2	Introduction.....	3
2.3	Field Deployment	4
2.3.1	Planning	4
2.3.2	Equipment	4
2.4	Processing of Imagery Data.....	6
2.5	Results and Discussion	8
2.5.1.	Correlation of Ground-Cloud Trajectory with Wind Direction	8
2.5.2.	Images of the Titan IV #K15 Exhaust Cloud.....	10
2.5.3.	Cloud Rise Times and Stabilization Heights	15
2.5.4.	Comparison of REEDM Prediction to Imagery Data: Rise Rate and Height	19
2.5.5.	Comparison of REEDM Prediction to Imagery Data: Trajectory and Speed	20
2.5.6.	Comparison of REEDM Prediction to Imagery Data: Summary Table	22
2.5.7.	Imagery-Derived Crosswind Growth Rate	23
2.6	Summary and Conclusions	24
3.	Aircraft Elevated HCl Measurements	27
3.1	Background.....	27
3.2	Introduction.....	28
3.3	Results and Discussion	29
3.3.1.	Overview of Aircraft Sampling Data	31
3.3.2.	HCl Concentration Hits as a Function of Bearing from SLC-4E.....	41

3.3.3. HCl Concentration Hits as a Function of Radial Distance from SLC-4E	42
3.3.4. HCl Concentration Hits as a Function of Altitude	43
3.3.5. HCl Concentration Hits as a Function of Altitude and Aircraft Position.....	44
3.4 Conclusions.....	49
4. Aircraft Elevated HCl Measurements—Spectral Sciences Data.....	51
5. Ground Level HCl Dosimetry	53
5.1 Dosimeter Monitoring	53
5.2 Ground Level Monitoring Results	53
5.3 Preparation of Geomet Instrument for Airborne Sampling	53
Appendix A—REEDM Code Calculations of Cloud Stabilization Heights and Ground-Level HCl Exposure Doses	59
Appendix B—Meteorological Data	95
Appendix C—Description of Sampling Aircraft	109
Appendix D—Spectral Sciences Inc. Report SSI-TR-274 “Measurement of Gas Phase Hydrogen Chloride in the Exhaust Cloud of a Titan Rocket”	121

Figures

1. Implementation of the “box” method with two imagers.....	7
2. Implementation of the six-sided polygon method for three imagers	8
3. A map documenting the locations of the three imagery	9
4. #K15 ground cloud and attached launch column as observed from Bldg 900 at 00:30 (mm:ss) after launch.....	11
5. #K15 “hour-glass shaped” ground cloud with attached but dissipating launch column as observed from Bldg 900 at 03:00 (mm:ss) after	12
6. #K15 “hour-glass shaped” ground cloud as observed by visible imagery from block wall site at 03:00 (mm:ss) after launch.....	13
7. #K15 “hour-glass shaped” ground cloud with attached but dissipating launch column as observed by visible imagery from Tetra Site at 03:00 (mm:ss) after launch.	13

8. #K15 ground cloud with attached launch column as observed from Bldg 900 at 08:00 (mm:ss) after launch	14
9. #K15 cloud bottom rise rate	16
10. #K15 cloud middle rise rate	17
11. #K15 cloud top rise rate	18
12. The imagery-derived heights for the top, middle, and bottom of the ground cloud (Figures 9–11) are plotted as $H(t)$ vs t	19
13. Ground track for the middle of the #K15 launch cloud	20
14. Ground distance for the middle of the #K15 launch cloud from the launch pad	21
15. Growth of the #K15 launch's exhaust cloud as observed from Block Wall site.....	24
16. Partial map of VAFB documenting the locations of the three imagery sites as well as the available ground cloud data	30
17. Cartesian plot documenting the aircraft's position relative to SLC-4e and the measured HCl concentration (based upon the Geomet detector) throughout the 110 min #K15 exhaust cloud sampling mission.	32
18. Geomet response curves illustrating rapid initial rise followed by rollover prior to reaching a plateau	33
19. #K16 pre-flight raw and integrated response of the Geomet.....	35
20. #K16 post-flight raw and integrated response of the Geomet.	35
21. Comparison of the #K15 exhaust cloud HCl concentration data obtained by the aircraft's two sensors.....	37
22. Comparison of the #K15 exhaust cloud HCl concentration data obtained by the aircraft's Geomet chemiluminescent detector with the Spectral Sciences GFC spectrometer's encounter data.....	38
23. Cartesian plot of 3.85-s averaged (unfiltered) GFC spectrometer and raw Geomet data collected by the aircraft while searching for the #K15 exhaust cloud	39
24. Effect of averaging time on GFC spectrometer data and comparison with the raw Geomet data for the #K15 exhaust cloud.....	40
25. Summary of the aircraft's HCl concentration measurements and its polar angles (rawinsonde convention) plotted against time (minutes) after the Titan IV #K15 launch.....	41
26. Summary of the aircraft's HCl concentration measurements and radial distances (m) from SLC-4E plotted against time (min) after the Titan IV #K15 launch.	42

27. Summary of the aircraft's HCl concentration measurements and altitude (m) plotted against time (minutes) after the Titan IV #K15 launch.	43
28. Summary Cartesian plot documenting the aircraft's position and measured HCl concentrations while sampling at altitudes between 800 to 1000 m by GPS after the Titan IV #K15	44
29. Summary Cartesian plot documenting the aircraft's position and measured HCl concentrations while sampling at altitudes between 600 and 800 m by GPS after the Titan IV #K15 launc	45
30. Summary Cartesian plot documenting the aircraft's position and measured HCl concentrations while sampling at altitudes between 400 to 600 m by GPS after the Titan IV #K15 launch.....	46
31. Summary Cartesian plot documenting the aircraft's position and measured HCl concentrations while sampling at altitudes between 200 to 400 m by GPS after the Titan IV #K15 launch.....	47
32. Summary Cartesian plot documenting the aircraft's position and measured HCl concentrations while sampling at altitudes below 200 m by GPS after the Titan IV #K15	48
33. Location of dosimeters for #K15 launch.....	56
34. #K15 launch dosage levels (ppm min)	57

Tables

1. Field-of-View (FOV) for Imagery Sites During the #K15 Mission	5
2. Imagery Site Positions and Angles to SLC-4E based upon 2-m Resolution GPS Survey	6
3. Summary for #K15 Launch Cloud Data Derived from Visible and Infrared Imagery, T-0.25 h Rawinsonde Sounding Data, and T-0 h REEDM Predictions.	23
4. Imagery-Derived Stabilization Heights and REEDM's Predicted Stabilization Height Expressed Relative to MSL (Comparable to the Aircraft's GPS Data) and Relative to SLC-4E (as Reported in Section 2).....	29
5. Portion of the Aircraft's Data File Provided to The Aerospace Corporation by NOAA....	31
6. HCl Dosimeter Locations and Calculated Dosages In Order of Proximity to Launch Point	55

Executive Summary

This report presents plume imagery and aircraft- and ground-based hydrogen chloride (HCl) sampling data documenting the development and dispersion of the Titan IV #K15 launch plume at Vandenberg Air Force Base (VAFB). The HCl is measured in both dry gas and aerosol forms. The report also presents pertinent meteorological data taken from towers and rawinsonde.

The imaging team successfully tracked the trajectory and time evolution of the vehicle's exhaust plume for 11 min following launch using one infrared and three visible light video camera systems. A twin-engine Piper Seminole aircraft, equipped with a Geomet total HCl analyzer and a Spectral Sciences hydrogen chloride gas analyzer, was used to measure HCl concentrations within the plume as a function of time for approximately two hours. In addition, a third team deployed HCl dosimeters at ground level to determine HCl concentrations at that level in the path of the ground cloud.

To provide modeling input data, rawinsonde data were measured shortly before launch, and meteorological tower data were measured before launch and during dispersion of the launch plume. These data and similar data on other Titan IV launches (past and future) will be used along with tracer gas release campaigns to determine the accuracy of atmospheric dispersion models such as REEDM in predicting toxic hazard corridors (THCs) at the USAF Eastern and Western Ranges. These THCs assess the risk of exposing the public to HCl exhaust from solid rocket motors or hypergolic propellant vapors accidentally released during launch operations.

The #K15 launch occurred on 5 December 1995 at 2118 Zulu time. The sampling aircraft entered the plume approximately 4 min after launch and made 13 passes through the plume. Comparable HCl data were obtained during the first eight passes from the onboard Geomet and SSI HCl sensors, but the SSI CO sensor proved to be inoperable. HCl concentrations from 10 ppm to 32 ppm were measured during these passes.

Imagery from coaligned visible and infrared imagers was obtained at one site, and visible-only imagers at two other sites. Reduction of the first 11 min of these data yielded the rise time, stabilization height, dimensions, ground track and speed, and growth rate of the ground cloud. Comparison to REEDM predictions show that the measured stabilization height is 28% higher than predicted, but the rise time to stabilization is very close to the predicted 2.8 min. Cloud trajectory direction and speed agrees well with the rawinsonde T-15 min data, but is 21% faster than REEDM, and 24° in a more clockwise direction. These data suggest that better prediction of stabilization height by REEDM would automatically correct the cloud speed and direction predictions.

Thirty-four dosimeters were deployed along the projected plume track 5 ft above the ground, including 20 placed in a 90° arc from 600 to 1400 ft from the launch point. All but three provided usable data; those three being damaged by launch blast or fire. Two of the dosimeters at 2600 and 5000 ft from the pad along the approximate launch azimuth did not detect measurable levels of HCl while others indicated from 13 to 340 ppm min. dosages.

1. Introduction

There is a strong need to collect launch cloud data that can be used to validate the performance of atmospheric dispersion models used to predict the transport and diffusion of hazardous species that may be released into the atmosphere during Air Force launch vehicle operations. Launch vehicles that employ solid propellant rocket motors release ground clouds into the Eastern Range and Western Range launch areas at Cape Canaveral Air Station (CCAS) and Vandenberg Air Force Base (VAFB), respectively, that contain large amounts of hydrogen chloride (HCl). Large quantities of hazardous hydrazine fuels or the nitrogen tetroxide oxidizer could also be accidentally released at the ranges during propellant transfer operations or due to a launch vehicle failure.

The Air Force launch range safety organizations of the 45th Space Wing at Patrick Air Force Base (45 SPW/SE) and 30th Space Wing at VAFB (30 SPW/SE) are responsible for assuring that launches are carried out only when meteorological conditions are such that nearby communities cannot be exposed to hazardous levels of HCl, the hydrazine fuels, or N_2O_4/NO_2 . Predictions of toxic hazard corridors (THCs) that extend into public areas can lead to costly launch delays. The present use of non-validated models requires the use of conservative launch criteria. The development and validation of accurate atmospheric dispersion models is expected to increase launch opportunities and significantly reduce launch costs. The Space and Missile System Center's Launch Programs Office (SMC/CL) established the Atmospheric Dispersion Model Validation Program (MVP). MVP is collecting data to determine the accuracy of current and future atmospheric dispersion and chemical kinetic models in predicting THCs during launches of Titan and other vehicles at CCAS and VAFB.

The MVP effort involves the collection of data during Titan launches at CCAS and VAFB to characterize HCl launch cloud rise, growth, and stabilization, as well as launch cloud transport and diffusion. These data, as well as data from tracer gas releases, will in particular be used to determine the capability of the Rocket Exhaust Effluent Diffusion Model (REEDM) for predicting THCs at the launch ranges. REEDM is used at CCAS and VAFB to predict the locations of THCs in support of launch operations. It is applied to large heated sources of toxic air emissions such as nominal launches, catastrophic failure fireballs, and inadvertent ignitions of solid rocket motors. It uses launch vehicle and meteorological data to generate ground-level concentration isopleths of HCl, hydrazine fuels, NO_2 , and other toxic launch emissions. Launch holds may occur when REEDM toxic concentration predictions exceed adopted exposure standards. REEDM is a unique and complex model based on relatively simple modeling physics. It has a long developmental history with the Air Force and NASA, but has never been fully validated. Validation of REEDM has been identified as a range safety priority.

The MVP has been organized and is being directed by the MVP Integrated Product Team (IPT). SMC/CL is serving as the IPT leader, while The Aerospace Corporation's Environmental Systems Directorate is the IPT technical manager. The IPT consists of personnel with expertise in atmospheric dispersion modeling, meteorology, and atmospheric concentration field measurements. MVP participants include personnel from 30 and 45 SPW, SMC, The Aerospace Corporation, NASA,

NOAA, and contractors. Key functions include program planning, field data collection, data review and compilation, range coordination, and model validation.

This report presents the results of measurements performed at VAFB during the Titan IV #K15 launch. Visible and infrared imagery measurements were made on the launch cloud to monitor its growth, stabilization, and trajectory. An aircraft equipped with two HCl detectors was flown through and below the visible cloud to measure HCl concentrations. Ground-level HCl doses were also measured during this launch at selected locations near the launch pad. The imagery results are presented in Section 2. The aircraft sampling results are presented in Sections 3 and 4, and the ground sampling results are presented in Section 5. REEDM predictions of ground-cloud stabilization heights and surface concentrations are presented in Appendix A. Measurements of meteorological data are tabulated in Appendix B. A description of the cloud sampling aircraft is presented in Appendix C.

The imagery data obtained show that, for the meteorological conditions present during the launch, the T-0.25 hour REEDM calculation underestimates the cloud's stabilization height (658m vs. 515m predicted). REEDM also underestimated the cloud's stabilization time (2.8 min vs. 3 to 5 min). The results presented in this, as well as previous and subsequent MVP reports, will allow the accuracy of REEDM and other launch range atmospheric dispersion models to be determined over the range of possible meteorological conditions.

2. Imagery of the Titan IV #K15 Ground Cloud

[The material in this section was contributed by R. N. Abernathy, K. L. Foster, B. P. Kasper, and R. F. Heidner III of the Environmental Monitoring and Technology Department of The Aerospace Corporation's Space and Environment Technology Center]

2.1 Background

The Aerospace Corporation has been deploying visible and/or infrared imaging systems to Titan IV launches since the #K10 Launch on 07 February 1994. These deployments include Titan IV missions #K02, #K07, #K09, #K10, #K14, #K15, #K16, #K19, #K21, #K22 and #K23. Typically, two-dimensional cloud images are recorded at each of two or three imaging sites and are combined in a pairwise fashion to produce stereoscopic 3-D information about the exhaust cloud. When atmospheric conditions were favorable and two (or more) imagery sites were manned (i.e., #K02, #K07, #K15, #K16, #K19, #K21, #K22, and #K23), the analysis of these data yields the ground cloud's rise time, stabilization height, dimensions, ground track, and ground speed. These imagery data and the resulting cloud characteristics are available to modelers as part of the model validation program (MVP).

For #K15, all three selected imagery sites yielded data useful for tracking the cloud. The analysis of the first 11 min of the imagery data yields the ground cloud's rise time, stabilization height, ground track, cloud growth rate, and speed. The raw infrared imagery data for the #K15 mission were recorded digitally by the AGEMA computer system. The raw visible imagery data were recorded by a VCR. Subsequently a PC-based image capture board allowed the digitization of selected images from the VCR tapes. Subsequently, all of the imagery data that were processed for this report were archived on magneto-optical disks as digital image files.

2.2 Introduction

On 5 December 1995, the Titan IV #K15 mission was successfully launched from VAFB SLC-4E at 13:18 PST (21:18 ZULU). This section describes the exhaust cloud imagery data collected by three imagery sites during the 30 min immediately following the launch. It also briefly describes the data acquisition hardware and analysis software. Analysis of the first 11 min of this imagery yields the stabilization time, the stabilization height, the growth rate, the ground track, and the speed of the ground cloud without recourse to additional data sources. Rudimentary knowledge of the rawinsonde wind data is needed for more quantitative interpretation of the imagery data reported in this section. These pre-launch rawinsonde data are documented in Appendix D and referenced in this section. REEDM predictions are documented in Appendix C and referenced in this section. An Aircraft sampled the HCl in the exhaust cloud, and that data is documented in Section 3.

2.3 Field Deployment

2.3.1 Planning

The Aerospace Corporation's participants are listed in various subteams below (members of the imaging teams for #K15 are indicated with asterisks and paired with the imagery sites they supported).

Technology Operations

Space and Environment Technology Center

Environmental Monitoring and Technology Department

R. N. Abernathy*	K. L. Foster* (<i>Building 900</i>)
G. J. Scherer*	J. T. Knudtson* (<i>Tetra Tech</i>)
R. A. Klingberg*	J. Y. Webb* (<i>Block Wall</i>)
R. F. Heidner III	B. P. Kasper

Space Launch Operations

Systems Engineering Directorate

Environmental Systems

N. F. Dowling, Systems Director
H. L. Lundblad

Western Range

Systems Engineering Directorate

E. J. Tomei, Systems Director
J. F. Kephart

2.3.2 Equipment

The equipment at each site includes all the hardware and software necessary to record and document the launch, to communicate between sites, and to supply backup power in case of a power outage. The Building 900 site used fixed power from the building while both Tetra Tech and Block Wall Sites used gasoline-powered generators. The launch of #K15 marked the fourth opportunity to deploy the Titan IV-dedicated Visible and Infrared Imaging System (VIRIS) hardware.

The VIRIS consists of an array of four cloud tracking systems and was designed and fabricated at the request of Space Launch Operations, Systems Engineering Directorate, at The Aerospace Corporation. Three of the tracking systems include coaligned visible and infrared (IR) (8–12 μm) imagers, mounted on an azimuth- and elevation-encoding tripod, with an associated data acquisition and display console. The fourth tracking system does not include an infrared imager. The combination of visible and IR imagers permits cloud tracking in both daylight and darkness. The #K15 launch represented a daylight launch. The unique capabilities built into the VIRIS hardware include digital insertion of imager azimuth (Az), elevation (El), time, and GPS location into the VCR recording of the imagery. The system electronics are integrated in a single package, which has been ruggedized for

field use. Prewiring of this package makes deployment of these imagery systems straightforward, usually requiring less than 45 min for instrumentation at a site to become fully operational. For the Titan IV #K15 mission, the operators at building 900 site set the field-of-view (FOV) of the IR imager to its maximum (i.e., $20_v^\circ \times 40_h^\circ$) value using the standard AGEMA IR lenses. The FOV of the visible imagers varied based upon the distance of the site from the launch complex and the size of the launch cloud from their perspective. The FOV of the Block Wall imager was changed once during the tracking of the exhaust cloud. The FOV of the imagers at the other sites remained constant throughout the tracking of the exhaust cloud. Table 1 summarizes the FOVs of the imagery sites for the #K15 launch.

The imaging systems deployed for the Titan IV #K15 mission were capable of total autonomy. Differential-ready GPS receivers documented each imager's position with moderate spatial resolution. Typically, 35 m is the precision in the horizontal plane for the differentially corrected data. At VAFB, the GPS receivers did not obtain differential correction broadcasts, and so a 100-m precision in the horizontal plan was used for the #K15 analysis. Subsequent to the analysis, the sites were resurveyed with a 2-m precision differential GPS receiver. These data were used to document that the 100-m precision data was adequate for the selected sites due to their large distance from reference sites and from the launch complex. Gasoline-powered AC generators (Honda Ex1000) are insurance against loss of fixed power and were used as the sole source of power at Tetra Tech and Block Wall Sites. The Stirling cooler option for the AGEMA 900 series IR imagers was chosen so that liquid nitrogen would not be required at the sites. Each unit was transported in a van.

The Az/El angle encoder for all imagery systems was calibrated using reference objects (e.g., SLC-4E) within the field-of-view of the imagers. When reference objects are not part of the geodetic survey database, the GPS location uncertainty is the dominant term in the positional accuracy. Imagery pixelation and operator error in edge detection also contribute to the error in defining the cloud boundary. Step-size in the tripod angle encoders is a third source of error. The accuracy is usually determined by the availability of optimal references for Az/El calibration. Based upon the 2-m survey, the 100-m precision GPS data provided better than 0.3° precision for the #K15 analysis. Table 2 documents the imagery site locations and the angles to SLC-4E pad based upon the 2-m precision GPS survey.

Table 1. Field-of-View (FOV) for Imagery Sites During the #K15 Mission

Imagery Site	Imager Type (Vis or IR)	Time Notes (switch time)	FOV(horizontal) (deg)	FOV(vertical) (deg)
Block Wall (early)	Visible	Up to 21:18:30 ZULU	6.72	4.37
Block Wall (late)	Visible	After 21:18:30 ZULU	13.95	9.46
Building 900	Visible	All Imagery	31.68	24.14
Building 900	Infrared	All Imagery	40.80	20.89
Tetra Tech	Visible	All Imagery	13.44	10.27

Table 2. Imagery Site Positions and Angles to SLC-4E based upon 2-m Resolution GPS Survey

Imagery Site	Latitude (deg)	Longitude (deg)	Altitude (MSL) (m)	AZ(SLC-4E) (deg)	EL(SLC-4E) (deg)
Block Wall	34.706202	-120.600496	5	186.41	1.02
Building 900	34.663684	-120.578843	114	219.57	0.48
Tetra Tech	34.692873	-120.537945	108	224.50	0.27

2.4 Processing of Imagery Data

The processing of the imagery data requires the following transformations to be performed upon return to The Aerospace Corporation.

1. Digitizing frames of visible imagery from the VCR tapes.
2. Measuring the pixel locations of the reference sites within each image (i.e., FOV and angular calibration).
3. Measuring the pixel locations of exhaust cloud features in digitized images.
4. Converting pixel locations to azimuth and elevation readings.
5. Calculating cloud characteristics (i.e., position in Cartesian coordinates relative to the launch

The processing requires the use of specialized hardware and software. Time, Az, and El are tabulated for each digitized image. Quartets of digitized images exist for selected times following the launch. A setup file containing all relevant information necessary to compute the cloud geometry is created for each of these pairs. The Aerospace program **PLMTRACK** is run to digitize the x, y, and z coordinates of cloud features.

PLMTRACK is a software program developed in the Environmental Monitoring and Technology Department (EMTD) of The Aerospace Corporation by Brian P. Kasper. It is designed to analyze pairs of cloud images synchronized in time. The operator selects the location of a particular cloud feature in the images from the two imagery sites by moving a screen pointer over the desired point in each image and clicking a mouse button. **PLMTRACK** then calculates the three-dimensional location of this point and writes the information to a data file.

Another implementation of **PLMTRACK** is the "box method," illustrated in Figure 1. The operator draws a rectangle about a cloud feature in the images from the two imagery sites by moving a screen pointer to the extreme corners of the rectangles and clicking a mouse button. **PLMTRACK** then calculates the closest approach for various rays as, illustrated in Figure 1 and described below. The top of the cloud is defined by rays determining T1 and T2 (i.e., $T1 \times T2$); the bottom is determined by rays defining B1 and B2 (i.e., $B1 \times B2$); and the middle is defined by the geometric mean of top and

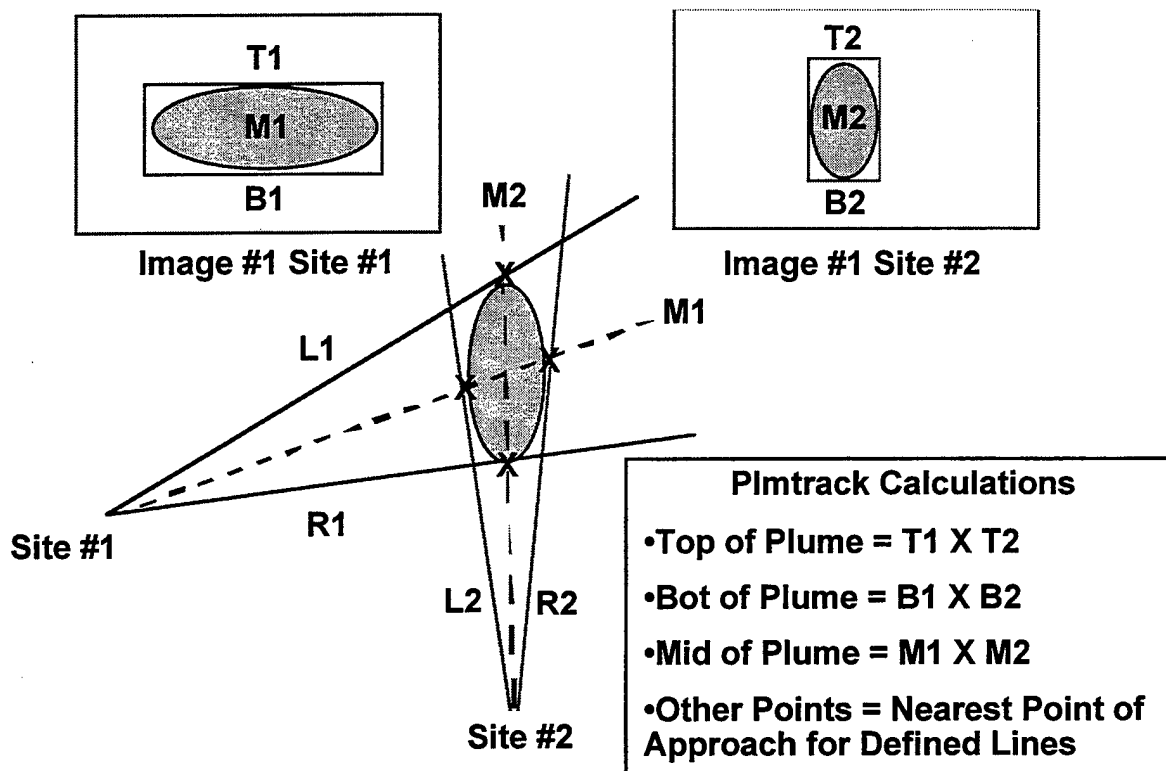


Figure 1. Implementation of the "box" method with two imagers.

bottom (i.e., $M1 \times M2$). To define the "faces" of the polygon surrounding the cloud, the points of closest approach for ray M1 with L2 and R2 (the left and right tangents to the cloud from Imager 2) are defined (i.e., $M1 \times L2$ and $M1 \times R2$). A similar procedure is used to define the points of closest approach for M2 with L1 and R1, yielding $M2 \times R1$ and $M2 \times L1$. Thus, seven points are defined for the "cell" surrounding the cloud (a point in the center of each of the six faces, plus a middle point). Four additional points are calculated by **PLMTRACK** ($L1 \times L2$, $L1 \times R2$, $R1 \times L2$, and $R1 \times R2$), and they define the extreme vertices of a polygon projected onto the ground plane and surrounding the observable cloud. All eleven points are written to a comma-separated-variable file.

When three (or more) imagers are viewing the cloud simultaneously (as accomplished for #K02, #K15, #K16, #K19, #K22, and #K23), a six-sided polygon method (documented in Figure 2) has been employed as an initial step in our plan to determine cloud volume as a function of time. With three imagers, there is a triply redundant determination of the top, middle, and bottom of the cloud by **PLMTRACK**. The horizontal extent of the cloud is determined by defining the rays from each imager that are tangential to the widest part of the cloud as seen from that site. Projection of these extreme rays for each imager on the x-y ground plane forms a six-sided polygon (for three sites) that bounds all material in the cloud at all altitudes, as shown in Figure 2. When the polygon area is combined with the mean cloud height (i.e., the difference between the top and the bottom) of the cloud, one can obtain an upper bound for cloud volume. This upper bound volume may *significantly* overestimate the volume of the cloud.

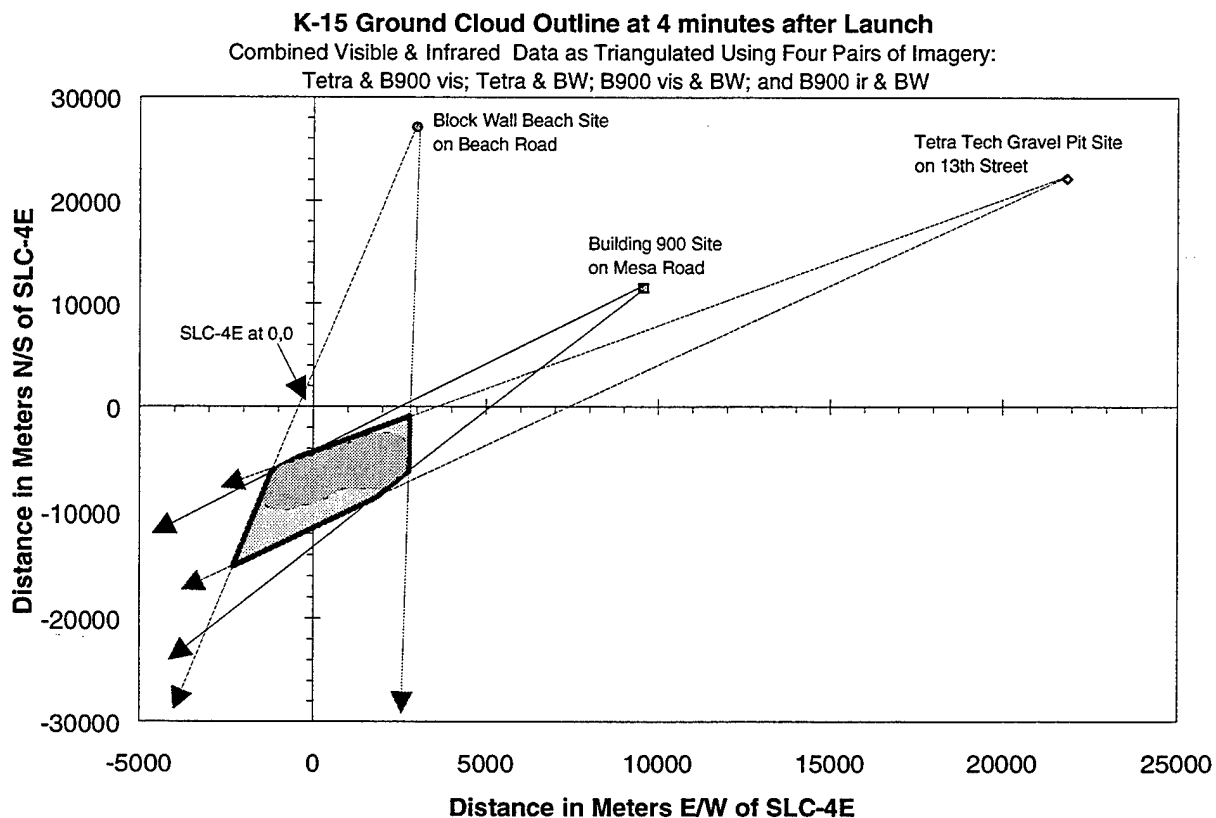


Figure 2. Implementation of the six-sided polygon method for three imagers. The imager positions and rays are actual #K15 data for imagery collected 4 min after launch. The cartoon of the cloud was synthesized for heuristic purposes to illustrate the potential for overestimation of the cloud's size by the polygon method.

Examination of Figure 2 reveals that all three imagery sites were in the northeastern quadrant relative to the SLC-4E pad. One would obtain better triangulation of the clouds position and closer estimates of its volume if one could find three imagery sites more evenly distributed about the launch pad. Unfortunately, there is a mountain to the east of the pad. As illustrated by the imagery included in this report, it is easier to image the cloud against the sky than against the terrain. Therefore, one prefers sites at or below the pad's altitude. We were not able to deploy south of the pad because of exclusion zones (chemistry and debris). The ocean is to the west of the pad. For future launches, we are investigating potential imagery sites to the southeast of the pad along the coast and beyond the exclusion zones.

2.5 Results and Discussion

2.5.1. Correlation of Ground-Cloud Trajectory with Wind Direction

Figure 3 plots various wind and cloud bearings using the rawinsonde convention (defined fully in section 2.5.5). The cloud trajectories are anchored to SLC-4E on the map. The heaviest arrow (i.e., thickest linewidth) is used to plot the 8° cloud direction derived from imagery. Three additional cloud vectors are included to document the REEDM output that applies to the predicted exhaust cloud

trajectory: (1) the 2° bearing to maximum concentration at 514 m (i.e., REEDM's T-0.25 hour prediction for the stabilization height); (2) the 14° bearing of the cloud when immediately after stabilization; and (3) the 344° average wind bearing for the second mixing layer (i.e., this dominates the vector of concentration isopleths for the stabilized cloud at later times). Since the #K15 imagery data extends to 11 min, well after stabilization, we will use the 344° REEDM prediction for the cloud trajectory after stabilization when comparing trajectories. To the far right of the map in Figure 3, three wind vectors document the rawinsonde-derived wind directions associated with the bottom (17°), middle (26°), and top (358°) of the imagery-derived cloud heights. Although the rawinsonde originated from building 900, the wind direction vectors are anchored to the right of the map to avoid clutter. Figure 3 also documents the locations of the three imagery sites chosen by The Aerospace Corporation for the #K15 imagery.

It is evident from examination of Figure 3 and from the discussion in the preceding paragraph that REEDM predicts a cloud track (344° based upon the wind for the second mixing layer) that is southeasterly while the imaged cloud track (8°) is southwesterly. Likewise, it is evident from examination of Figure 3 that the imagery-derived southwesterly cloud direction is qualitatively consistent with the wind directions measured at the top, middle, and bottom of the imaged cloud. It should be noted that

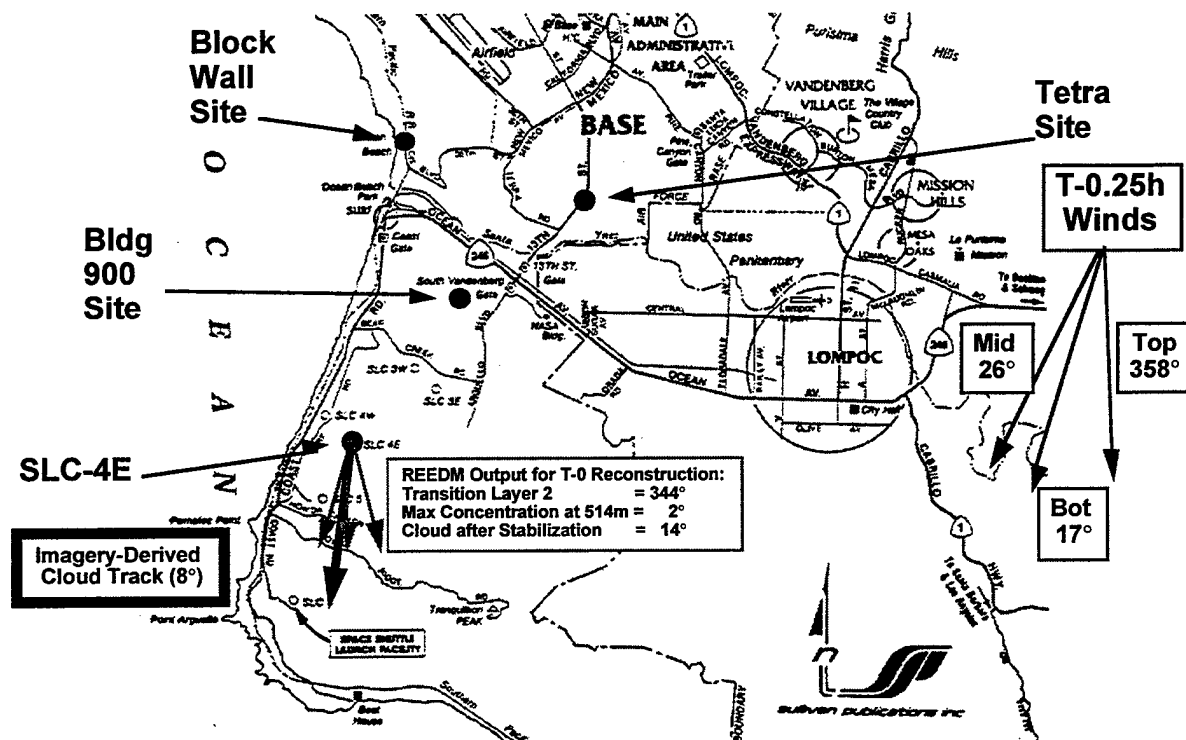


Figure 3. A map documenting the locations of the three imagery sites, the observed #K15 ground cloud's track (8°), the REEDM predictions for the #K15 exhaust cloud (2° to maximum concentration at stabilization height, 14° for the stabilized cloud, and 344° for the average wind in the second mixing layer), and the wind direction for the top (358°), middle (26°), and bottom (17°) altitudes for the imaged cloud. The rawinsonde sounding was at 21:03 ZULU (T-0.25 h) from building 900 site and was modified using DAS data to synthesize the T-0 h reconstruction. The cloud track vectors are anchored to SLC-4E pad on the map.

the low-altitude winds (shown on Figure 3) are out of the northeast ($17\text{--}26^\circ$) while the high-altitude winds are out of the northwest (358°). This is qualitatively consistent with the shearing of the launch column from the ground cloud. As illustrated by Figure 3 and discussed in the next section, the imagery documents that the ground cloud rises and stabilizes to the south of the pad. The T-0.25 hour rawinsonde data in Figure 3 are documented in Appendix D. The REEDM predictions in Figure 3 are documented in Appendix C.

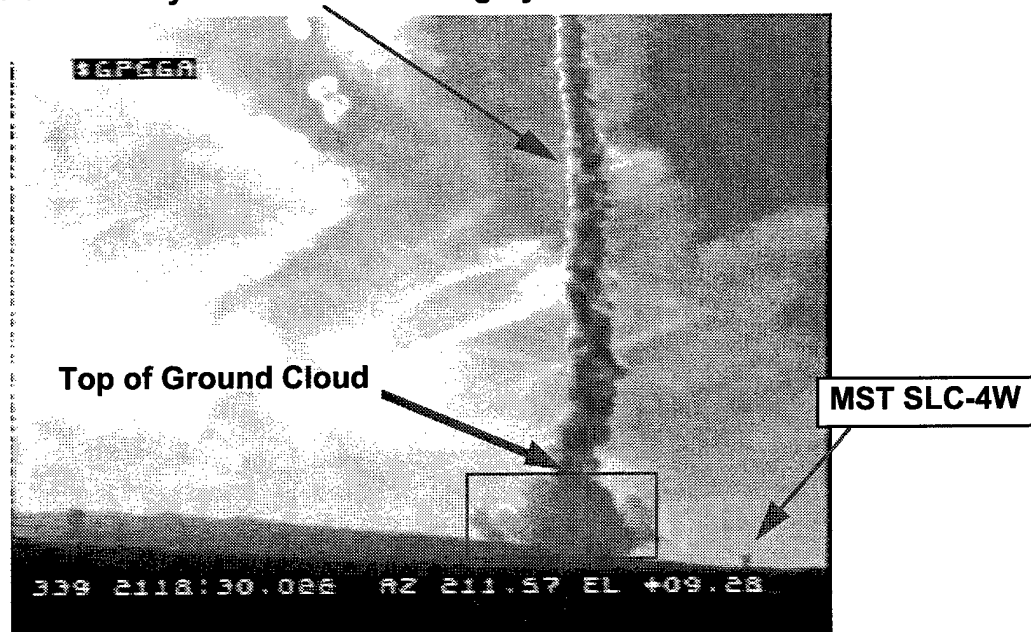
2.5.2. Images of the Titan IV #K15 Exhaust Cloud

As discussed in the previous section, the imagery data is qualitatively consistent with the T-0.25 hour rawinsonde wind directions. In contrast, the imagery documents a southwesterly cloud track while REEDM predicts a southeasterly cloud track. Figures 4 through 8 are infrared and visible images of the Titan IV #K15 exhaust cloud as seen from the imagery sites at the specified times after launch. For clarity, boxes have been drawn about the “ground cloud,” and arrows are used to identify the top of the ground cloud, the launch column, and launch complex structures. It is immediately obvious that the cloud is not spherically symmetric in any of these images.

Figure 4 documents (a) visible and (b) infrared imagery of the exhaust cloud at 30 s after launch as observed from building 900, which is north (and slightly northeast) of the launch pad. In these images, the analyst identified the ground cloud as the wide portion of the cloud with the launch column extending upward from its middle. The analyst used the width of the ground cloud to differentiate it from the launch column during the first several minutes after launch. Comparison of the visible to the infrared imagery illustrates the complimentary nature of the techniques. The IR sees the hot exhaust cloud in emission against the background (i.e., the cool sky and warm ground) while the visible imagery sees the cloud as illuminated by the sun (i.e., reflection and shadows depending upon the illumination angle). The background for the visible imagery is dominated by scatter from high-altitude clouds as well as from aerosols in the lower atmosphere. Since the high-altitude atmospheric clouds are cooler than the ground cloud and the launch column, they do not contribute significantly to the IR background. However, the warmer low-altitude atmosphere and the warm hillside do contribute to the IR background. Hence, the signal-to-noise ratio for the IR image increases with elevation as evidenced by the dark background at the top of the IR images and the bright background at the bottom of the IR images.

Figure 5 documents the “hour-glass shaped” ground cloud at 3 min after launch as observed from building 900. The analyst used the darkness of the ground cloud in the visible (5a) and the brightness of the ground cloud in the infrared (5b) to discriminate against the launch column, which was sheared to the south at the top of the ground cloud. As mentioned above, the signal-to-noise increases with elevation for the IR imagery, which easily reveals the launch column against the cold high-altitude atmospheric clouds. In contrast, the visible imagery easily detects the low-level remnants (tail) of the ground cloud (not observable in the IR) but has difficulty differentiating the launch column from the atmospheric clouds.

Launch Column Easily Seen in Visible Imagery



Launch Column Easily Seen in Infrared Imagery

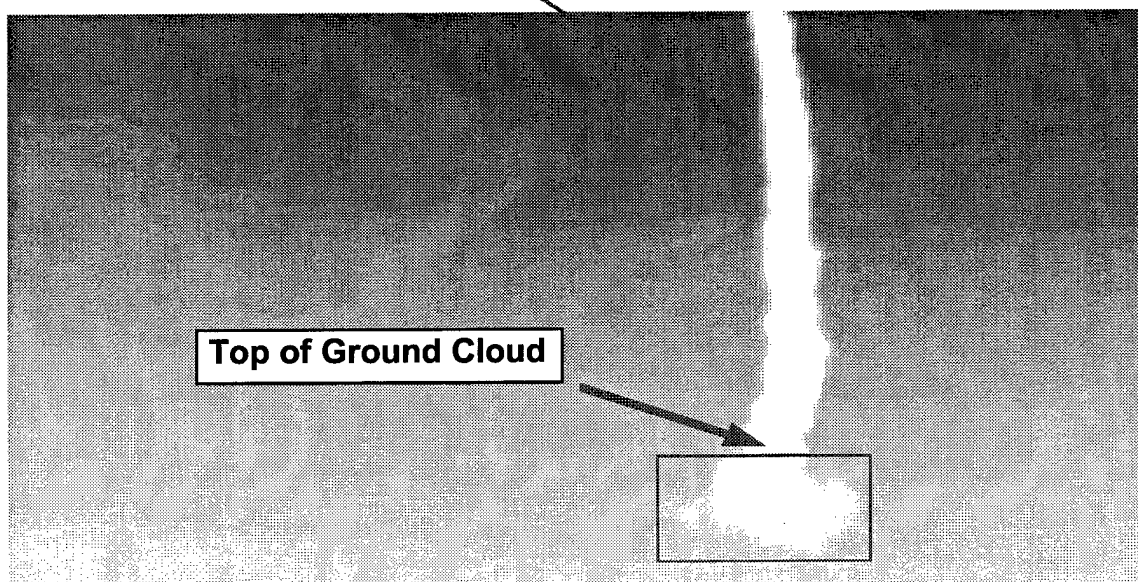


Figure 4. #K15 ground cloud and attached launch column as observed from Bldg 900 at 00:30 (mm:ss) after launch: (a) Visible imagery and (b) Infrared imagery.

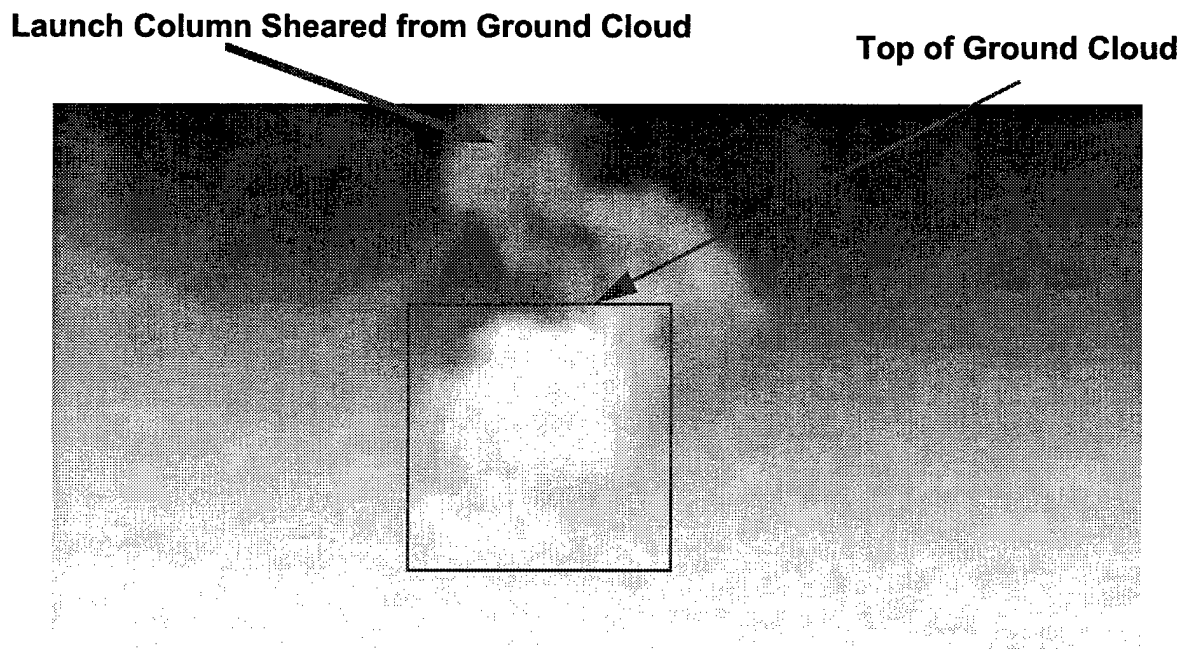
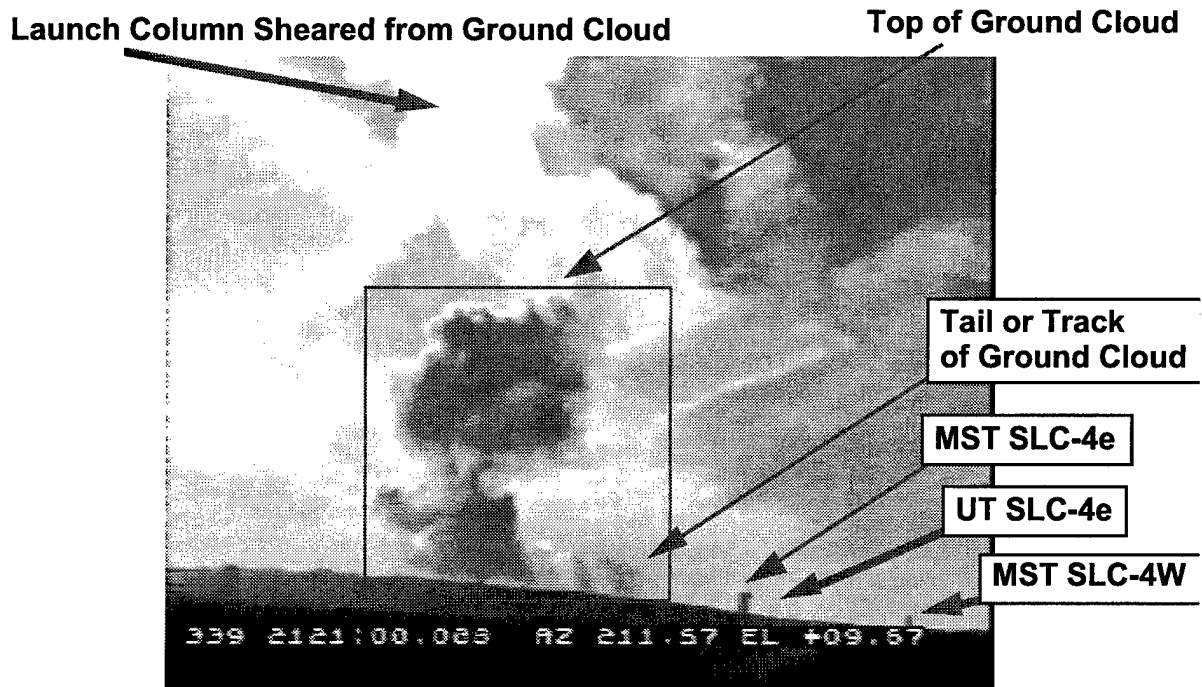


Figure 5. #K15 “hour-glass shaped” ground cloud with attached but dissipating launch column as observed from Bldg 900 at 03:00 (mm:ss) after launch: (a) visible imagery and (b) infrared imagery.

Figures 6 and 7 document visible imagery of the “hour-glass shaped” cloud at 3 min after launch as observed from Block Wall Beach and the Tetra Tech Gravel Pit, respectively. These images document the decrease in signal-to-noise with distance from the cloud. Both of these sites are further from the ground cloud than Building 900.

Launch Column Sheared from Ground Cloud

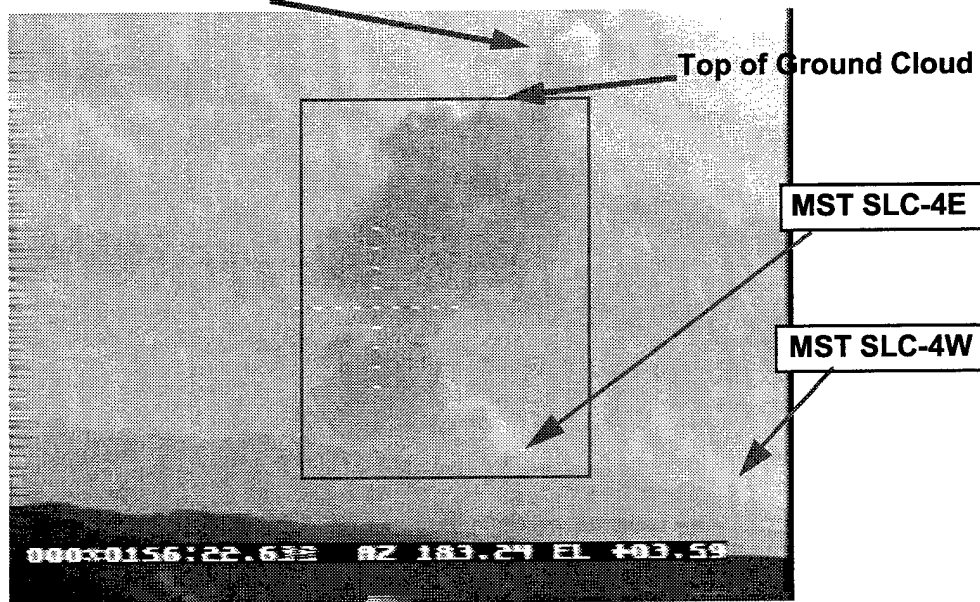


Figure 6. #K15 “hour-glass shaped” ground cloud as observed by visible imagery from block wall site at 03:00 (mm:ss) after launch.

Launch Column Sheared from Ground Cloud

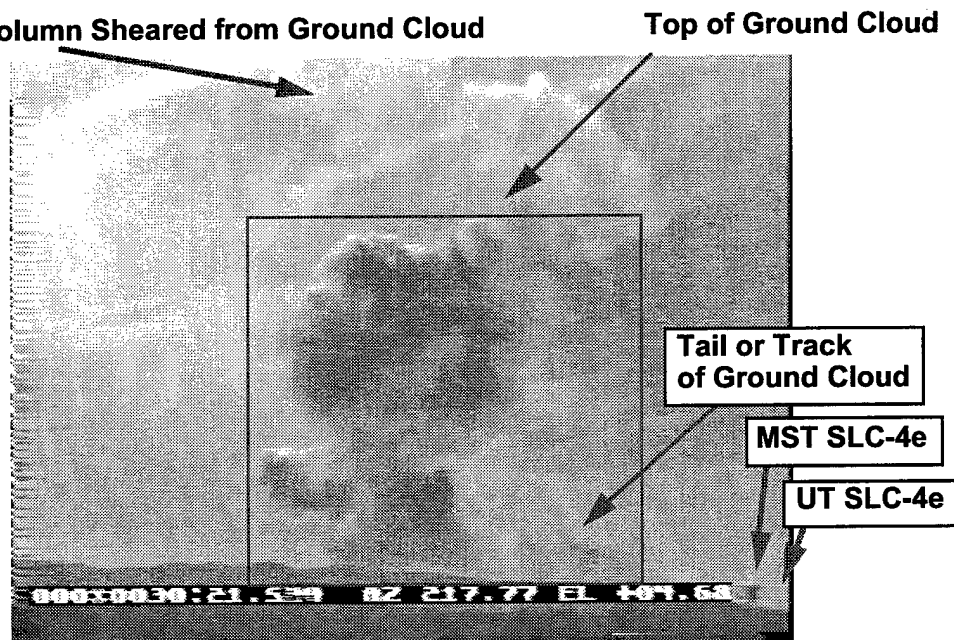
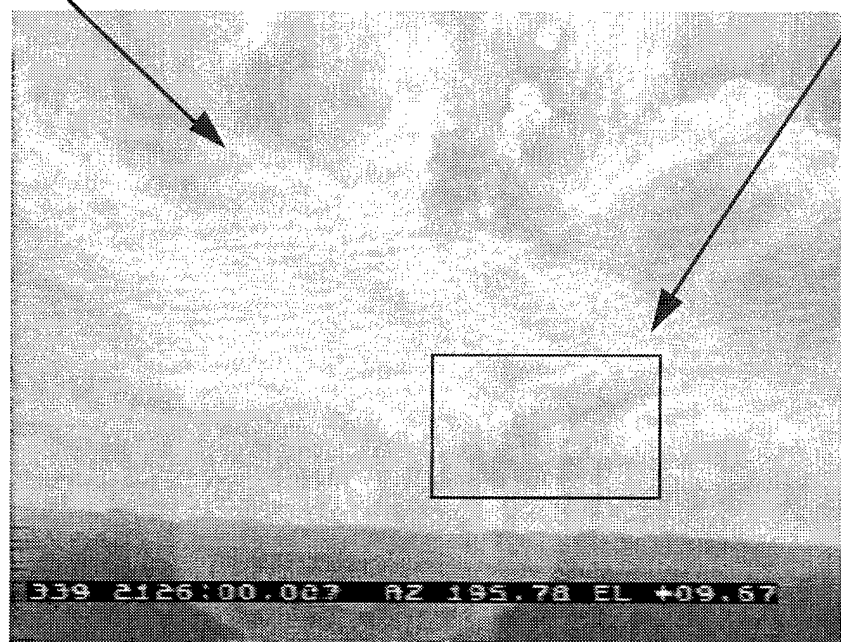


Figure 7. #K15 “hour-glass shaped” ground cloud with attached but dissipating launch column as observed by visible imagery from Tetra Site at 03:00 (mm:ss) after launch.

Figure 8 documents (a) visible and (b) infrared imagery of the exhaust cloud at 8 min after the launch as observed from building 900. It is evident that the (a) visible and (b) infrared imagery are complimentary and provide the analyst a better picture of the shape of the ground cloud and launch column. The visible imagery is complicated by sunlight reflections in the optics. The infrared

Launch Column Difficult to See in Visible Imagery **Top of Ground Cloud**



Launch Column Testifies to Changing Wind Direction with Altitude

Top of Ground Cloud

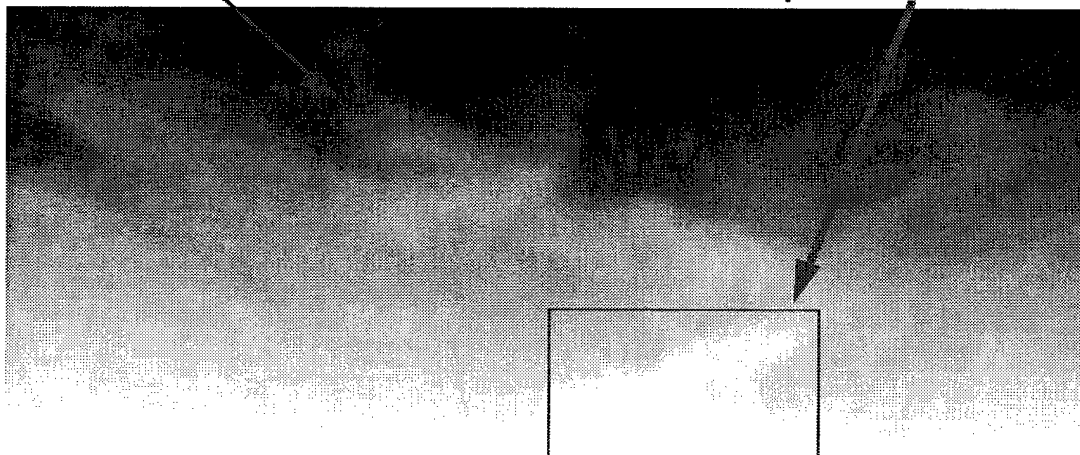


Figure 8. #K15 ground cloud with attached launch column as observed from Bldg 900 at 08:00 (mm:ss) after launch: (a) visible imagery and (b) infrared imagery.

imagery is not affected by the such scattering and reveals the affect of the shifting wind direction with altitude upon the ground cloud and launch column shapes. The analyst included the bright "sideways V" as the ground cloud and ignored the launch column, which is sheared from the top of the ground cloud in this image (8b).

The top and bottom of the "ground cloud" are defined by the analyst after careful review of previous and subsequent imagery from all imagery sites. The analyst draws his "box" about the mass of the cloud that contributes to the stabilized ground cloud.

2.5.3. Cloud Rise Times and Stabilization Heights

The plots presented in Figures 9-11 show the time-dependent altitude (meters above SLC-4E = m AS4E) of the "bottom," the "middle," and the "top" of the ground cloud as documented by the imagery from three camera sites. The "a" plots label the data according to the type of imagery and the camera site as follows:

vteb9	=	visible only from Tetra Site and Building 900 Site
vtebw	=	visible only from Tetra Site and Block Wall Site
vb9bw	=	visible only from Building 900 and Block Wall Site
ib9bw	=	infrared imagery from building 900 and visible from Block Wall Site

The labels on the "a" plots not only allow one to look for trends associated with certain combinations of imagery sites but also allow direct comparison of infrared to visible imagery for identical camera sites. Review of the "a" plots reveals that no single combination of sites or cameras produces systematically different results when compared to the other data over the entire monitoring time. However, for the first several minutes after launch, data biased by the block wall perspective reports negative "Bottom" heights (relative to SLC-4E). This is physically possible since SLC-4E is 153 m (501 ft) above MSL. At later times, data biased by the block wall perspective is often higher than determined by other perspectives. Certainly the random nature of the scatter in the "a" plots support the treatment of the imagery data as one set as done in the "b" plots. The "b" plots include a polynomial fit to the combined data and horizontal lines illustrating the stabilization height as well as the $\pm 3\sigma$ error levels.

It is evident from review of Figures 9-11 that the shapes of the cloud rise curves for the top, middle, and bottom of the ground cloud are as dramatically different as their stabilization times. The top of the cloud reaches its stabilization height within 2.5-4 min while the bottom continues to rise until 9-11 min after launch (possibly a result of decreasing signal-to-noise for the remote cloud). The height of the top of the ground cloud decreases only slightly after rising to its maximum. The cloud was not imaged for long enough times to see a similar trend for the bottom of the ground cloud. The middle of the cloud is calculated from the top and bottom and therefore presents an intermediate behavior. The cloud's characteristic rise times and stabilization heights are compared to REEDM predictions in the next section.

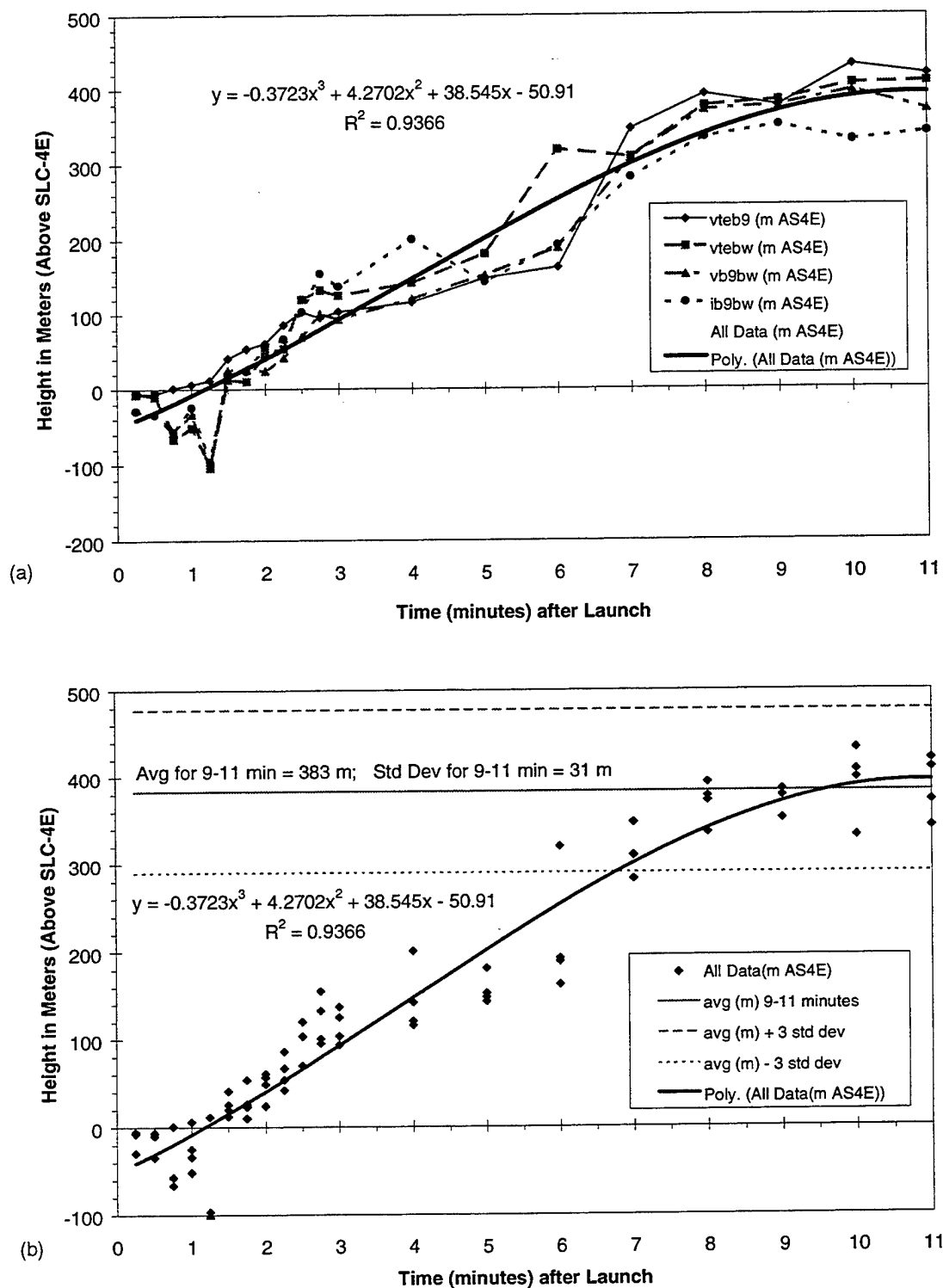


Figure 9. #K15 cloud bottom rise rate. (a) Raw imagery data displaying the rise of the cloud bottom for #K15 with the data labeled by imagery pairs. (b) a plot of the height above ground vs time as 3rd-order polynomial fits to all data and lines, documenting the 3- σ error bands as well as the 383-m (1258-ft) stabilization height above launch pad ground level. The variance (R^2) of 0.9366 indicates a high quality of fit.

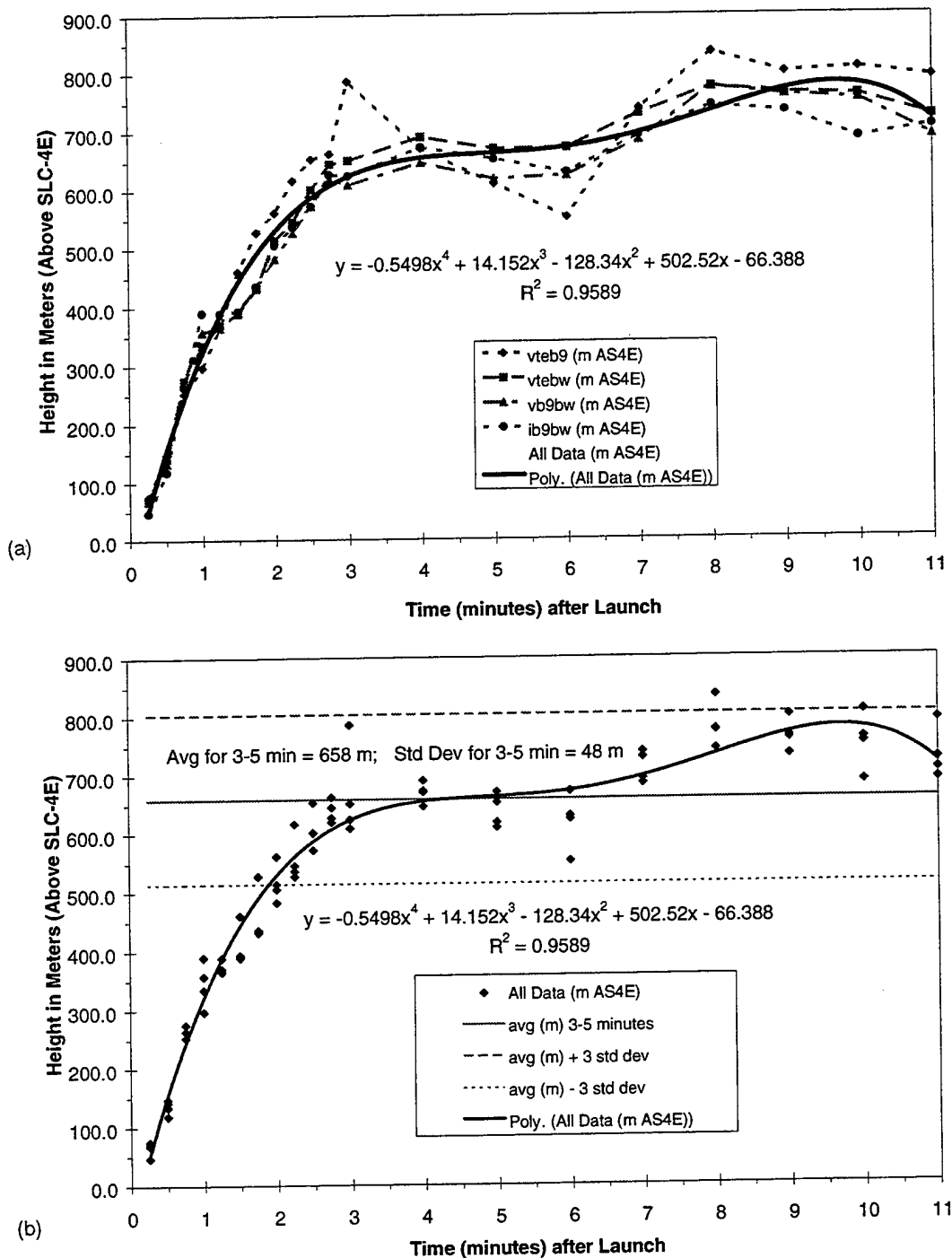


Figure 10. #K15 cloud middle rise rate. (a) Raw imagery data displaying the rise of the cloud middle for #K15 with the data labeled by imagery pairs. (b) a plot of the height above ground vs time as 4th-order polynomial fits to all data and lines, documenting the 3- σ error bands as well as the 658-m (2160-ft) stabilization height above launch pad ground level. The variance (R^2) of 0.9589 indicates a high quality of fit.

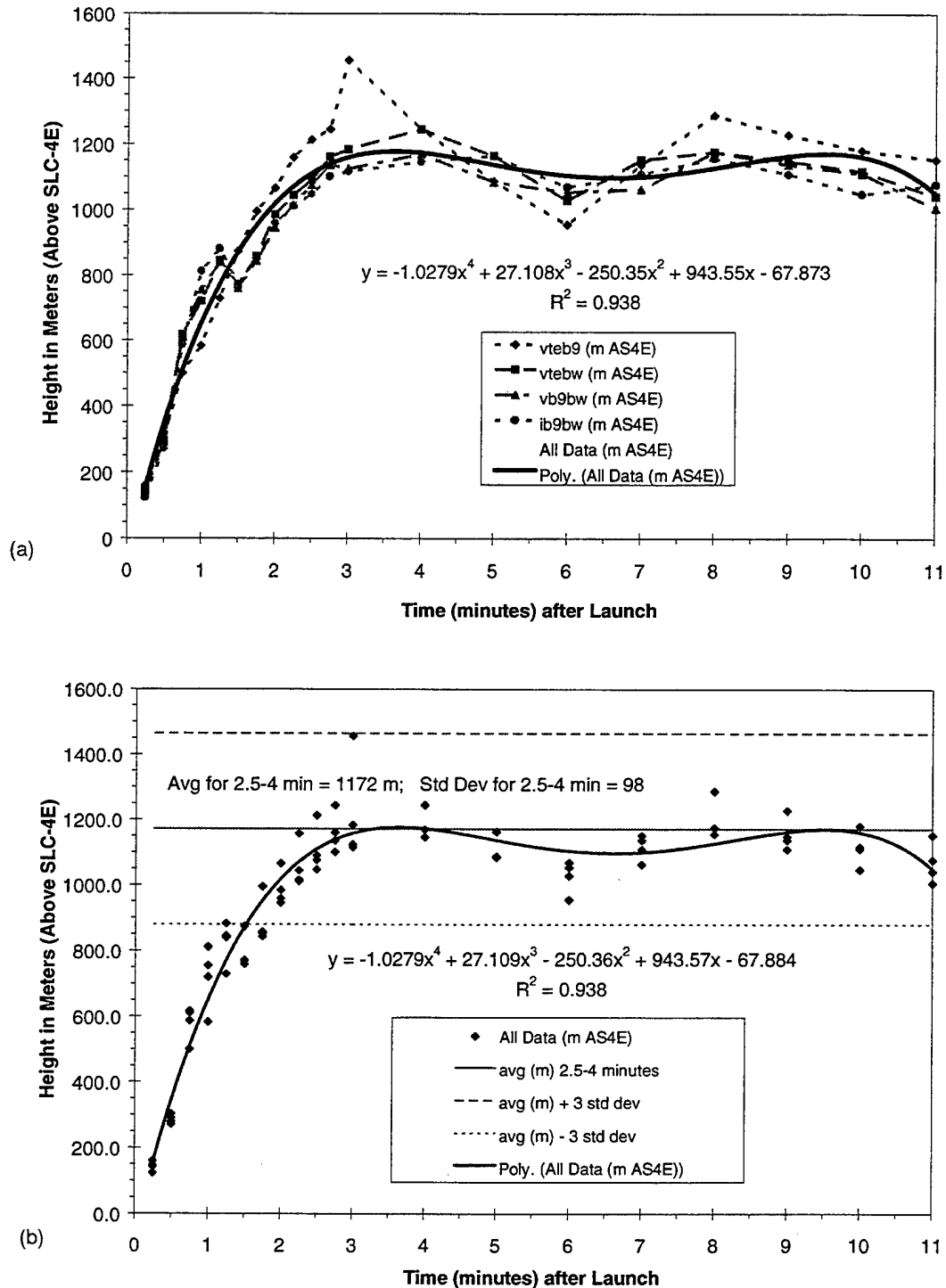


Figure 11. #K15 cloud top rise rate. (a) Raw imagery data displaying the rise of the cloud middle for #K15 with the data labeled by imagery pairs. (b) A plot of the height above ground vs time as 4th-order polynomial fits to all data and lines, documenting the 3- σ error bands as well as the 1172-m (3844-ft) stabilization height above launch pad ground level. The variance (R^2) of 0.938 indicates a high quality of fit.

2.5.4. Comparison of REEDM Prediction to Imagery Data: Rise Rate and Height

In Figure 12, the imagery-derived heights for the cloud's top, middle, and bottom are plotted with the T-0.25 hour REEDM prediction of the height for the cloud's middle against time. It can be seen that the measured stabilization height of the cloud's center (658.4 ± 48 m above SLC-4E) is 28% higher than the value predicted by REEDM (514 m in Appendix C) using pre-launch rawinsonde data (Appendix D). The amount of time required to reach the stabilization height (approximately 3–5 min from the imagery) is very close to the 2.8 min predicted by REEDM. This is qualitatively evident from comparison of the shapes of the "middle" curves in Figure 12.

The variances (R^2) of the polynomial fits to the data (i.e., Figures 9–11) indicate that the fits are very good. A polynomial fit was used in those figures as a convenient method to permit the representation of cloud overshoot and subsequent damped oscillation around the stabilization height. To be consistent with REEDM, stabilization time and height refer to the first maximum in these fits. REEDM predicts that the cloud goes through damped oscillatory motion with a period of $2\pi/S^{1/2}$,

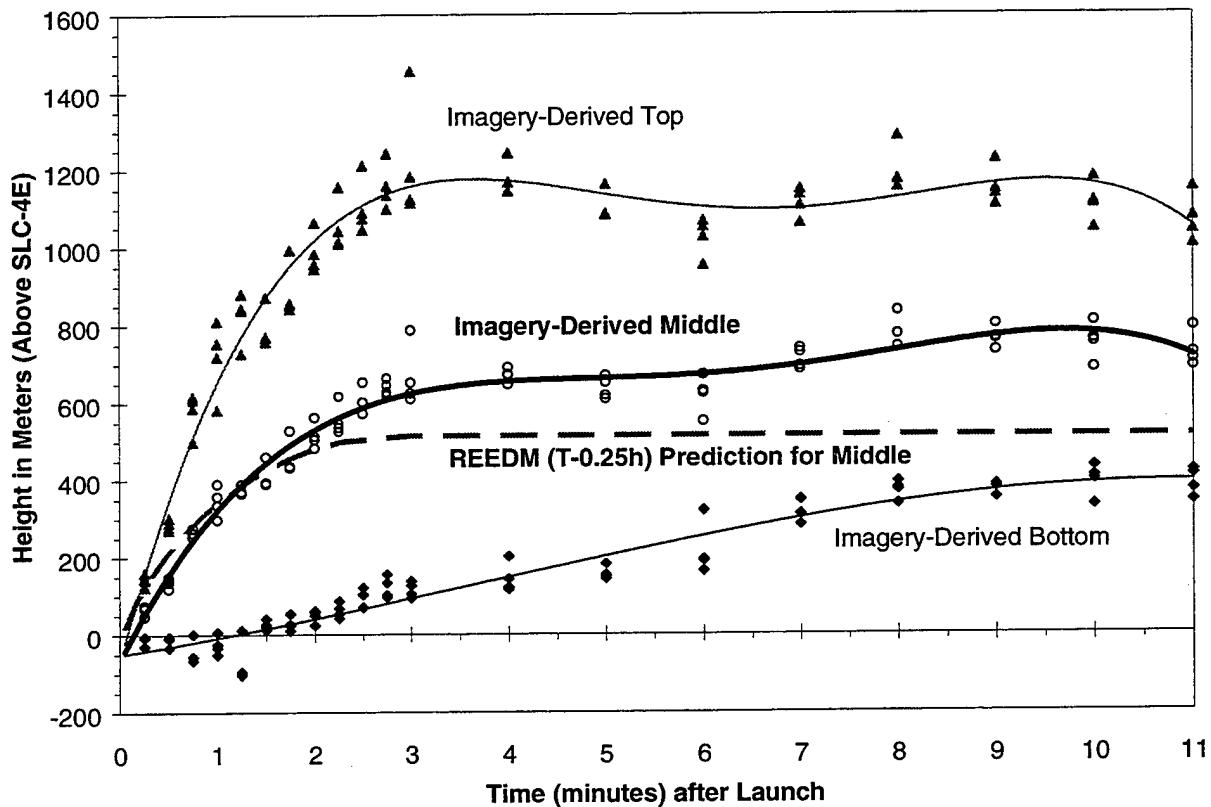


Figure 12. The imagery-derived heights for the top, middle, and bottom of the ground cloud (Figures 9–11) are plotted as $H(t)$ vs t . The T-0.25 h REEDM modeling run predictions for the cloud middle (514 m after stabilization) are presented for comparison to the middle curve derived from the imagery (658 m to first maximum), which is 28% higher than the REEDM prediction.

where S is the static stability parameter [Ref. 1, Eq. (7)]*. Examination of Figures 10 and 12 shows that stabilization time is approximately 3–5 min for the #K15 ground cloud compared to 2.8 min for REEDM. Sensitivity of REEDM predictions to input parameters has been examined by Womack.[†] Careful imaging of launch ground clouds under a variety of meteorological conditions is a vital element in REEDM evaluation.

2.5.5. Comparison of REEDM Prediction to Imagery Data: Trajectory and Speed

Figures 13 and 14 present data for the ground track and for the displacement of the cloud from the launch pad as determined by imagery. The “box” method of analysis for the imagery data does not yield independent values of the cloud track for the top, middle, and bottom of the cloud. We have chosen to present data for the middle of the cloud as defined by **PLMTRACK**.

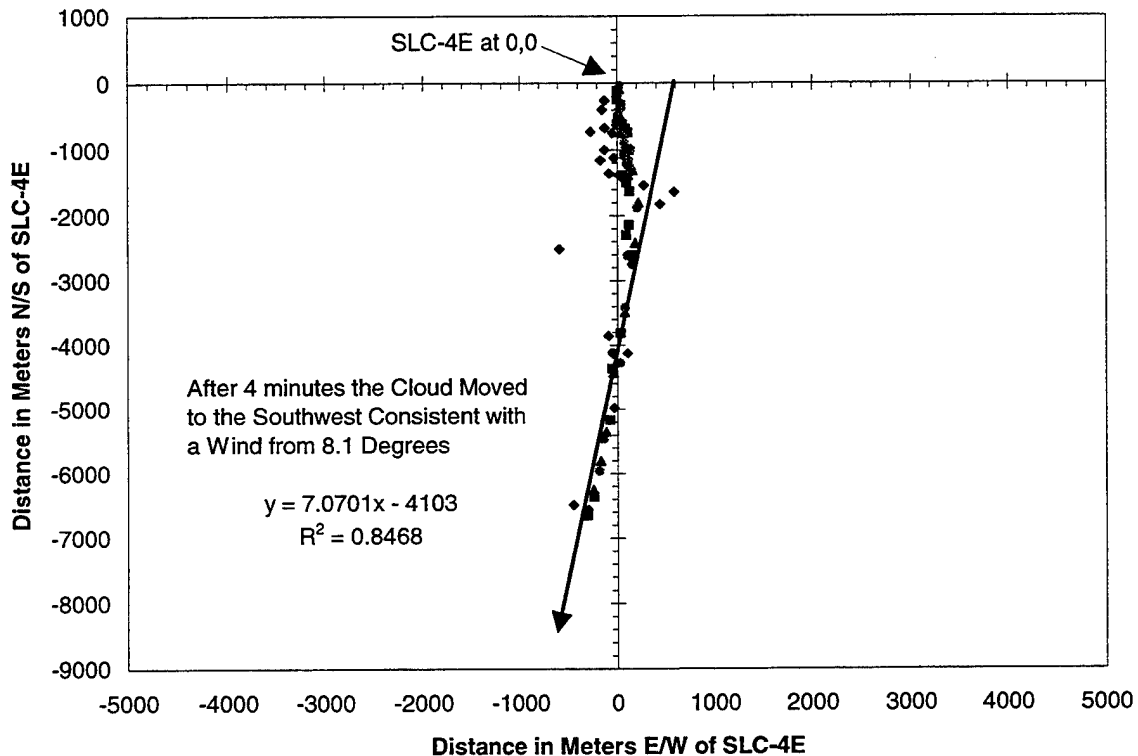


Figure 13. Ground track for the middle of the #K15 launch cloud. Due to the changing direction and strength of the winds experienced by the cloud as it rises, the early cloud trajectory data appears scattered. However, once the cloud reached stabilization height, the cloud followed a southwesterly path as illustrated by fitting only the data collected after stabilization (i.e., greater than 4 min after launch). This 8.1° trajectory is bracketed by vectors reported by REEDM: (1) the 2° maximum concentration at the 514 m, (2) the 14° trajectory at the end of cloud rise, and (3) the 344° wind for the second mixing layer. Likewise, the winds at the top (358°), middle (26°) and bottom (17°) of the imaged cloud are consistent with the observed cloud trajectory (8.1°).

* J. R. Bjorklund, User's Manual for the REEDM Version 7 (Rocket Exhaust Effluent Diffusion Model) Computer Program, Vol. I, TR-90-157-01, AF Systems Command, Patrick AFB, FL (April 1990).

† J. M. Womack, *Rocket Exhaust Effluent Diffusion Model Sensitivity Study*, TOR-95(5448)-3, The Aerospace Corporation, El Segundo, CA (May 1995).

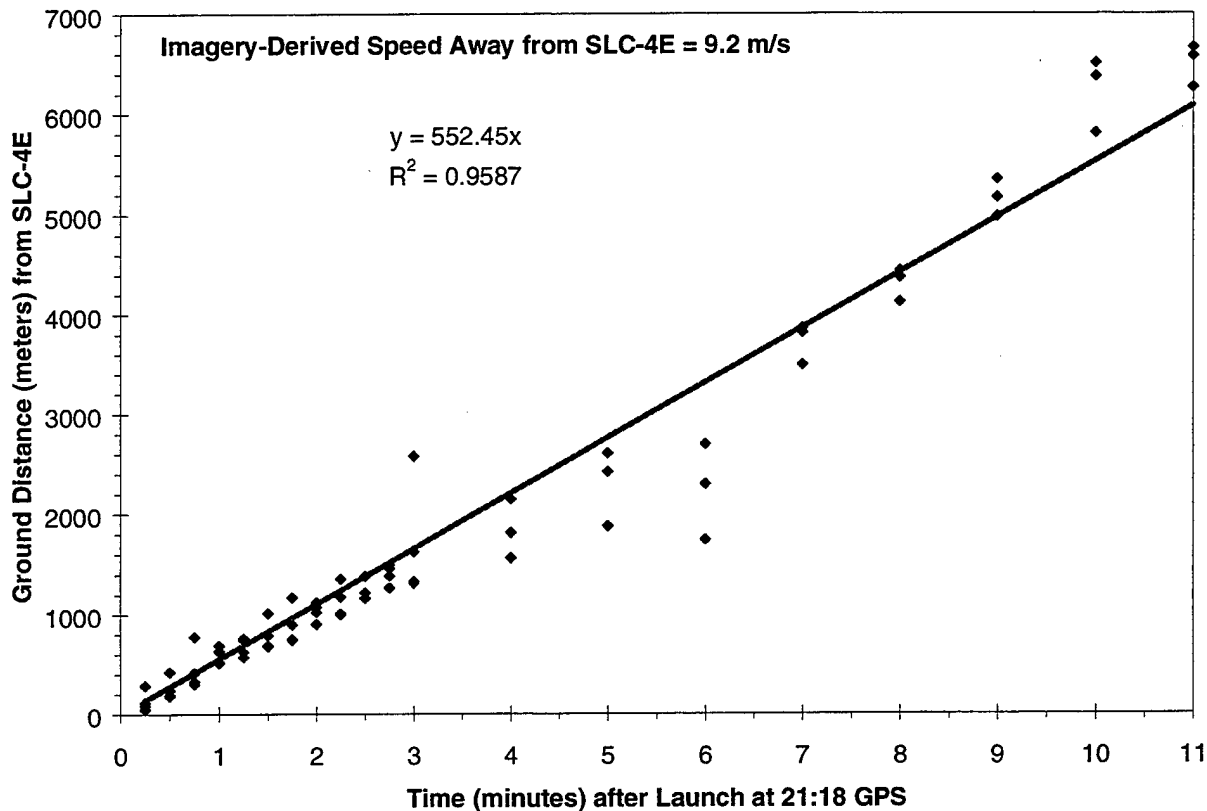


Figure 14. Ground distance for the middle of the #K15 launch cloud from the launch pad. The slope yields a speed of 9.2 m/s away from SLC-4E. The high value for the variance ($R^2 = 0.9587$) indicates the quality of this linear fit to these data. For comparison, REEDM predicts 7.6 m/s (during rise), and the rawinsonde sounding (T-0.25h) documents 7.3–8.9 m/s at the height of the imaged cloud. The rawinsonde was launched from Building 900 (i.e., north-northeast of the pad).

To be precise, the ground track in Figure 13 represents the ground-plane projection of the trajectory of the middle of the cloud as a function of time. For higher wind speeds, an “average” ground track is normally computed as a single linear fit to the position data using the following formula:

$$Y = mX + b,$$

where Y is the distance in meters along the north-south axis, m is the slope of the fit, X is the distance in meters along the east-west axis, and b is the intercept for the fit. We normally permit the intercept (b) to be nonzero since the cloud origin may differ from the location of the launch complex due to low-altitude winds and exhaust duct geometry. That displacement can also be modeled within the REEDM code.

In this report, the angles will conform to the convention of rawinsonde wind vectors (the angle from which the wind originates that would push the cloud to its imaged position). Thus, the angles are related by

$$J = 180 + \Phi,$$

where ϑ is the equivalent rawinsonde wind angle, and Φ is the measured polar angle of the cloud relative to SLC-4E and clockwise of true north. For example, when the cloud is due east of SLC-4E, Φ is 90° , and ϑ is 270° . The slope (m) of the fitted line is determined by the angle θ , where $\theta = \tan^{-1} m$, and therefore $\Phi = 90^\circ - \theta$.

Figure 14 presents the distance of the cloud from the launch pad as derived from analysis of pairs of imagery. The ground distance of the cloud from SLC-4E increases with time. As with the cloud trajectory, the speed varies slightly as the cloud rises. A linear fit to the imagery data provides the velocity of the ground cloud. The imagery documents 9.2 m/s cloud velocity away from SLC-4E. The high value for the variance for this linear fit (i.e., $R^2 = 0.9587$) illustrates the quality of these data. By comparison, REEDM (T-0.25 h) predicts a cloud speed of 7.6 m/s (during rise), which is significantly lower than the observed speed. Likewise, the rawinsonde sounding (Appendix D) documents lower wind speeds (7.3 to 8.9 m/s) at the height of the imaged cloud. The winds at the height of the stabilized cloud are derived from rawinsonde measurements at T-0.25 hour from building 900 area (i.e., north-northeast of the pad). Therefore, there are offsets both in time and distance between the rawinsonde sounding and the exhaust cloud rise.

2.5.6. Comparison of REEDM Prediction to Imagery Data: Summary Table

Table 3 summarizes the imagery-derived, rawinsonde-measured (T-0.25 h), and REEDM-predicted (T-0 h reconstruction) data for the #K15 launch cloud. Several conclusions are derived from review of the contents of this table:

- (1) the imagery-derived direction and speed of the cloud are, qualitatively, in agreement with the T-0.25 hour rawinsonde data at the imagery-derived stabilization height of the cloud;
- (2) the imagery-derived stabilization height (658 m) is 28% higher than predicted by REEDM (515 m);
- (3) the imagery-derived velocity (9.2 m/s) of the ground cloud is 21% faster than predicted by REEDM (7.6 m/s); and
- (4) the imagery-derived cloud track (8°) is 24° more clockwise than predicted by REEDM (344°).

These data suggest that better prediction of stabilization height by REEDM would automatically correct the wind direction and the wind speed predictions, which are based upon the rawinsonde data at the stabilization height.

Table 3. Summary for #K15 Launch Cloud Data Derived from Visible and Infrared Imagery, T-0.25 h Rawinsonde Sounding Data, and T-0 h REEDM Predictions.

Attribute	Feature	Imagery (IR & Vis)	Rawinsonde (T-0.2 h)	REEDM 7.07 (T-0.2 h)
Height (m)	Top	1172	#N/A	#N/A
Above SLC-4E	Middle	658	#N/A	515
	Bottom	383	#N/A	#N/A
Time (min)	Top	2.5-4	#N/A	#N/A
After Launch	Middle	3-5	#N/A	2.8
	Bottom	9-11	#N/A	#N/A
Bearing (deg) (Rawinsonde)	Top	#N/A	358	#N/A
	Middle	8.1	26	344-14
	Bottom	#N/A	17	#N/A
Speed (m/s)	Top	#N/A	7.8	#N/A
Away from	Middle	9.2	8.9	6.3-7.6
SLC-4E	Bottom	#N/A	7.3	#N/A

2.5.7. Imagery-Derived Crosswind Growth Rate

The imagery from the Block Wall site documented the cross-wind growth in the diameter of the ground cloud as a function of time. The cloud moved to the south-southwest of SLC-4E, which was almost directly away from the Block Wall site, which was to the north-northeast of SLC-4E. Figure 15 presents a plot of the exhaust cloud width against distance from SLC-4E. The cross-wind diameter was measured using the azimuthal width of the cloud as seen from Block Wall site and the triangulated position of the cloud relative to Block Wall site. Therefore:

$$W = 2 \cdot D \cdot \text{TAN}(dAZ / 2),$$

where W is the crosswind width of the cloud in meters, D is the distance in meters of the center of the cloud from the Block Wall site, and dAZ is the azimuthal crosswind width in degrees of the cloud as observed from the Block Wall site. Figure 15 includes three sets of determinations for the cloud's crosswind width using Tetra Tech Site's visible imagery, Building 900 Site's visible imagery, and Building 900 Site's infrared imagery paired with Block Wall Site's visible imagery. The crosswind width increases linearly for the first 6.5 min after launch and is fit to the following functions:

$$W = 0.3133 D + 457.3 \quad (R^2 = 0.9543)$$

$$W = 147.19 t + 464.8 \quad (R^2 = 0.9443)$$

where t is time after launch. The apparent stabilization in the cloud's crosswind width at times greater than 6.5 min after launch is probably a result of poor signal-to-noise for detecting the edge of the remote cloud.

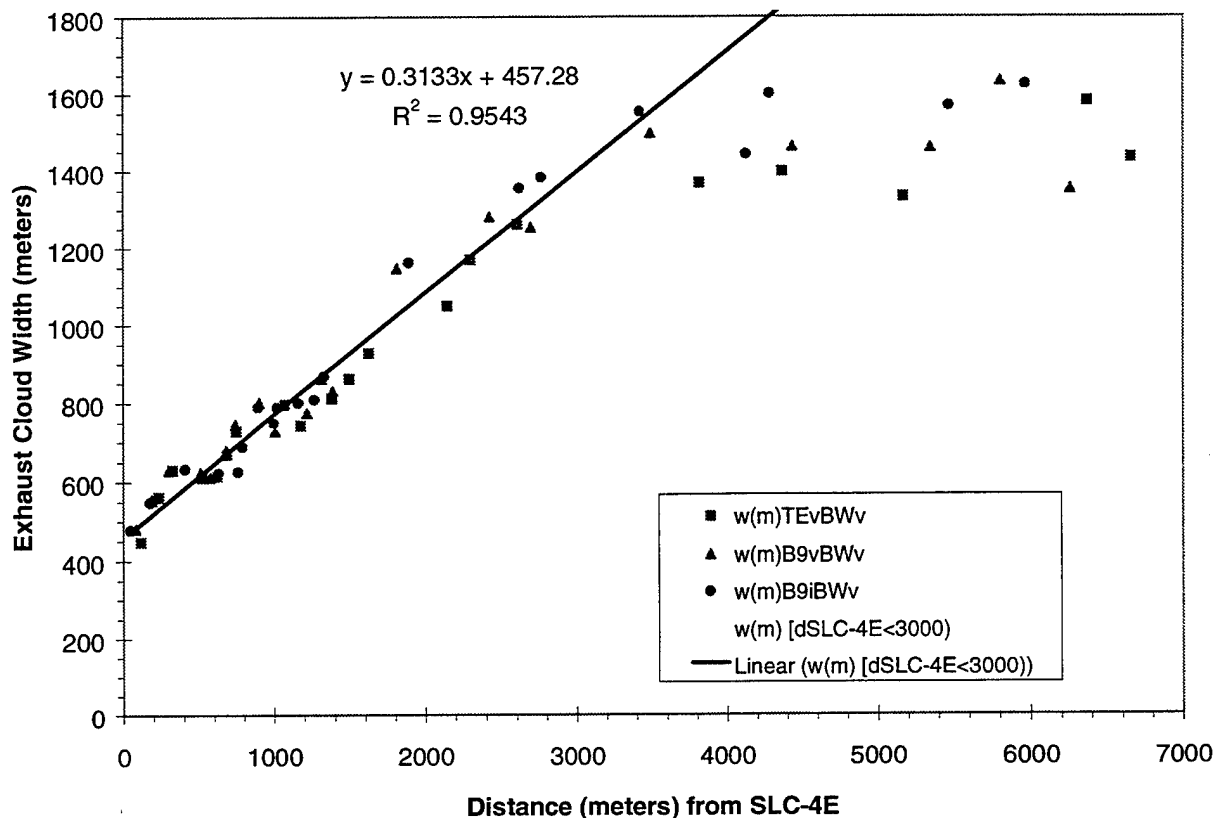


Figure 15. Growth of the #K15 launch's exhaust cloud as observed from Block Wall site. A linear fit to the cloud's crosswind width documents a steady increase in width until 6.5 min after launch. At longer times, the width appears to remain constant, which is probably an artifact due to low signal-to-noise for detecting the cloud's edges at longer distances and greater dilutions. The high value for the variance ($R^2 = 0.9543$) indicates the quality of this linear fit to these data. These data are derived from the angular width observed from Block Wall Site combined with the cloud's position derived by triangulation using Block Wall visible imagery paired with Tetra Tech visible imagery, Building 900 visible imagery, and Building 900 infrared imagery.

2.6 Summary and Conclusions

The Titan IV #K15 mission was launched successfully from the Western Range (SLC-4E) at 13:18 PST (21:18 ZULU) on 5 December 1995. Personnel from The Aerospace Corporation deployed one IR imaging system and three visible imagery systems to monitor this daylight launch and to track the time evolution and the ground trajectory of the solid rocket motor exhaust cloud. The three imagery sites were located to the northeast, north-northeast, and north relative to launch complex SLC-4E. Imagery data were recorded for 30 min, and the cloud was tracked for 11 min. When combined with the Az/El readings and the IRIG-B time data, the imagery was used to quantify movement, rise, and growth of the cloud for 11 min after the launch. The launch of #K15 marked the fourth deployment of the Titan IV-dedicated VIRIS imaging platforms and the first VIRIS deployment for VAFB launch.

The definition of exhaust cloud geometric features was complicated by multiple contributions to the complex shape of the evolving cloud (i.e., rapid rise of the hot ground cloud and separation of the

high-altitude launch column). The analyst included only the portions of the exhaust cloud that became incorporated into the stabilized ground cloud.

Analysis of the imagery data presented in this report has focused on determining parameters that are directly comparable to REEDM predictions. The most accurately determined quantities by imagery are the cloud rise time, its stabilization height, cloud speed, and ground track. In addition, the imagery documented the rate of growth in the size of the #K15 exhaust cloud. Using the T-0.25 hour rawinsonde data, REEDM predicted a stabilization height of 514 m above ground level and a stabilization time of 2.8 min, while the imagery yielded values of 658 m above SLC-4E and 3-5 min. The imagery-derived cloud trajectory was 8° , and the cloud's ground speed was 9.2 m/s away from SLC-4E. This compares to 344° and 7.6 m/s predicted by REEDM (T-0.25 h). Therefore, the imaged cloud stabilized at a height that was 28% higher than predicted by REEDM (T-0.25 h), traveled at a speed 21% faster than predicted by REEDM (T-0.25 h), and headed in a direction 24° more clockwise than predicted by REEDM (T-0.25 h).

3. Aircraft Elevated HCl Measurements

[The material in this section was contributed by Dr. R. N. Abernathy, Brian P. Kasper, Karen L. Foster, and Dr. R. F. Heidner III of the Environmental Monitoring and Technology Department of The Aerospace Corporation's Space and Environment Technology Center.]

3.1 Background

On 5 December 1995, the Titan IV #K15 mission was successfully launched from VAFB at 13:18 PST (21:18 GMT). This section describes the HCl concentration data collected by an aircraft that sampled that portion of the exhaust cloud known as the ground cloud. The aircraft used a modified Geomet total hydrochloric acid (HCl) detector to measure the HCl concentrations within the ground cloud for 110 min subsequent to the launch. This aircraft sampling campaign involved Air Force, NASA, NOAA, and contractor (I-NET and SRS) organizations. The Aerospace Corporation analyzed the aircraft's HCl concentration data. Based upon sampling at altitudes below 1000 m, the aircraft's HCl concentration data document the movement of the ground cloud to the south immediately following the launch, the mixing of HCl to altitudes as low as 150 m, and a shift in cloud direction to a southeasterly trajectory, at later times. The aircraft's altitude was measured using a global positioning system (GPS) receiver with regular service (± 100 m in latitude and in longitude and ± 250 m in altitude). Differential GPS service was not available for this mission at VAFB.

The aircraft's Geomet data (i.e., total HCl concentration measurements) are reported here in several graphical formats to facilitate comparison with REEDM predictions (Appendix A), meteorological data (Appendix B), gaseous HCl measurements (Section 4), and imagery data (Section 2). The aircraft setup is described in Appendix C. For clarity, this section includes some data from other sections in its figures, tables, and text. It is apparent from review of this section, that these data will be useful for validating current and future dispersion models. In fact, we discovered an error in the REEDM output of cloud height relative to mean sea level while writing this report.

The purpose of this report is to document the quality and quantity of the aircraft data available for validating dispersion models. However, it is difficult to extract the data for a single pass through the cloud from summary plots that contain 41 passes through the cloud. Therefore, in order to facilitate the comparison of these data to individual dispersion model runs, two subsequent reports will provide: (1) a detailed correlation between imagery and aircraft data for the first 11 min after launch and (2) a detailed graphical analysis of the aircraft's HCl concentration profiles using polar and Cartesian coordinates for each 10-min time window throughout the 110-min flight time. These subsequent detailed analyses will provide the data in a format that will allow direct comparison to model runs for specific times, altitudes, and distances from the release site. The aircraft data are also available as comma-separated-variable files providing time, latitude, longitude, altitude, Geomet response, and HCl concentration.

3.2 Introduction

As described in detail in Section 5, I-NET, a NASA contractor, modified a Geomet for mounting in the nose of a Piper (PA-44-180) Seminole (a twin-engine, four-seat aircraft). (See Appendix C for installation details.) The Geomet is a total HCl monitor that produces a response proportional to the combined HCl present in both the vapor or the aerosol phases. It reports the HCl concentration as parts-per-million (ppm) by volume (i.e., $V_{\text{HCl}} 10^6/V_{\text{total}}$). This instrument sampled the air through a horizontal four-foot-long ceramic inlet wetted with a bromate/bromide-containing reagent. The HCl diffuses to the wetted walls of the ceramic tube and produces bromine vapor through reactions with the reagent. The bromine vapor is swept into a buffered hydrogen peroxide/Luminol solution resulting in photoluminescence detected by a filtered photometric detector. I-NET disabled the Geomet's autoranging electronics so that a single range produced a millivolt response that was proportional to the combined HCl vapor and aerosol concentration entering the inlet. I-NET calibrated the Geomet against HCl vapor before and after the #K15 mission as described in Section 5 and discussed in this section.

SRS Technologies Inc., a contractor, provided an interface between the I-NET laboratory and the Florida Institute of Technology (FIT) flight crew. NASA, NOAA/Air Resources Laboratory/Field Research Division, I-NET, SRS, and FIT cooperated in the integration of the NOAA data system, the FIT aircraft, and the Air Force Geomet into an airborne sampling and data logging system. FIT personnel piloted the aircraft during the #K15 mission, while 45th AMDS/SGPB personnel operated the NOAA data system and the Geomet detector. The NOAA data system logged GPS time and position as well as the Geomet response every 0.25 s during the flight. NOAA provided a comma-separated-variable (csv) data file to The Aerospace Corporation.

The Aerospace Corporation imaged the rise, movement, and growth of the ground cloud for the first 11 min subsequent to the #K15 launch, as documented in Section 2. This quantitative imagery documented the stabilization height (above SLC-4E) and the trajectory (relative to SLC-4E) of the ground cloud. Rudimentary knowledge of the rawinsonde wind data (Appendix B), REEDM predictions (Appendix A), and the imagery data (Section 2) was required for the interpretation of the aircraft's HCl sampling data as reported in this section.

As stated previously, the aircraft's altitude was measured using a global positioning system (GPS) receiver using regular service (no differential corrections were available for the VAFB area during this mission). The GPS altitude data were recorded as meters relative to mean sea level (MSL). Upon landing at the Santa Maria airport, the GPS altitude of the aircraft varied by 100 m over a 5-min period, ranging from 40 to 140 m. The actual runway height was 79 m (259 ft) MSL. Therefore, the GPS receiver appeared to function as expected while on the runway, delivering altitude data well within the regular GPS precision of ± 250 m.

When comparing the aircraft's GPS-derived altitude to the imagery, rawinsonde, and REEDM data, it is essential to use the same frame of reference for measuring the height. REEDM reports the predicted height of the exhaust cloud relative to MSL and relative to ground level but incorrectly assumes that the height of the rawinsonde release site is the same as the height of the launch pad. This is the case for Cape Canaveral, but is not the case for VAFB and results in a significant error in REEDM's output. We assert that REEDM's predicted height above ground level (AGL) was intended to be height above origin, which for a launch is height above the launch pad NOT above the

rawinsonde release site. Therefore, in Section 2, the observed height of the imaged cloud and the predicted (i.e., by REEDM) height of the stabilized cloud were reported in meters above SLC-4E (i.e., above the launch pad). For this conversion, we assumed the height AGL reported by REEDM was the same as the height above SLC-4E. Since SLC-4E is 501 ft (153 m) above MSL, height relative to SLC-4E is converted to height MSL by adding 501 ft (153 m). Since REEDM incorrectly uses the height of the rawinsonde release site (368 ft, 112 m) rather than the height of the launch pad (501 ft, 153m) for its conversion of height AGL to height MSL, the height MSL reported by REEDM in Appendix A is low by 41 m (133 ft). Table 4 provides the imaged and the predicted (i.e., by REEDM) heights relative to MSL and to SLC-4E by correctly using the launch pad as the origin for the launch:

Table 4. Imagery-Derived Stabilization Heights and REEDM's Predicted Stabilization Height Expressed Relative to MSL (Comparable to the Aircraft's GPS Data) and Relative to SLC-4E (as Reported in Section 2). Note that SLC-4E is 501 ft (153 m) above MSL.

Stabilized Exhaust Cloud Characteristic	H (m MSL) (comparable to the aircraft's GPS data)	H (ft MSL) (501 + H (ft SLC-4E))	H (m SLC-4E) (as reported in Section 2)	H (ft SLC-4E) (unit conversion from H (m SLC-4E))
Imaged Bottom	536	1758	383	1257
Imaged Middle	811	2660	658	2159
Imaged Top	1327	4353	1174	3852
REEDM's Middle	667	2187	514	1686

3.3 Results and Discussion

The aircraft's data are most easily interpreted in light of some rudimentary knowledge of the rawinsonde and imagery results. Figure 16 plots various wind and cloud bearings using the rawinsonde convention [defined fully in Subsection 3.3.2]. The cloud trajectories are anchored to SLC-4E on the map. The heaviest arrow (i.e., thickest linewidth) is used to plot the 8° cloud direction derived from imagery. Three additional cloud vectors are included to document the REEDM output that applies to the predicted exhaust cloud trajectory: (1) the 2° bearing to maximum concentration at 667m MSL (or 514 m AGL, which was REEDM's T-0.25 h prediction for the stabilization height); (2) the 14° bearing of the cloud at stabilization; and (3) the 344° average wind bearing for the second mixing layer (i.e., this dominates the trajectory for the stabilized cloud at later times). Therefore, REEDM's cloud trajectory predictions could be interpreted as a 2° bearing during rise, a 14° bearing at stabilization, and a 344° bearing after stabilization. The 8° bearing derived from the #K15 imagery data applies from 4 to 11 min after launch (during and shortly after stabilization). To the far right of the map in Figure 16, three wind vectors document the rawinsonde-derived wind directions associated with the bottom (17°), middle (26°), and top (358°) of the imagery-derived cloud heights. Although the rawinsonde launch originated from Building 900, the wind direction vectors are anchored to the right of the map to avoid clutter. Figure 16 also documents the locations of the three imagery sites chosen by The Aerospace Corporation for the #K15 imagery.

It is evident from examination of Figure 16 and from the discussion in the preceding paragraph that REEDM predicts a cloud trajectory at the stabilization height starting at 2°-14° and shifting to 344° while the imagery-derived cloud trajectory was a constant 8° during and shortly after stabilization. Likewise, it is evident from examination of Figure 16 that the imagery-derived southwesterly cloud direction is consistent with the pre-launch wind directions measured at heights equivalent to the top,

middle, and bottom of the stabilized ground cloud as determined by imagery. It should be noted that the low-altitude winds (shown on Figure 16) are out of the northeast (17–26°) while the high-altitude winds are out of the north (358°). This is consistent with shearing of the ground cloud as a function of altitude. REEDM predicts the dispersion of the cloud using a single rawinsonde sounding from a site that is remote from the launch pad. One can imagine that the winds can vary substantially with time and terrain. The REEDM predictions in Figure 16 are extracted from the REEDM output (T-0.25 h) in Appendix A. The T-0.25 h rawinsonde data in Figure 16 are extracted from rawinsonde sounding data in Appendix B.

The following sections of this report will document that the aircraft's HCl concentration measurements are consistent with the trajectory of the cloud measured by imagery during the first 11 min after launch and predicted by REEDM at and after stabilization. The aircraft data documents an initial southerly cloud trajectory that is in agreement with the imagery data (8° between 4 and 11 min) and the REEDM prediction (2°–14°) during and shortly after stabilization. At later times, the aircraft data documents a shift in trajectory to a southeasterly direction consistent with REEDM's prediction (344°) for the average wind in the second mixing layer.

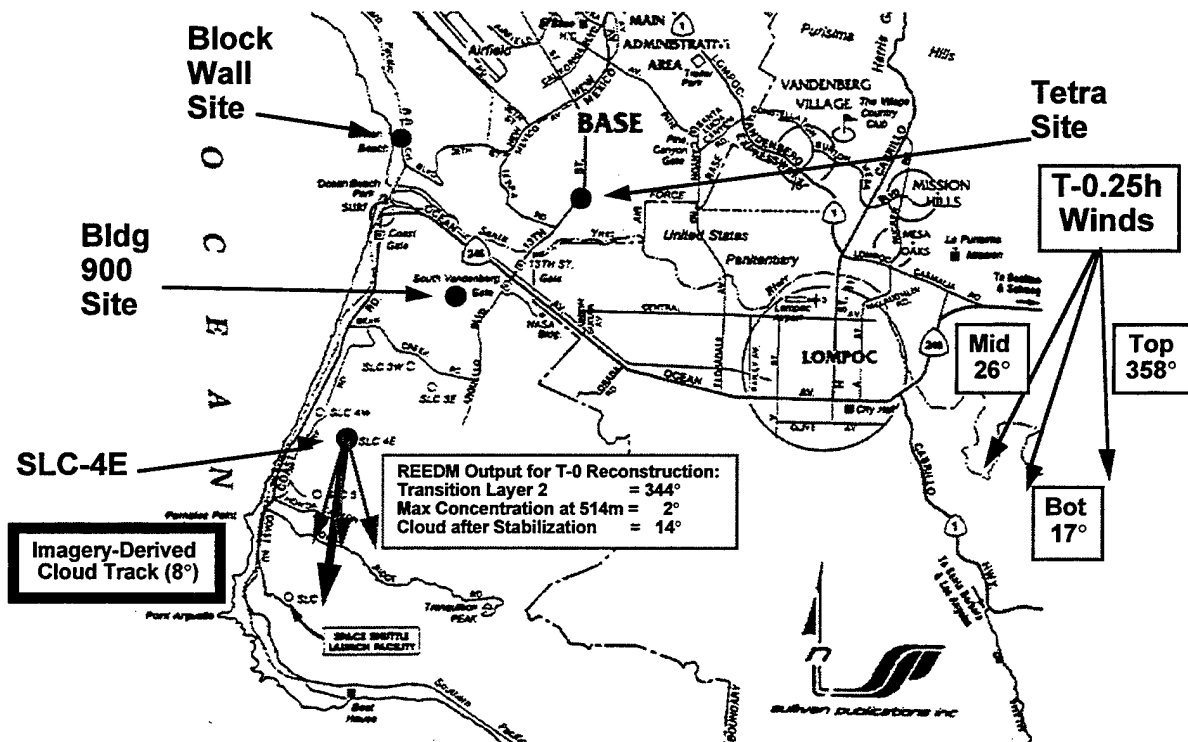


Figure 16. Partial map of VAFB documenting the locations of the three imagery sites as well as the available ground cloud data. The exhaust cloud data includes the imagery-derived #K15 ground cloud track (8° between 4 and 11 min after launch), the REEDM predictions for the #K15 ground cloud track (2° to maximum concentration at stabilization height, 14° for the initially stabilized cloud, and 344° after stabilization), and the wind direction for the top (358°), middle (26°), and bottom (17°) altitudes as determined from quantitative cloud imagery. The rawinsonde sounding was at 21:03 GMT (T-0.25 h) from Building 900 site and was modified using Doppler acoustic sounder data to synthesize the T-0 hour reconstruction. The cloud track vectors are anchored to SLC-4E pad.

3.3.1. Overview of Aircraft Sampling Data

3.3.1.1 Raw Aircraft Data

Table 5 presents a sample of the aircraft's data as delivered to The Aerospace Corporation with added headings. The headings are as follows: Log (mission log number assigned by NOAA); yr (year); d (Julian day of the year); hm (local time by inaccurate data logger clock in hour and minutes, two digits each); s (seconds); ppm (raw HCl concentration based upon single-point calibration and mV response from the Geomet); rng (range of the Geomet, disabled function); mV (Geomet response in millivolts); tGPS (GPS receiver GM time in hhmmss [documenting hours minutes seconds as six digits without separation]); lat (latitude, ddmm.mmmm, in degrees and decimal minutes); N/S (label for latitude, North/South); lon (longitude, ddmm.mmmm, in degrees and decimal minutes); E/W (label for longitude, East/West); diff (differential, 2, or normal, 1, GPS mode); # Sat (number of GPS Satellites); HDOP (horizontal dilution of precision [measure of GPS accuracy]); alt (altitude reported from GPS receiver); and units (M, meters for alt). The hm column is local and inaccurate computer time. Therefore, tGPS was used to interpret the aircraft data (using the "s" column to bin data reproducibly). The hm data were only used to interpolate between valid tGPS entries when the GPS failed to log time. Personnel from The Aerospace Corporation have reviewed these data in 10-min increments and applied baseline corrections to eliminate negative HCl concentrations. Personnel from The Aerospace Corporation have also performed the conversions necessary to report distance, polar angles, and Cartesian position in meters relative to SLC-4E.

Table 5. Portion of the Aircraft's Data File Provided to The Aerospace Corporation by NOAA. These data include the first aircraft detection of the Titan IV #K15 exhaust cloud. Note that the "hm" column does not agree with the "tGPS" column. The Aerospace Corporation registered all data to the GPS time using the seconds from the "s" column. When "tGPS" was not available, the computer time ("hm" column) was used to interpolate the time between valid "tGPS" entries.

Log	yr	d	hm	s	ppm	rng	mV	tGPS	lat	N/S	lon	E/W	diff	# Sat	HDOP	alt	units
113	1995	339	1315	46.5	-0.006	208	-157.7	212150	3437.0662	N	12036.5972	W	1	8	0.9	905	M
113	1995	339	1315	46.75	-0.006	208	-157.7	212150	3437.0662	N	12036.5972	W	1	8	0.9	905	M
113	1995	339	1315	47	-0.002	203.3	-60.89	212150	3437.0662	N	12036.5972	W	1	8	0.9	905	M
113	1995	339	1315	47.25	0.311	1387	77.9	212150	3437.0662	N	12036.5972	W	1	8	0.9	905	M
113	1995	339	1315	47.5	0.264	831	658.8	212151	3437.0281	N	12036.5902	W	1	8	0.9	906	M
113	1995	339	1315	47.75	0.116	834	291.1	212151	3437.0281	N	12036.5902	W	1	8	0.9	906	M
113	1995	339	1315	48	0.067	199.3	1667	212151	3437.0281	N	12036.5902	W	1	8	0.9	906	M
113	1995	339	1315	48.25	0.642	1387	160.4	212151	3437.0281	N	12036.5902	W	1	8	0.9	906	M
113	1995	339	1315	48.5	2.895	1386	724	212152	3436.9902	N	12036.5834	W	1	8	0.9	906	M
113	1995	339	1315	48.75	6.975	1385	1744	212152	3436.9902	N	12036.5834	W	1	8	0.9	906	M
113	1995	339	1315	49	8.97	1385	2244	212152	3436.9902	N	12036.5834	W	1	8	0.9	906	M
113	1995	339	1315	49.25	10.35	1823	258.9	212152	3436.9902	N	12036.5834	W	1	8	0.9	906	M
113	1995	339	1315	49.5	10.35	1824	258.9	212153	3436.9525	N	12036.577	W	1	8	0.9	907	M
113	1995	339	1315	49.75	10.18	1823	254.5	212153	3436.9525	N	12036.577	W	1	8	0.9	907	M
113	1995	339	1315	50	7.52	1384	1879	212153	3436.9525	N	12036.577	W	1	8	0.9	907	M
113	1995	339	1315	50.25	4.834	1385	1208	212153	3436.9525	N	12036.577	W	1	8	0.9	907	M
113	1995	339	1315	50.5	3.447	1385	862	212154	3436.9148	N	12036.5707	W	1	8	0.9	907	M
113	1995	339	1315	50.75	1.609	1385	402.3	212154	3436.9148	N	12036.5707	W	1	8	0.9	907	M
113	1995	339	1315	51	1.093	1385	273.2	212154	3436.9148	N	12036.5707	W	1	8	0.9	907	M
113	1995	339	1315	51.25	0.913	1385	228.3	212154	3436.9148	N	12036.5707	W	1	8	0.9	907	M
113	1995	339	1315	51.5	0.699	834	1748	212155	3436.8773	N	12036.5645	W	1	8	0.9	909	M
113	1995	339	1315	51.75	0.613	834	1532	212155	3436.8773	N	12036.5645	W	1	8	0.9	909	M
113	1995	339	1315	52	0.591	834	1477	212155	3436.8773	N	12036.5645	W	1	8	0.9	909	M
113	1995	339	1315	52.25	0.607	834	1516	212155	3436.8773	N	12036.5645	W	1	8	0.9	909	M

3.3.1.2 Cartesian Plot of Aircraft Data Relative to SLC-4E

Figure 17 plots the spatial extent of aircraft's sampling during the 110 min following the launch of #K15. It represents conversion of the latitude and the longitude of the aircraft's position to Cartesian coordinates centered on the SLC-4E launch complex. The aircraft's position is labeled with HCl concentration at each sampling by the use of different plot symbols. The HCl concentrations are based on calibrations performed by the NASA Toxic Vapor Detection/Contamination Monitoring Laboratory personnel and applied to the logged data files by NOAA personnel. The Aerospace Corporation personnel applied a small constant baseline offset to eliminate negative HCl concentrations and filtered incorrect positional and time entries when GPS coverage was intermittent. As shown in Figure 17, the aircraft's flight pattern was largely confined to a 16 km \times 70 km rectangle to the south of the launch complex. Time (0–110 min), polar angle (0° to 360° in the rawinsonde convention), distance (0–70,000 m), and altitude (0–1000 m by regular GPS service) are variables in the flight tracks presented in Figures 18 through 20. Thus, the HCl concentration hits noted in Figure 17 can be interpreted in light of these other critical variables.

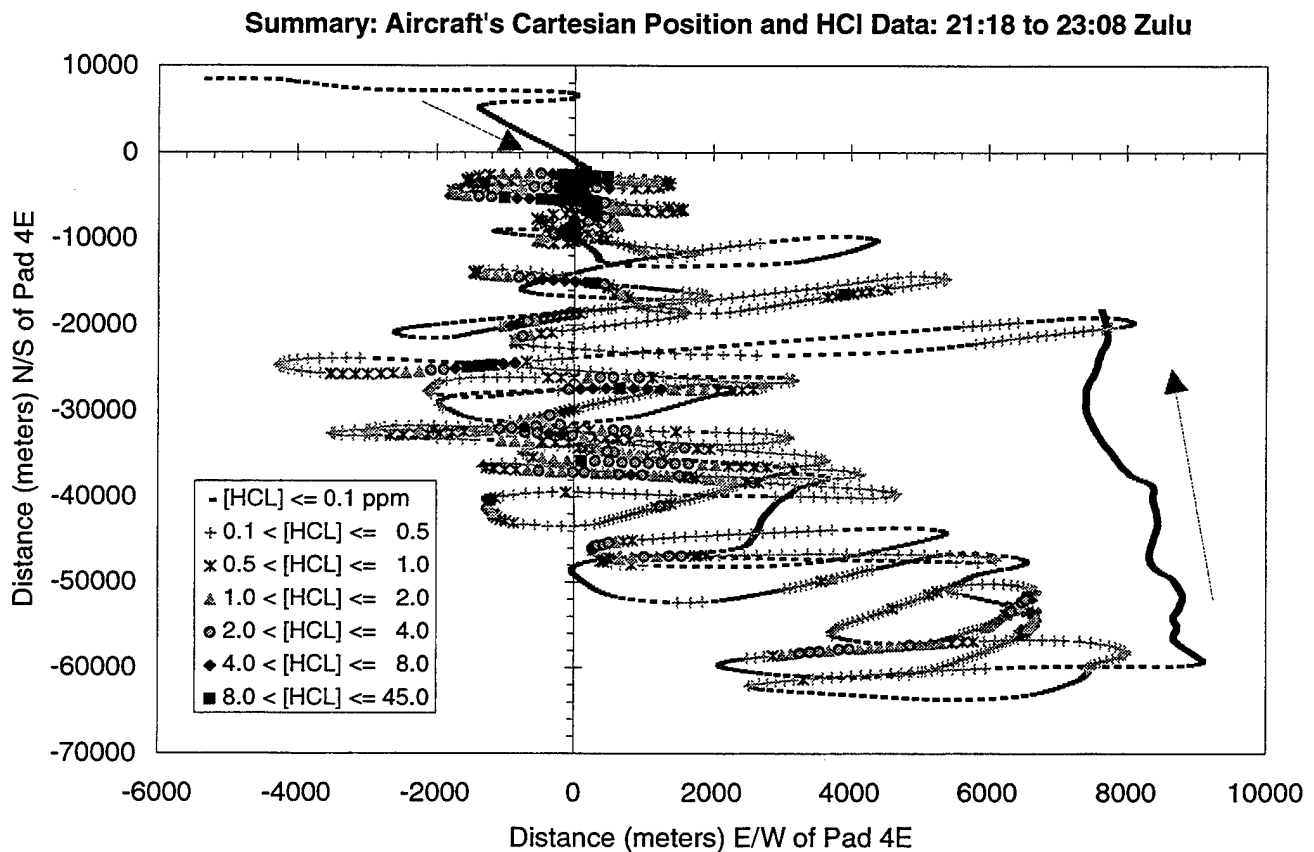


Figure 17. Cartesian plot documenting the aircraft's position relative to SLC-4E and the measured HCl concentration (based upon the Geomet detector) throughout the 110 min #K15 exhaust cloud sampling mission.

3.3.1.3 Geomet Detector Response to Calibration Gases

Figure 18 documents typical calibration gas response curves recorded using a data logger for the Geomet as deployed for the #K16 mission. The Geomet's configuration was equivalent for the #K23, #K15, K22, and #K16 missions. However, I-NET did not log the calibration response curves for the #K15 mission. Instead, for the #K15 calibrations, I-NET personnel merely noted the values of the plateau responses of the Geomet while being challenged against the calibration gas prior to the mission, subsequent to the mission with depleted reagent, and subsequent to the mission after recoating the inlet with reagent. For the #K15 mission, the plateau responses ranged from 0.92 V prior to launch, 0.585 V after launch (before recoating the inlet with reagent and with a -0.019 offset for zero air), and 0.662 V after recoating the inlet and rezeroing the detector. Therefore, the Geomet's plateau response to the calibration vapor degraded to 66% of its pre-flight value during the #K15 mission. Recoating the inlet with reagent recovered a few additional percent of the loss in response, yielding only 72% of the pre-flight value. This behavior is qualitatively consistent with the #K16 response curves in Figure 18.

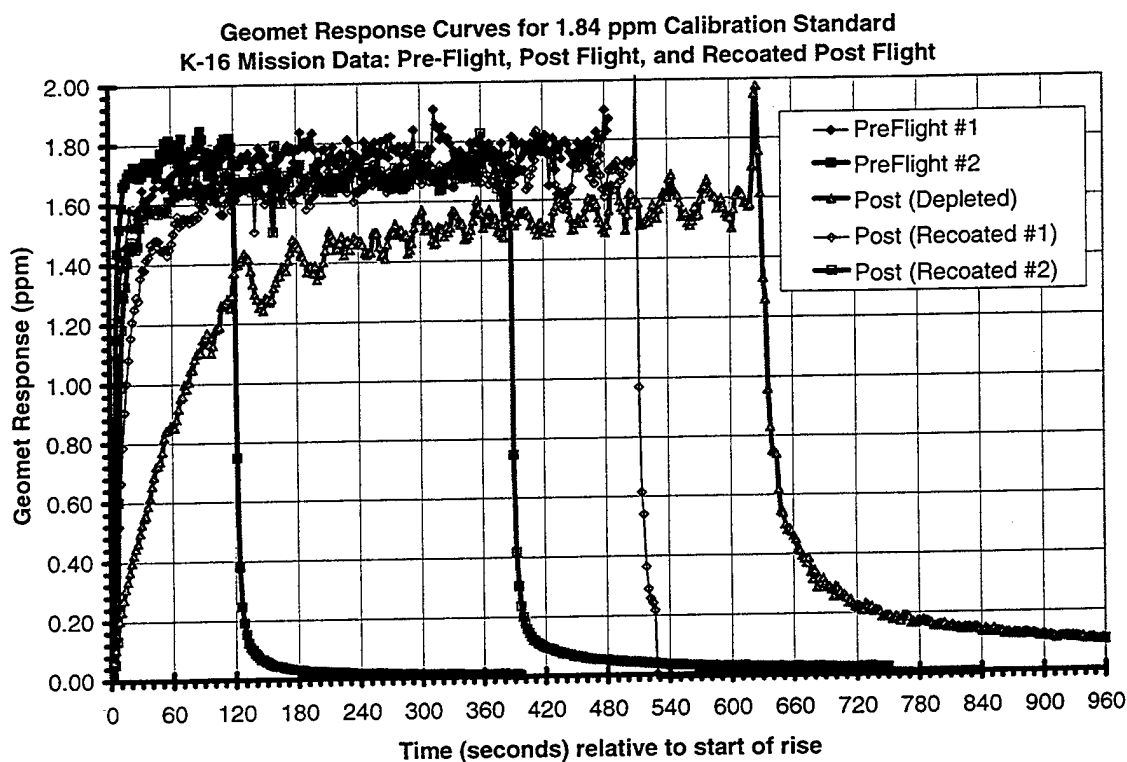


Figure 18. Geomet response curves illustrating rapid initial rise followed by rollover prior to reaching a plateau. These data are for #K16 mission that used a data logger to record the Geomet data. The identical hardware was used for the #K15 mission; however, the rise curves were not logged during field calibration. "Pre-Flight" #1 and #2 refer to the first and second exposure to the calibration gas after a single pre-flight coating of the inlet. Likewise, "Post (Recoated)" #1 & #2 refer to the first and second exposure to the calibration gas after washing and recoating the inlet after the flight (post-flight). "Post (Depleted)" refers to the exposure to the calibration gas after the flight (post-flight) but prior to washing and recoating of the inlet.

The data plotted in Figure 18 represent five challenges of the Geomet against a constant concentration of HCl vapor. For each challenge, the total exposure time can be calculated as the time between the start of the response to the calibration gas and the start of the fall at the end of the plateau. It is readily apparent that the exposure times were not a constant for these five calibrations. The inlet was coated with reagent prior to the first pre-flight calibration and after the post-flight challenge of the "reagent depleted" inlet to the calibration gas. It is apparent from Figure 18 that the post-flight "reagent depleted" inlet requires a longer time to reach a lower plateau response than any of the other challenges.

The response characteristics of the Geomet detector are not perfectly matched to aircraft sampling. As configured for Titan IV missions (#K23, #K15, #K16, and #K22) and as illustrated by Figure 18 (#K16 data), the Geomet requires more than 15 s to reach 90% of its plateau response as deployed for the Titan IV missions. Figure 18 documents that the response time changes as a result of exposure to HCl vapor (i.e., the second exposures were faster than the first exposures after coating the inlet). This is consistent with passivation of active sites within the freshly coated inlet. Figure 18 also documents that the magnitude of plateau response, as well as the time to reach it, can worsen when the exposure times are extremely long (as in the #K16 mission, which had an hour hold prior to extended sampling of the launch cloud). This is consistent with depletion of the reagent that coats the inlet. For all of the Titan IV missions, the Geomet's inlet was coated with reagent once prior to the flight. Therefore, one would expect some variation in response characteristics during each sampling mission.

Since the aircraft is moving at more than 70 m/s and it takes 15 (or more) seconds for the Geomet to provide 90% response to the new HCl concentration, it is likely that the Geomet may underestimate the maximum HCl concentration for short encounters with the cloud. However, Figure 18 illustrates that the initial response to 10% of the plateau response is extremely rapid. Thus, there should be little offset between the Geomet's first indication of change and the aircraft's encounter with the edge of the exhaust cloud. Therefore, we use the Geomet's HCl data to establish the position and relative strength of the exhaust cloud with the realization that the reported HCl concentration is an average value that depends upon the exposure history of the Geomet and the abruptness of HCl concentration changes.

In Figures 19 and 20, the Geomet's raw response and its integrated response are plotted against time for pre-flight and post-flight calibrations (data previously included in Figure 18). The integrated response is normalized in these figures to the total HCl dose (i.e., the total exposure time multiplied by the average value of the plateau response). The total HCl dose is the area under the square calibration exposure function (i.e., the Geomet is exposed to a constant concentration for a given period of time). The integrated Geomet response is the area under the actual Geomet calibration response curve (which includes the sharp initial rise, the slower rollover to plateau, the plateau, the sharp falloff after the exposure is ended, and the slow recovery to baseline). The normalized integrated response (plotted in Figures 19 and 20) is the integrated response divided by the total HCl dose. These plots document that the Geomet accurately integrates the total HCl dose for these HCl vapor exposures. Unfortunately, I-NET did not record all of the "tail" of the Geomet's response to the post-flight calibration. Therefore, we can only say that the integrated response accounted for more than 92% of the total dose for the post-flight "depleted" inlet. On the other hand, there is quantitative behavior (i.e., more than 98% of total dose) for the pre-flight challenges.

The Geomet calibrations are HCl vapor challenges using constant concentration for long exposure times. These data illustrate that the Geomet has an almost instantaneous response to sudden large changes in HCl vapor concentration but requires longer time to reach the plateau response. Therefore, the Geomet should accurately map the extent but not necessarily the strength of the Titan IV exhaust cloud.

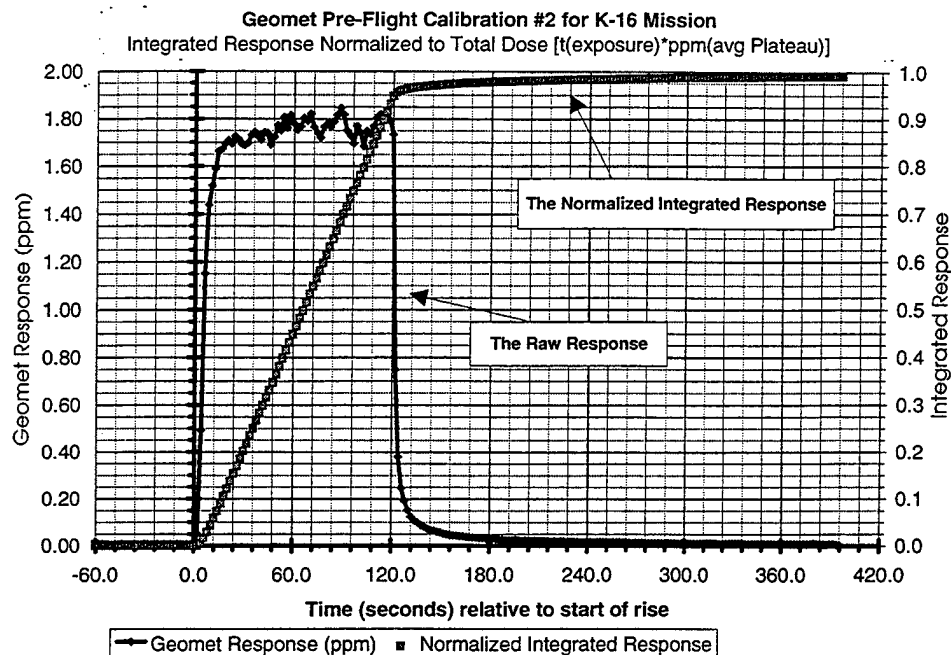


Figure 19. #K16 pre-flight raw and integrated response of the Geomet.

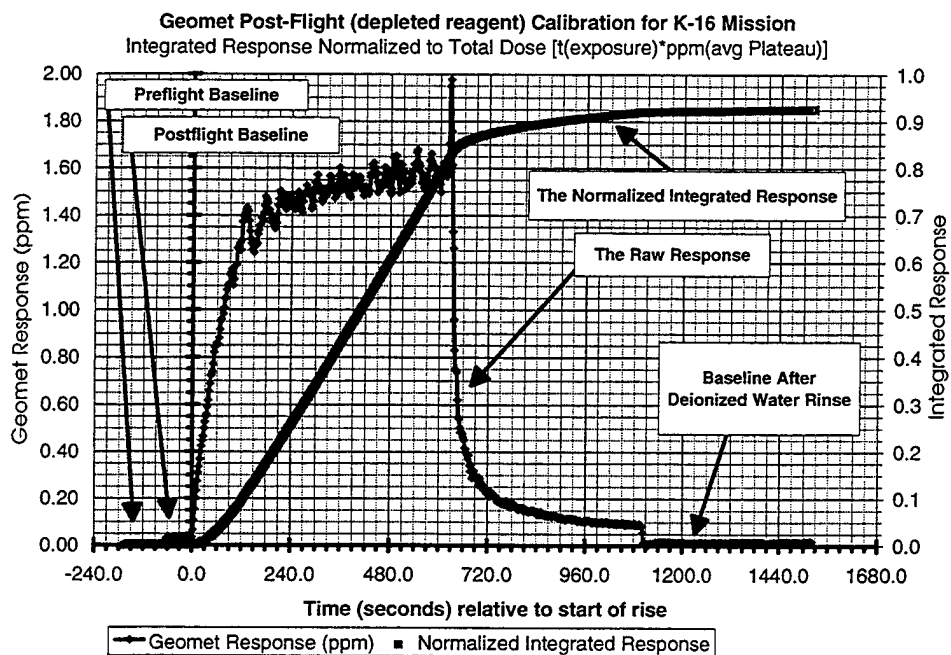


Figure 20. #K16 post-flight raw and integrated response of the Geomet.

3.3.1.4 Geomet vs GFC Response to the Titan IV #K15 Exhaust Cloud

The temporal, relative, and absolute accuracy of the Geomet's response to the Titan IV #K15 exhaust cloud is documented for the first few minutes after launch by comparison of the Geomet's cloud data to that of the Spectral Sciences gas filter correlation (GFC) spectrometer that flew on the same aircraft for the #K15 mission. The GFC spectrometer provided an instantaneous response to the exhaust cloud and was mounted beneath the aircraft. The inlet to the Geomet extended out of the front of the same aircraft.

Spectral Sciences provided a description of the GFC spectrometer setup, its calibration, and their analysis of the #K15 exhaust cloud data in Section 4. In that chapter, they documented that the GFC spectrometer's optics were irreversibly coated with exhaust cloud aerosols every pass through the cloud. This resulted in a dramatic decrease in signal-to-noise ratio with every encounter with a cloud. However, the GFC technique, as deployed for #K15, has an almost instantaneous response to HCl vapor since there was no inlet to their GFC cell (i.e., that's why it was directly exposed to the exhaust cloud). In future missions, Spectral Sciences will have to shield their optics from direct contact with the cloud.

In this section, we compare the GFC data (i.e., from Section 4) to the Geomet data to establish the significance of the Geomet's response characteristics for actual aircraft sampling of Titan IV #K15 exhaust cloud. This comparison documents excellent temporal agreement between the GFC spectrometer and the Geomet detector for actual exhaust cloud encounters. Due to the changing signal-to-noise ratio for the GFC spectrometer, there are only a few useful exhaust cloud encounters for the GFC technique. Considering these limited data, it appears that the Geomet provides reasonable response characteristics for mapping the location of the edges of the exhaust cloud. Therefore, the start of response upon entering the edge of the cloud and initial fall upon exiting the cloud should accurately map the extent of the cloud. This is consistent with the Geomet's rapid initial response to sudden changes in HCl concentration (i.e., the calibration data). These same comparisons document excellent positional accuracy for the maximum concentration reported by the Geomet relative to that recorded by the GFC technique. Therefore, the Geomet's 15-s rise time to 90% response does not seem to affect its temporal accuracy when chasing Titan IV launch clouds. Instead, the Geomet's fast initial response to significant changes seems to make it useful for mapping the position and shape of Titan IV launch clouds.

The GFC spectrometer data in Section 4 included raw and averaged GFC spectrometer data. For comparison to the Geomet, we will include the GFC data after using a moving 11-point average to smooth the data (3.85 s average). As illustrated in Section 4, this averaging results in almost a factor of 5 attenuation in the peak response of the GFC data for the #K15 mission. However, it also provided a significant increase in signal-to-noise for detecting the exhaust cloud encounters. In addition to the averaged GFC data, we also compare the filtered GFC results. As discussed in Section 4, each encounter with a cloud coated the optics (reduced light throughput) and was detectable as a temperature fluctuation. Spectral Sciences used the temperature sensor data to filter GFC data for times when an exhaust cloud encounter was probable. This filtered data correlates with the Geomet's encounters with the exhaust cloud, suggesting a useful method for reducing false hits by the noisy GFC technique. However, the Geomet's HCl concentrations are about 50% of those measured by the 3.85 s averaged and filtered GFC technique. This is a believable result considering the short encounter times with the exhaust cloud and relatively long response times for the Geomet. Indeed, the Geomet

response matches that of the GFC technique when using longer averaging times (18 s average). Since the Geomet has both fast and slow components of response, it appears that the Geomet is able to accurately map the extent and shape of the exhaust cloud by virtue of its fast response to large changes in concentration.

Figure 21 overlays the aircraft's GFC data (after application of a 3.85-s moving average) with the aircraft's raw Geomet data in a plot of HCl concentration versus time after launch for the #K15 mission. In Figure 21, the GFC data is plotted on an axis using 90 ppm HCl as full scale, while the Geomet data is plotted using 45 ppm as full scale. Figure 21 documents that the Geomet and the GFC spectrometer provided good temporal agreement for the position and relative shape of the HCl concentration profiles at early times (i.e., up to 6 min after the launch). As discussed by Spectral Sciences in their report, the optics of the GFC spectrometer were coated with each encounter with the exhaust cloud resulting in dramatic decreases in signal-to-noise ratio (S/N) with each encounter. Considering the relative response of the GFC and the Geomet to the HCl at 5 min, there was approximately a factor of 2 difference in the magnitudes of their responses at early times. Since the HCl concentrations change rapidly as the aircraft passes through the exhaust cloud at 70 m/s, and the Geomet has a documented 15-s rise time to obtain 90% response, it is reasonable that the GFC data averaged with a 3.85-s period documents higher concentration than the Geomet, which has a longer effective averaging time. As the optics coated, the S/N decayed, and the GFC data quickly became useless (i.e., provided false hits) as revealed by large noise spikes between the exhaust cloud encounters (see Geomet peaks) after 6.5 min. The tail on the Geomet peaks is consistent with the tail (i.e., slow recovery to baseline) observed during challenges against calibration vapors as documented by Figures 18–20.

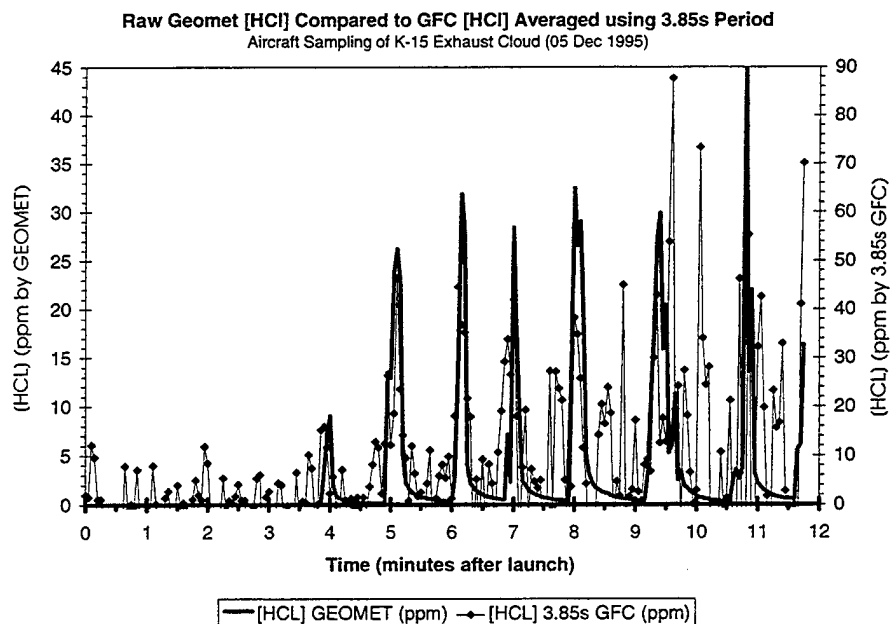


Figure 21. Comparison of the #K15 exhaust cloud HCl concentration data obtained by the aircraft's two sensors: (1) the Geomet Chemiluminescent Detector and (2) the Spectral Sciences GFC Spectrometer. Note the dramatic decrease in S/N for the GFC spectrometer at later times (greater than 6.5 min) and the coincident peaks from the two detectors at early times (less than 6.5 min). The tail on the Geomet peaks is consistent with calibration data.

Figure 22 presents a subset of the data presented in Figure 21 and includes only the GFC data identified by Spectral Sciences as being possible exhaust cloud encounters. As detailed in Section 4 and discussed in this section, Spectral Sciences filtered the GFC data using other evidence of exhaust cloud encounters. The evidence included the degradation in transmission through the optics with each encounter and measurable temperature changes with each encounter. In Figure 22, the GFC data is plotted on an axis using 70 ppm HCl as full scale, while the Geomet data is plotted using 35 ppm as full scale. As illustrated previously by Figure 21, the data in Figure 22 document that the Geomet and the filtered GFC data provided good temporal agreement for the position and relative shape of the HCl concentration profiles at times up to 8 min after the launch. In addition, the data in Figure 22 document that Spectral Sciences successfully filtered the GFC noise spikes that complicated Figure 21 at times past 6.5 min. The peak in HCl concentration at 5 min illustrates almost perfect coincidence for the two detectors and represents the best S/N for the GFC spectrometer. There is a factor of 2 difference in peak response for this measurement. Careful comparison of these data reveals no shift in time between the maximum concentration reported by the GFC spectrometer for encounter 2 (E2) and the maximum reported by the Geomet detector. A 6-12-s shift in time would have corresponded to a 0.5-1 km shift in position for the maximum of the cloud based upon a 70 m/s aircraft speed. The width (i.e., onset of rise and start of fall) is identical for the Geomet and for the GFC spectrometer for this encounter. This is consistent with good edge detection by both detectors.

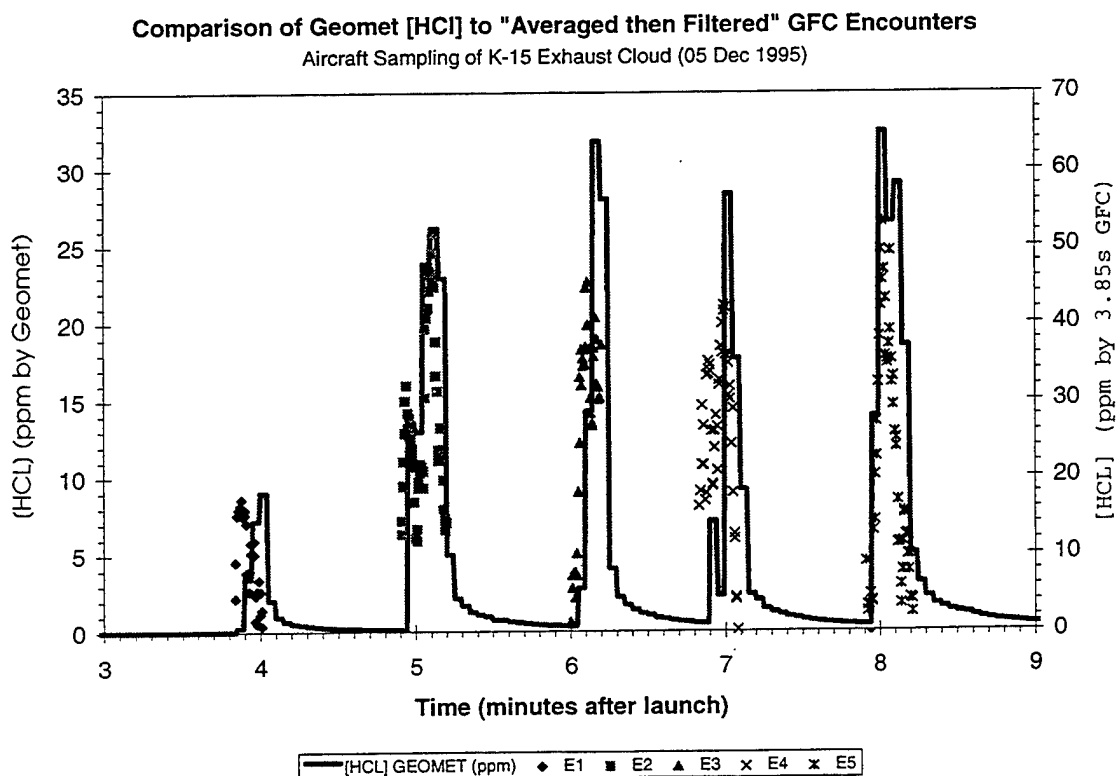


Figure 22. Comparison of the #K15 exhaust cloud HCl concentration data obtained by the aircraft's Geomet chemiluminescent detector with the Spectral Sciences GFC spectrometer's encounter data. Note the coincidence between the Geomet's HCl concentration peaks and the Spectral Sciences GFC spectrometer's encounters with the Titan IV #K15 Exhaust cloud.

Figure 23 is a Cartesian plot of the aircraft's position relative to the launch pad during the first three encounters with the Titan IV #K15 exhaust cloud. Each sampling point is labeled to indicate a "hit" or "miss" by each of the HCl detectors (i.e., the Geomet chemiluminescent detector and the Spectral Sciences GFC spectrometer). As expected, the GFC "hits" are initially coincident within the Geomet "hits." At later times when the GFC became very noisy, it started reporting apparent "hits" (i.e., concentrations greater than 20 ppm) even when outside of the cloud. Since the Geomet is much quieter (i.e., less noisy), we used a 2 ppm threshold for identifying its "hits."

Figure 23 is included with the intent of mapping the distances associated with the data plotted in Figures 21, 22, and 24. Encounters 2 and 3 correspond to a cloud encounter lasting just over 1000 m along the aircraft's trajectory. For encounter 2, the thresholds used in Figure 23 document the same location for the cloud by both detectors. However, one can see that the noisy GFC response bounces above and below the threshold while within the cloud. For encounter 3, the thresholds used in Figure 23 document the same location for the cloud by both detectors. However, the lower threshold for the Geomet reveals the cloud as wider than mapped by the noisy GFC technique that required a higher setting for its threshold. As discussed in Section 4, the GFC noise increased dramatically with each encounter with the exhaust cloud. After the third encounter, the GFC detector's noise level grew above the 20 ppm threshold used to label "hits" in Figure 23. Therefore, some noisy GFC data appears outside of Geomet data. As mentioned previously in this section and later in Section 4, these noise spikes can be filtered by using other evidence for cloud encounters, such as coating of the optics and temperature fluctuations.

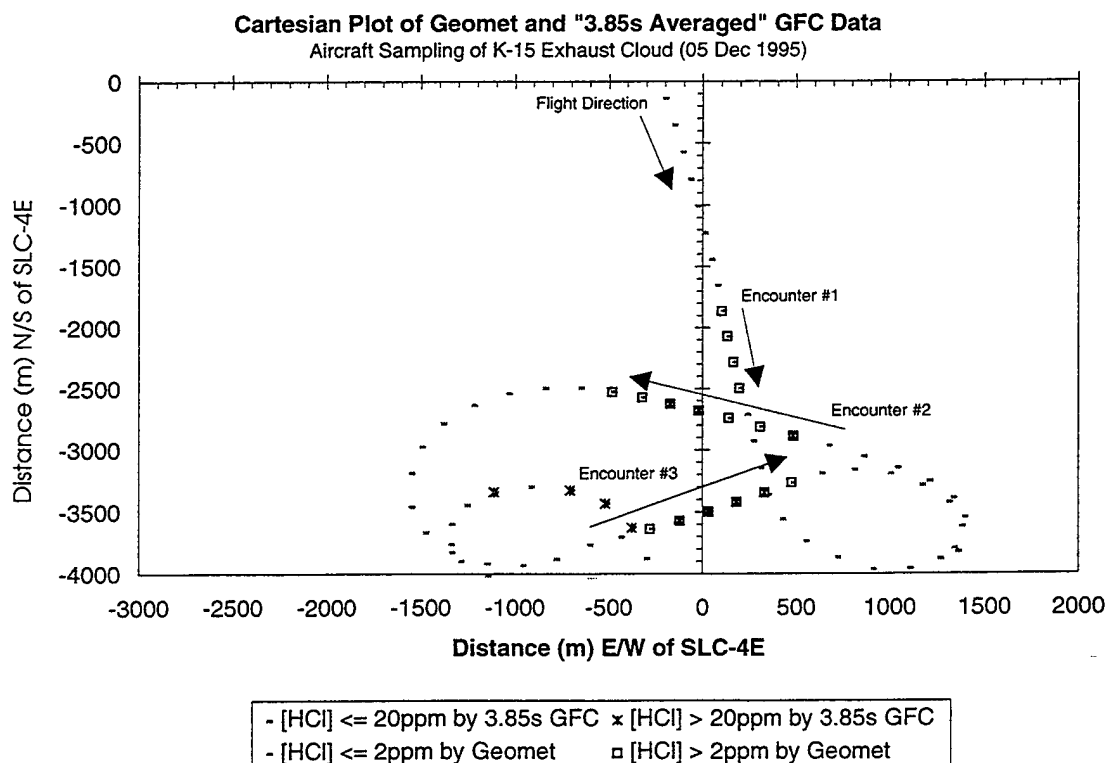


Figure 23. Cartesian plot of 3.85s averaged (unfiltered) GFC spectrometer and raw Geomet data collected by the aircraft while searching for the #K15 exhaust cloud.

Figure 24 documents the effect of averaging time upon the comparison of GFC to Geomet data. In Figure 24, the HCl concentration is plotted against time for encounter 2 with the #K15 ground cloud. The HCl concentration is derived in three ways: (1) Geomet response, (2) 3.85-s averaging of the GFC data, and (3) 18-s averaging of the GFC data. The 3.85-s GFC data and the Geomet data were plotted in Figures 21, 22, and 23. We previously discussed the excellent temporal (i.e., positional) agreement between the 3.85-s GFC data and the Geomet data. Both sets of HCl concentration data map the edges and the maximum of the cloud to the same locations in time and space. Figure 24 reveals this comparison in greater detail and adds 18-s GFC data. The 18-s GFC data reports the same value for the maximum HCl concentration as the Geomet data but does not agree with the Geomet's temporal (i.e., positional) mapping of the cloud. We believe that the data in Figure 24 are consistent with the Geomet's documented two-part response curve: (1) rapid initial response to a change in HCl concentration and (2) a slower rollover in response prior to reaching a plateau. Figure 24 documents that the Geomet's fast component allows it to map the extent and position of the launch cloud as well as 3.85-s averaged GFC data. The GFC data had to be averaged with an 18-s period to equal the Geomet's maximum response, which is consistent with the longer times required for full Geomet response. Since the GFC technique only responds to vapor, while the Geomet responds to total (aerosol and vapor) HCl, this treatment cannot provide quantitative rise characteristics for the Geomet. In addition, the noisy GFC data may overestimate the integrated HCl (i.e., bigger area than Geomet). Therefore, in addition to providing quantitative integrated HCl for each pass through the cloud, the Geomet accurately maps the extent and position of the cloud by virtue of the fast component of its complicated response function.

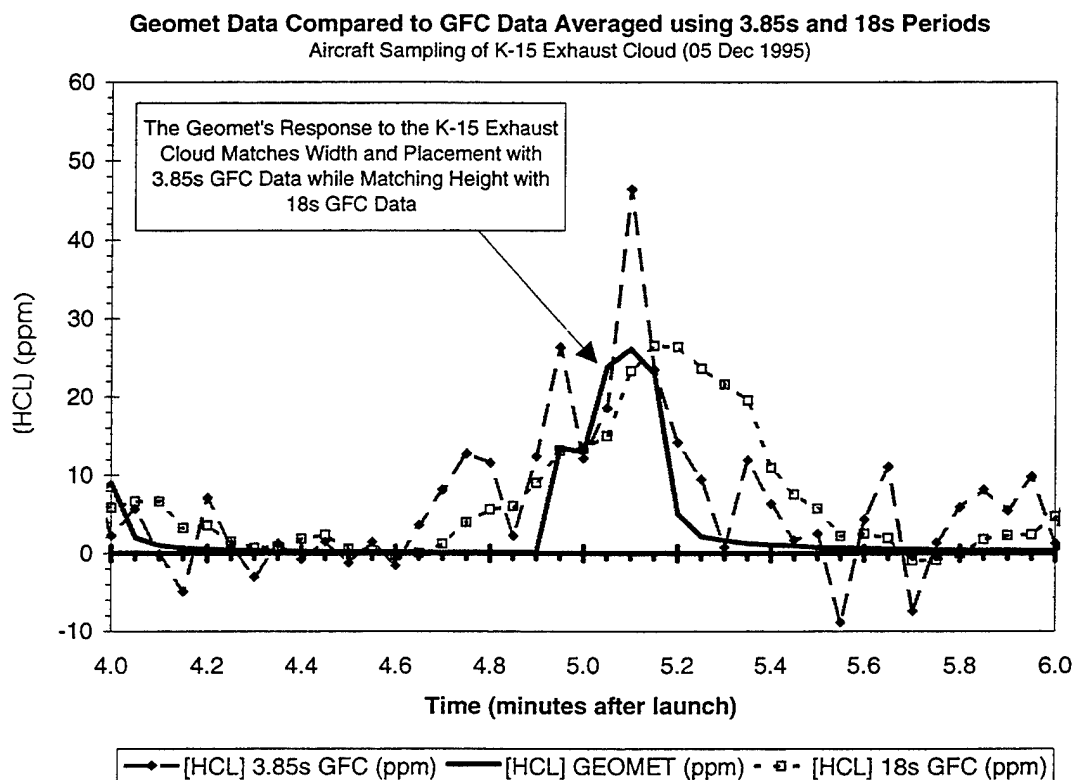


Figure 24. Effect of averaging time on GFC spectrometer data and comparison with the raw Geomet data for the #K15 exhaust cloud.

3.3.2. HCl Concentration Hits as a Function of Bearing from SLC-4E

Figure 25 substantiates that the aircraft focused on a modest range of polar angles relative to the launch complex. In this report, the angles reported will conform to the convention of rawinsonde wind vectors (the angle from which the wind originates that would push the cloud to the sampled position). Thus, the angles are related by

$$J = 180 + F,$$

where ϑ is the equivalent rawinsonde wind angle, and Φ is the measured polar angle of the aircraft relative to SLC-4E and clockwise of true north. For example, when the aircraft is due east of SLC-4E, Φ is 90° , and ϑ is 270° . The nominal trajectory of the ground cloud during the first 11 min after launch was shown by imagery to be 8° in the previous report (Section 2) and in Figure 16. The T-0.25 hour rawinsonde wind vectors at the bottom, middle, and top of the observable ground cloud were 17° , 26° , and 358° , respectively, as documented in Figure 16. Referring to Figure 25, we will document that these data are consistent with the movement of the ground cloud to the south, initially, and, at later times, to the southeast relative to SLC-4E. It is our conclusion that these HCl hits derive from sampling of the ground cloud as it is defined by REEDM and visualized by imagery.

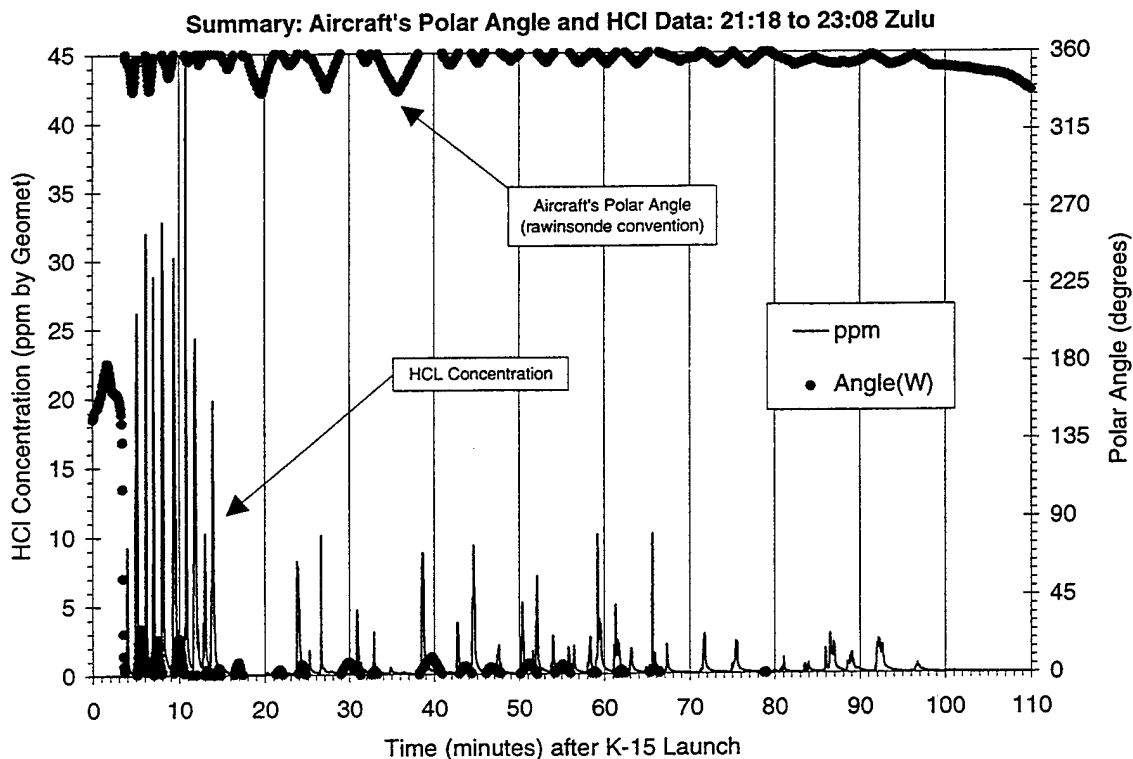


Figure 25. Summary of the aircraft's HCl concentration measurements and its polar angles (rawinsonde convention) plotted against time (minutes) after the Titan IV #K15 launch. This plot documents that the cloud was to the south and southeast of SLC-4E.

3.3.3. HCl Concentration Hits as a Function of Radial Distance from SLC-4E

Figure 26 is a plot of the HCl concentration and the aircraft's radial distance from SLC-4E against time after launch. Figure 26 can be used to illustrate several logical conclusions regarding the aircraft's sampling campaign. The highest HCl concentrations are encountered at early times and near (<10 km) to the launch complex. However, significant HCl concentrations (2–10 ppm) were observed at later times and at ranges of 10 to 60 km from SLC-4E. The most remote detection of the ground cloud occurred more than 95 min after launch and approximately 60 km from SLC-4E launch pad. All HCl hits, both initially and after downwind dispersion, were observed to the south and southeast of SLC-4E, as discussed in the previous section. As shown in Figure 27 and discussed below, all aircraft sampling was at altitudes below 1000 m according to the GPS receiver. As documented in later discussions and Figures 27–32, the bulk of the HCl was at altitudes greater than 400 m according to the GPS receiver.

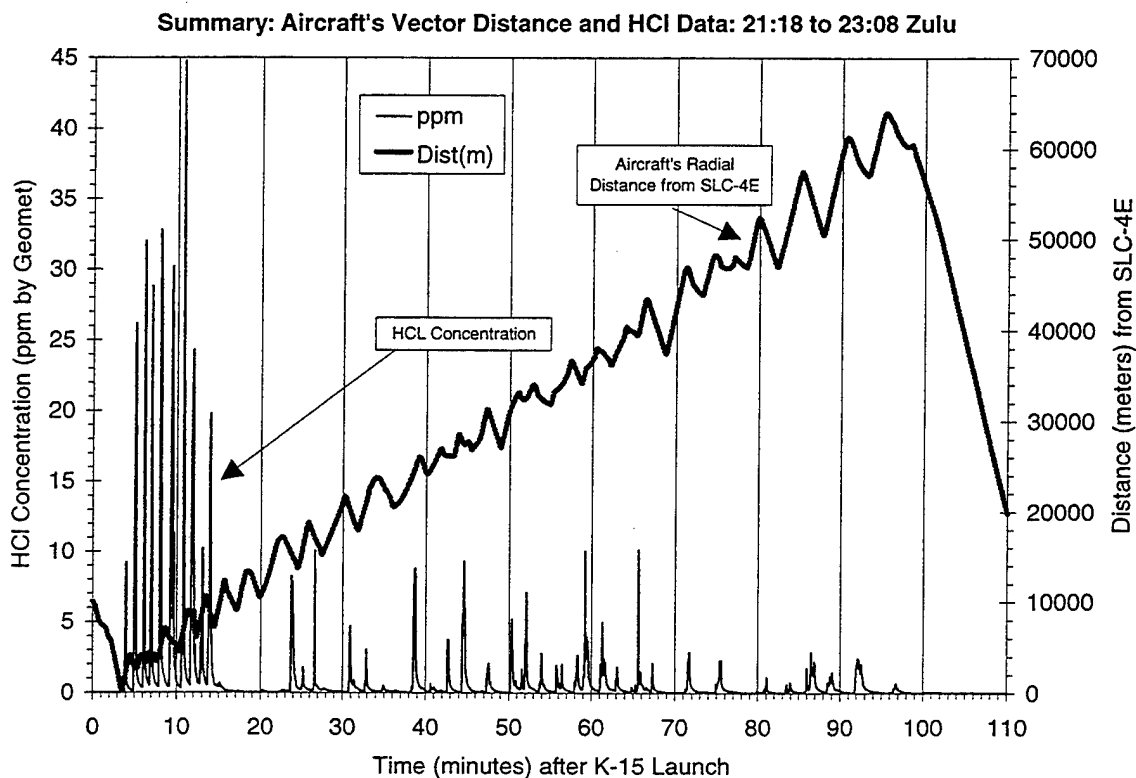


Figure 26. Summary of the aircraft's HCl concentration measurements and radial distances (m) from SLC-4E plotted against time (min) after the Titan IV #K15 launch.

3.3.4. HCl Concentration Hits as a Function of Altitude

Figure 27 is a plot of the HCl concentration and the aircraft's GPS altitude against time after launch. Figure 27 documents that at early times (i.e., 4–11 min after launch) the HCl hits are at altitudes between 500 and 1000 m by GPS, which is consistent with the extent of the ground cloud as revealed by the imagery (Section 2) during that same period. The imagery revealed that the top of the ground cloud stabilized within 3 to 5 min at an altitude of 1327 m MSL (± 98 m). The imagery documented that the bottom of the cloud continued to rise throughout the 11 min of monitoring and stabilized at 536 m MSL (± 31 m). Given the altitude range, radial distance range, and polar angle range covered by the aircraft in the time period of 10–110 min, it is not surprising that so many HCl hits were observed. Examination of Figure 20 shows that the pilot concentrated on altitudes (~ 400 to 800 m by GPS) near the bottom to middle of the visible cloud as documented by the 0–11 min imagery data (Section 2). As noted in Figure 16, T–0.25 hour rawinsonde wind vectors at the altitudes (536 to 1327 m MSL) reached by the stabilized ground cloud (i.e., revealed by imagery) ranged between 17° and 358° (i.e. consistent with the aircraft's HCl data).

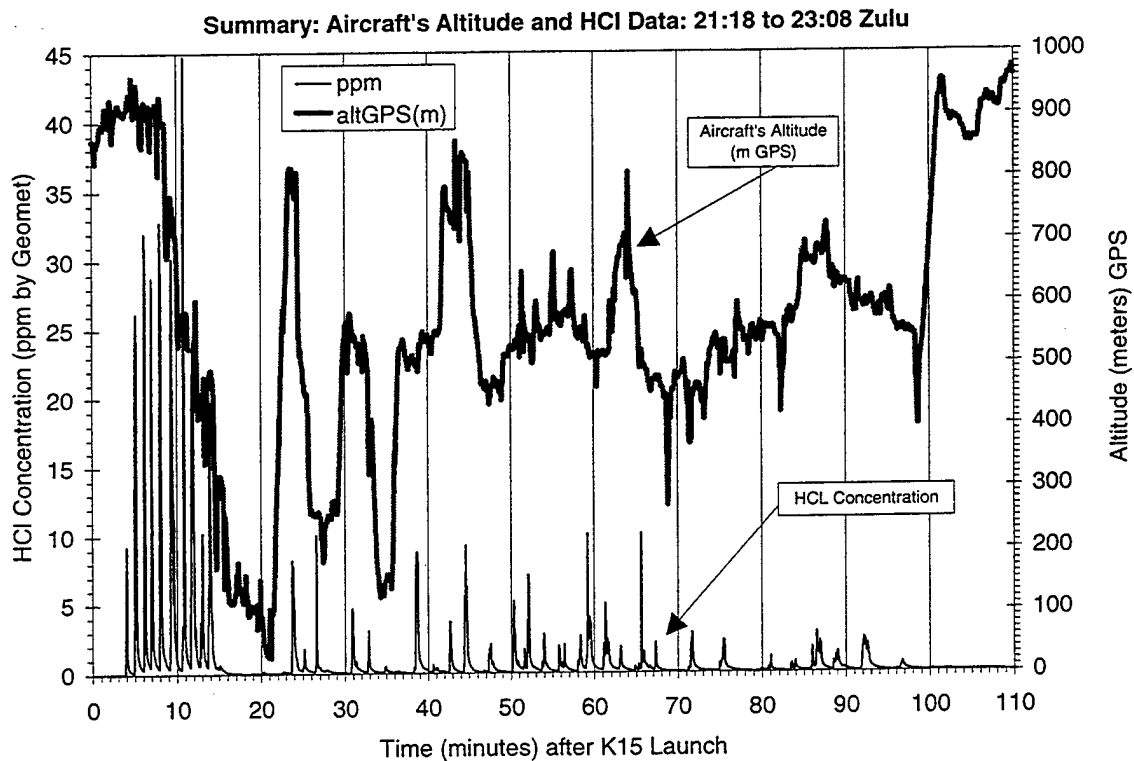


Figure 27. Summary of the aircraft's HCl concentration measurements and altitude (m) plotted against time (minutes) after the Titan IV #K15 launch.

3.3.5. HCl Concentration Hits as a Function of Altitude and Aircraft Position

This section will provide substantiation for observations made in previous portions of this overview of the aircraft's sampling data. The figures referenced in this section are subsets of the data presented in the Cartesian plot in Figure 17.

3.3.5.1. HCl Hits at Altitudes Greater than 800 m and Less than 1000 m

Figure 28 is a Cartesian plot, centered at SLC-4E, of the aircraft's sampling data collected at altitudes between 800 and 1000 m by GPS. The aircraft's HCl concentration profiles document a southerly trajectory for the cloud at these high altitudes. The early data can be directly compared to the imagery data collected during the first 11 min after launch. The imagery not only documented a southerly trajectory for the cloud but also reported stabilization heights of 536, 811, and 1327 m MSL for the bottom, middle, and the top, respectively, of the ground cloud. Therefore, the aircraft's data presented in Figure 28 represent sampling in the top half of the stabilized ground cloud (as defined by imagery).

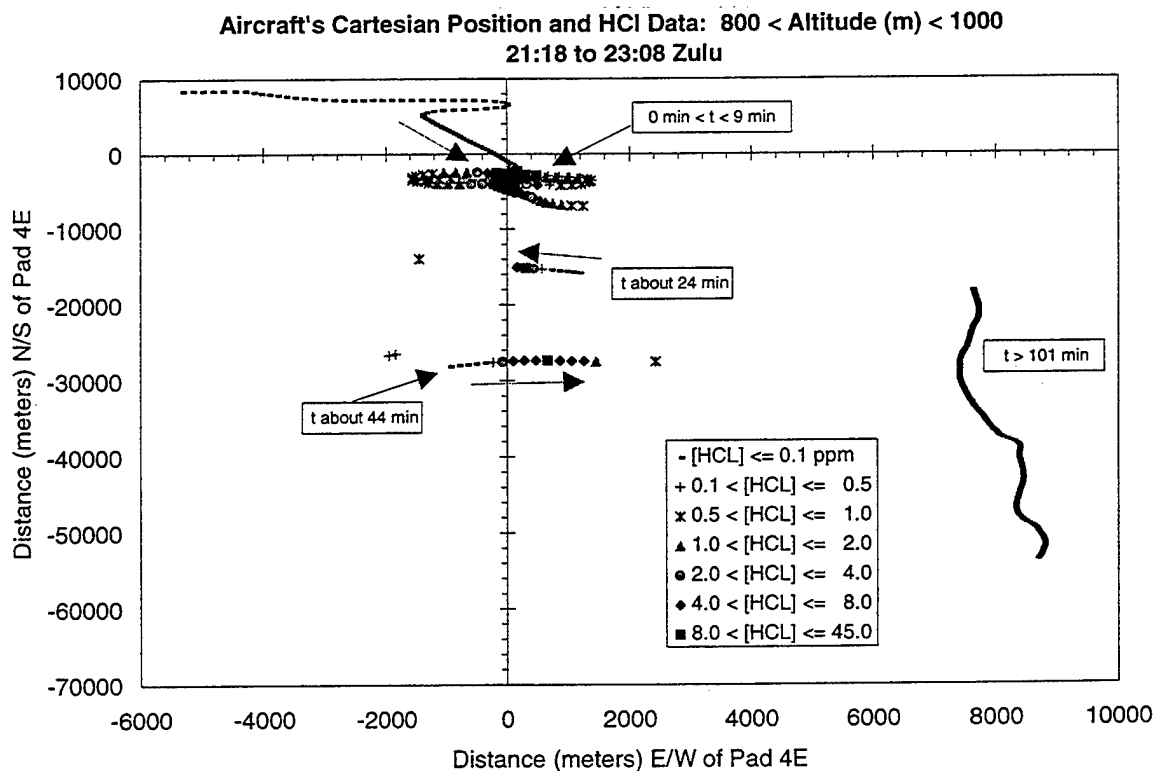


Figure 28. Summary Cartesian plot documenting the aircraft's position and measured HCl concentrations while sampling at altitudes between 800 to 1000 m by GPS after the Titan IV #K15 launch. These data document a southerly cloud track at altitudes within the top half of the ground cloud. For comparison, the imagery-derived altitudes were 536, 811, and 1327 m MSL for the bottom, middle, and top, respectively, of the stabilized cloud on a southerly track.

3.3.5.2 HCI Hits at Altitudes Less than 800 m and Greater than 600 m

Figure 29 is a Cartesian plot, centered at SLC-4E, of the aircraft's sampling data collected at altitudes between 600 and 800 m by GPS. The HCI concentration profiles document a southerly track at early times (up to 25 min). These early data are consistent with the higher altitude data (i.e., Figure 28) and with the imagery data (Section 2) collected during the first 11 min after launch. However, the HCI concentration profiles in Figure 29 are along a more southeasterly track at later times, suggesting a shift in trajectory. The aircraft did not sample these distances at the higher altitudes (i.e., in Figure 28). The imagery-derived altitudes (measured 4–11 min after launch) were 536, 811, and 1327 m MSL for the bottom, middle, and top of the stabilized ground cloud along a southerly track. Therefore, the aircraft data presented in Figure 29 represent sampling at or slightly below the center of the ground cloud (as defined by imagery). The rawinsonde data near the middle of the imaged cloud is from 26°, which would push the cloud to the southwest as observed at early times. At later times, the cloud moves in a southeasterly direction closer to the 344° predicted by REEDM for the second transition layer.

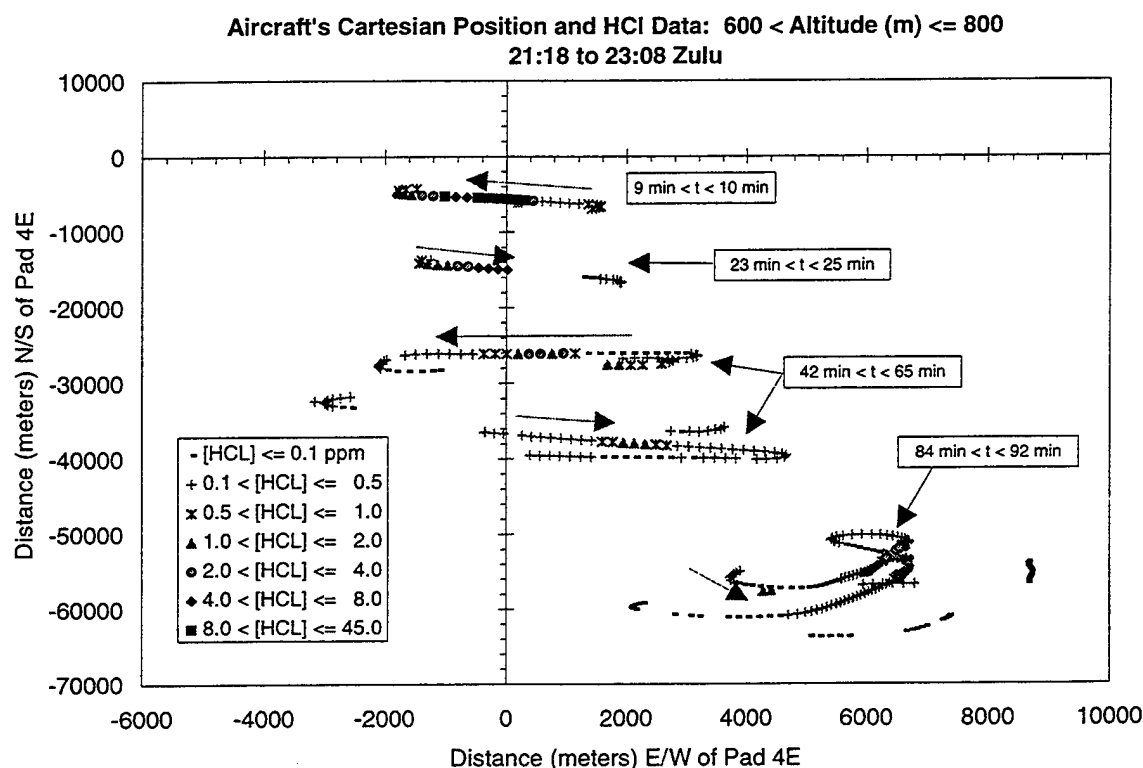


Figure 29. Summary Cartesian plot documenting the aircraft's position and measured HCI concentrations while sampling at altitudes between 600 and 800 m by GPS after the Titan IV #K15 launch. These data document a shift in cloud trajectory at later times. For comparison, the imagery-derived altitudes were 536, 811, and 1327 m MSL for the bottom, middle, and top, respectively, of the stabilized cloud on a southerly track (4–11 min after launch). Therefore, these aircraft data are collected at altitudes at and slightly below the altitude of the center of the initially stabilized ground cloud.

3.3.5.3 HCI Hits at Altitudes Less than 600 m and Greater than 400 m

Figure 30 is a Cartesian plot, centered at SLC-4E, of the aircraft's sampling data collected at altitudes between 400 and 600 m by GPS. The aircraft's HCI concentration profiles at these altitudes document an initial southerly track that shifts to a southeasterly track at later times. Therefore, these data are consistent with higher-altitude data in Figures 28 and 29. The imagery-derived altitudes (measured 4–11 min after launch) were 536, 811, and 1327 m MSL for the bottom, middle, and top, respectively, of the stabilized ground cloud along a southerly track. The aircraft data in Figure 30 represent sampling near the bottom of the ground cloud. The aircraft data collected at early times are consistent with the southerly track derived from imagery during the first 11 min after launch.

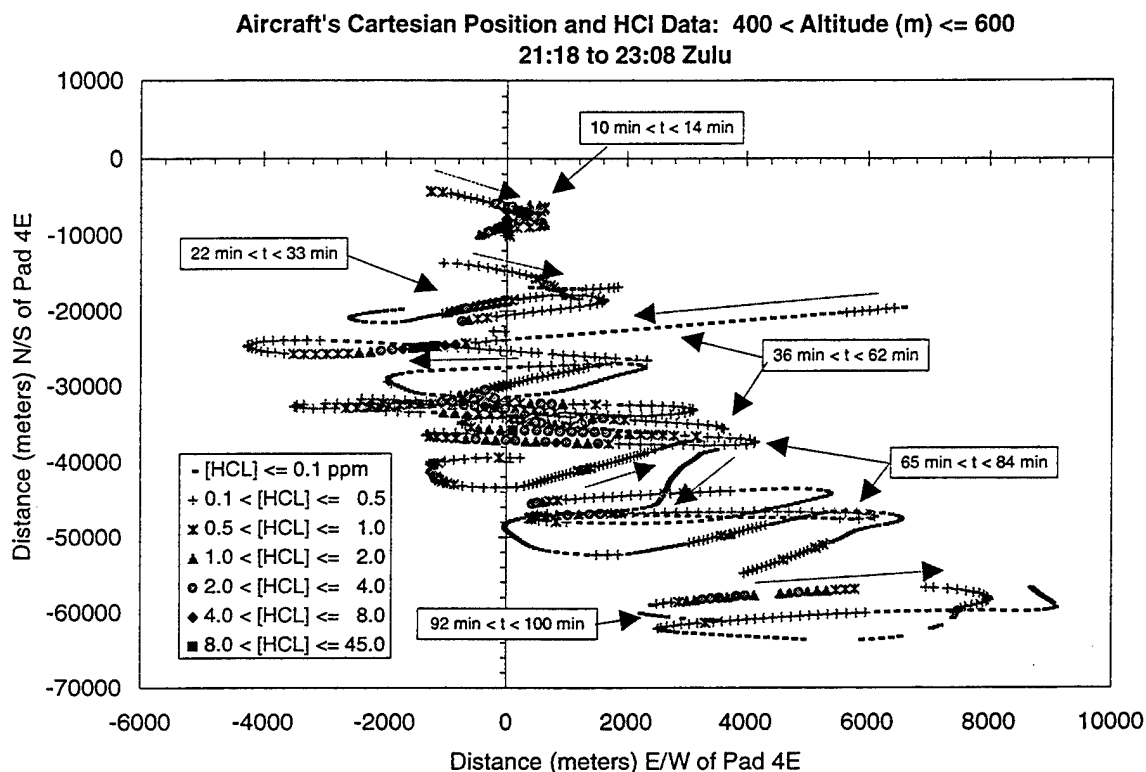


Figure 30. Summary Cartesian plot documenting the aircraft's position and measured HCI concentrations while sampling at altitudes between 400 to 600 m by GPS after the Titan IV #K15 launch. These data document a shift in cloud trajectory from southerly at early times to southeasterly at later times. For comparison, the imagery-derived altitudes were 536, 811, and 1327 m MSL for the bottom, middle, and top, respectively, of the stabilized cloud on a southerly track (4–11 min after launch). Therefore, these aircraft data are collected at altitudes near the bottom of the initially stabilized ground cloud.

3.3.5.4. HCI Hits at Altitudes Less than 400 m and Greater than 200 m

Figure 31 is a Cartesian plot, centered at SLC-4E, of the aircraft's sampling data collected at altitudes between 200 and 400 m by GPS. At early times, these data document the same southerly track that was observed by the imagery (0–11 min) and at higher altitudes (Figures 28–30). At later times, the data show a dramatic shift in cloud trajectory to the southeast at much earlier times than observed at higher altitudes (Figures 28–30). Since the imagery documented a stabilization height of 536 m MSL for the bottom of the ground cloud, the aircraft data in Figure 31 represent sampling below the bottom of the imagery-defined ground cloud. One should remember two things when comparing the aircraft and imagery data: (1) the GPS altitude could be off by ± 250 m, and (2) the aircraft sampled for longer times than available by imagery. In addition, the absolute error in GPS position fluctuates as a function of time and can result in discontinuities in plots that use altitude as a filter. We believe such GPS fluctuations have shifted some of the higher-altitude cloud sampling data into Figure 31 as incomplete aircraft passes. In several cases, only a few contiguous points are registered in this figure, while the rest of the encounter is documented in the next higher altitude range (i.e., in Figure 30).

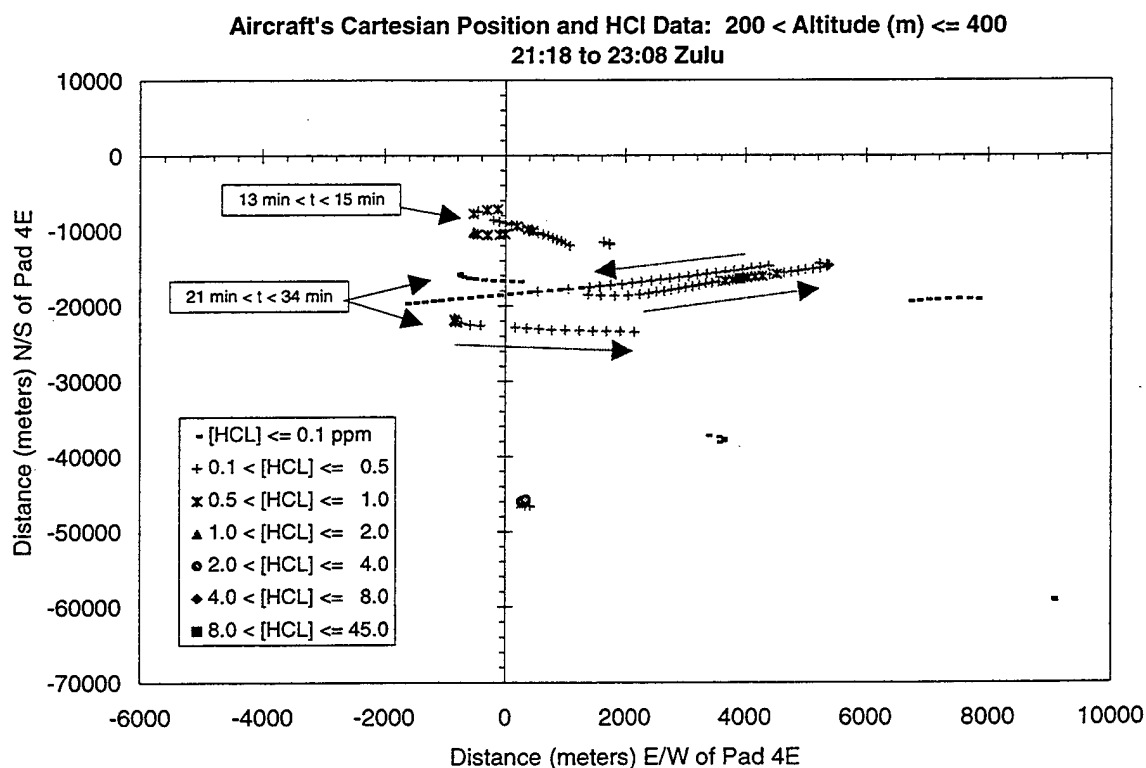


Figure 31. Summary Cartesian plot documenting the aircraft's position and measured HCI concentrations while sampling at altitudes between 200 to 400 m by GPS after the Titan IV #K15 launch. The cloud track appears to be much more southeasterly than documented by the aircraft data at higher altitudes. For comparison, the imagery-derived altitudes were 536, 811, and 1327 m MSL for the bottom, middle, and top, respectively, of the stabilized cloud on a southerly track (4–11 min after launch). Therefore, these aircraft data are collected at altitudes below the altitude of the bottom of the initially stabilized ground cloud.

3.3.5.5. HCI Hits at Altitudes Less than 200 m

Figure 32 is a Cartesian plot, centered at SLC-4E, of the aircraft's sampling data collected at altitudes between 25 and 200 m by GPS. The aircraft's HCI concentration profiles at these altitudes document both southerly (strong and narrow) and southeasterly (weak and broad) cloud tracks at early times. The strongest hits, at these extremely low altitudes, are along a southerly trajectory consistent with the early aircraft data and imagery. The weaker and broader southeasterly hits (i.e., 150 m by GPS, 344° bearing, and 34–36 min after launch) document a much stronger shift to the southeast than observed at higher altitudes at these distances and times. Therefore, the aircraft data in Figure 32 are consistent with a strong altitude-dependent shear in cloud trajectory. Since the imagery documented a stabilization height of 536 m MSL for the bottom of the ground cloud, these aircraft data represent sampling below the bottom of the imagery-defined ground cloud. The imagery also documented a shear in cloud trajectory with altitude that resulted in a sideways V shape for the cloud at later times.

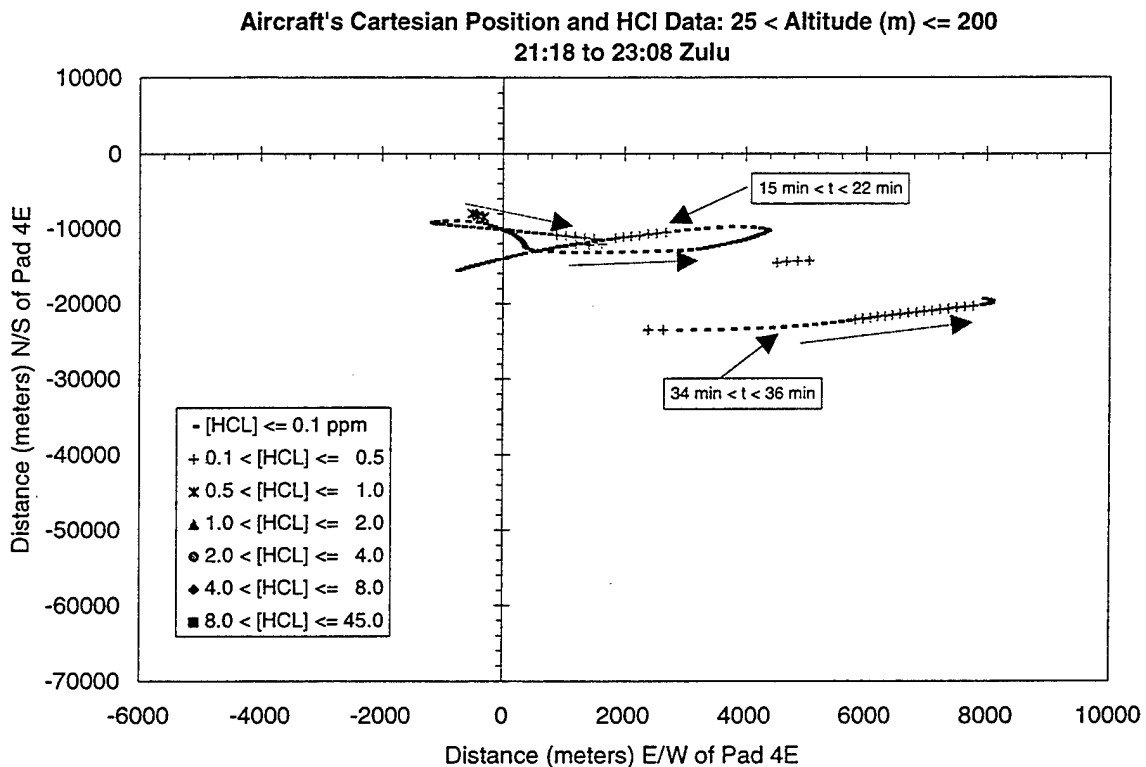


Figure 32. Summary Cartesian plot documenting the aircraft's position and measured HCI concentrations while sampling at altitudes below 200 m by GPS after the Titan IV #K15 launch. These data document a narrow concentrated cloud along a southerly track at early times and a broad dilute cloud along a southeasterly track at later times. The southeasterly shift occurred at much earlier times than observed at higher altitudes. For comparison, the imagery-derived altitude was 536 m MSL for the bottom of the stabilized cloud on a southerly track (4–11 min after launch). Therefore, these aircraft data are collected at altitudes below the altitude of the bottom of the initially stabilized ground cloud.

3.4 Conclusions

The aircraft's Geomet total HCl detector monitored the ground cloud from the Titan IV #K15 launch and obtained a large quantity of HCl concentration data as a function of time and aircraft position. The aircraft's HCl concentration data documented a shifting trajectory for the launch's ground cloud. At early times (4–20 min), the aircraft documented a southerly trajectory that was consistent with the imagery-derived cloud track and with REEDM's prediction for the rising ground cloud. At later times, the aircraft documented a shift in trajectory towards the southeast, which was consistent with REEDM's prediction for times after stabilization. This trend was reproduced by aircraft sampling at various altitudes between 400 and 1000 m by GPS. For comparison, the imagery-derived altitudes for the bottom, middle, and top of the ground cloud were 536, 811, and 1327 m, respectively, along a southerly track. Therefore, most of the aircraft's HCl measurements were at altitudes within the stabilized ground cloud (as defined by imagery during the first 11 min after launch). One should remember two things when comparing the aircraft and imagery data: (1) the GPS altitude could be off by ± 250 m, and (2) the aircraft sampled for longer times than available by imagery. The aircraft also sampled at altitudes below 400 m by GPS. These low-altitude data document a shift in cloud trajectory below 400 m. These data suggest that the lowest altitude portion of the ground cloud moved to the southeast faster than the bulk of the ground cloud (i.e., above 400 m by GPS).

The aircraft's data document measurable levels of HCl to altitudes as low as 150 m by GPS. The aircraft's data includes HCl detection at times greater than 95 min after the launch and as great as 60 km from SLC-4E. In a subsequent report, we will correlate the aircraft's HCl measurements with the imagery for the first 11 min after launch to document the dimensions and concentration distributions within the rising and the stabilized ground cloud. In a third report, we will provide a series of polar, Cartesian, and time plots for each ten-minute increment in the aircraft's #K15 mission. In addition to cloud concentrations, one can extract angular spreads and along-wind cloud dimensions for favorable transects. These subsequent detailed data reviews will provide the data in a format that will facilitate direct comparison to individual dispersion model runs (i.e., for a specific time after launch, altitude above the pad, and distance from the pad). The intent of this program is to document the results in sufficient detail to validate dispersion models.

As discussed in this report, the Geomet detector is useful for aircraft sampling of launch clouds. We provide data that illustrate quantitative integrated response as well as excellent temporal and spatial accuracy for mapping the extent and position of Titan IV clouds. We also include data that document significant differences in the HCl concentrations reported by the Geomet and another detector that flew on this mission. These data illustrate that the concentration reported by both detectors is a strong function of their response functions (i.e., averaging time). These data suggest that the Geomet reports an HCl concentration that represents an average value for at least an 18-s period. In contrast, the temporal and spatial accuracy of the Geomet is consistent with an averaging time of only 3 to 4 seconds. We recommend the use of caution when comparing measured HCl concentration to predicted HCl concentration since the averaging times associated with the detectors are not the same as those used by typical models.

We discovered an error in the REEDM output while comparing the REEDM predictions to imagery-derived and aircraft-derived altitude-dependent measurements. REEDM converts the height above ground level (AGL) to height above mean sea level (MSL) by using the height of the rawinsonde release site (112 m, 368 ft) instead of the height of launch pad (153 m, 501 ft). Therefore, the height MSL reported by REEDM in Appendix A is 41 m (133 ft) too low (i.e., 153–112 m).

4. Aircraft Elevated HCl Measurements—Spectral Sciences Data

Spectral Sciences, Inc. of Burlington, Massachusetts was retained to integrate and operate sensors on the twin-engine Piper aircraft in conjunction with the Geomet instrument described in Chapter 3. The instruments were based on earlier instruments flown on remote-piloted vehicles, and were modified somewhat for this mission to measure gas-phase hydrogen chloride (HCl) and carbon monoxide (CO). The data were collected and reported by Spectral Sciences. That report is reproduced in Appendix D.

5. Ground Level HCl Dosimetry

[The material in this section was contributed by Paul W. Yocom, Toxic Vapor Detection/Contamination Monitoring Laboratory, NASA Kennedy Space Center]

NOTE: In addition to the dosimeter preparation and operations and the preparation and operation of the Geomet monitors flown on the aircraft (see Chapter 3), the NASA laboratory also provided two Interscan HCl monitors, which were to be used by the Air Force mobile monitoring teams, and provided on-site calibration and operator training on these instruments. However, the mobile monitoring teams could not obtain access into the area of the exhaust plume after launch, and hence the Interscans were not used.

5.1 Dosimeter Monitoring

The primary goal for HCl dosimetry during this Titan IV launch was the collection of ground level data around the launch facility. Dosimeters were fabricated on 28 Nov 1995,

The dosimeters were provided to Air Force personnel for near-field placement around the launch complex along the projected plume track from Complex 4E the morning of the launch. Twenty dosimeters were placed in two lines within 90° arcs from the predicted plume track about 600 and 1400 ft from the launch mount. The remaining 14 dosimeters were placed between 1800 and 5000 ft from the launch point placed roughly along a line running approximately northwest to southeast. See Figure 33 for the placement pattern and dosimeter numbers.

5.2 Ground Level Monitoring Results

After the launch, the dosimeters were collected and returned to the Bioenvironmental Engineering lab for reading. Of the 34 dosimeters deployed, three (#7, #29 and #30) were destroyed in a brush fire, and two others (#3 and #4) were saturated beyond readability. See Figure 34 and Table 6 for the calculated HCl dosage in ppm minutes at each location.

5.3 Preparation of Geomet Instrument for Airborne Sampling

At the request of the 30th AMDS Bioenvironmental Engineering (BEE) office at VAFB, one Geomet Model 401B HCl detector was modified and calibrated for airborne effluent plume sampling. It was sent to VAFB for use during this launch, along with two unmodified Geomet units as backup units. A test flight was conducted to verify instrument operation on 4 Dec 95, L-1 day. The instrument was first calibrated at the field lab in the BEE office using a verified vapor sample of 1.1 ppm HCl at approximately 50% relative humidity and 75°F. The instrument was then delivered and installed in the Piper Seminole aircraft. After installation, functional verification tests were performed. The unit was functioning properly and responded as expected during the preflight tests. After the flight test, the instrument was returned to the field lab for postflight calibration. The instrument was turned on and allowed to stabilize while sampling air free of HCl vapor. A baseline shift of <0.01 ppm was

noted. The unit calibration stability was then evaluated by alternately sampling clean air and 1.1 ppm HCl vapor in air. The instrument responded within 10% of the calibration value during this test. The ceramic sample tube was then rinsed with deionized water, and coating solution was applied, after which the instrument responded as it did during preflight calibration, with the 1.1 ppm HCl sample and returned to zero upon removal from the standard.

On the day of launch, the Geomet was calibrated at the BEE field lab using a verified vapor sample of 0.9 ppm HCl at approximately 50% relative humidity and 75°F ambient. It was then installed in the aircraft, and functional verification tests were performed. The unit was functioning properly. After the Titan IV launch, the aircraft was flown into the launch plume numerous times over a 90-min period with the Geomet sampling. After aircraft landing, the Geomet was again returned to the field lab for postflight calibration. As before, the instrument was powered up and stabilized, and the baseline shift was measured. Again, a shift of <0.01 ppm was noted. Stability was evaluated by alternately sampling clean air and 0.7 ppm HCl vapor in air. The instrument responded within 10% of the calibrated value. The ceramic sample tube was then rinsed with deionized water, and coating solution was applied, after which the instrument read the 0.7 ppm HCl standard accurately and returned to zero upon removal.

The implementation of the Geomet calibration and test procedures, as well as the establishment of a good working relationship with other elements of the Titan IV plume monitoring program, has laid the foundation for future airborne measurement and monitoring activities at VAFB, if required. The credibility of the data collected and reported in Section 3 of this report and in the future will only increase with the routine execution of the procedures established for this launch.

Table 6. HCl Dosimeter Locations and Calculated Dosages In order of Proximity to Launch Point

Site No.	Location	Calculated Dosage (ppm min)
32	Near Field, Row 1	332.248
4	Near Field, Row 1	Saturated
3	Near Field, Row 1	Saturated
2	Near Field, Row 1	320.296
1	Near Field, Row 1	332.603
28	Near Field, Row 1	63.397
21	Near Field, Row 1	41.361
22	Near Field, Row 1	90.455
23	Near Field, Row 1	90.091
24	Near Field, Row 1	111.488
6	Near Field, Row 2	333.313
7	Near Field, Row 2	Destroyed by fire
8	Near Field, Row 2	340.100
9	Near Field, Row 2	36.807
29	Near Field, Row 2	Destroyed by fire
27	Near Field, Row 2	31.290
26	Near Field, Row 2	68.659
25	Near Field, Row 2	63.094
30	Near Field, trailing	Destroyed by fire
31	Near Field, trailing	25.254
14	Ridgeline, NW to SE	94.891
13	Ridgeline, NW to SE	275.345
12	Ridgeline, NW to SE	52.846
11	Ridgeline, NW to SE	20.434
10	Ridgeline, NW to SE	21.086
15	Ridgeline, NW to SE	30.878
5	Ridgeline, NW to SE	81.222
41	Ridgeline, NW to SE	13.197
16	Ridgeline, NW to SE	22.086
42	Ridgeline, NW to SE	16.709
17	Ridgeline, NW to SE	16.709
18	Ridgeline, NW to SE	No data, slight color change
19	Ridgeline, NW to SE	No data, slight color change
20	Ridgeline, NW to SE	No data, slight color change

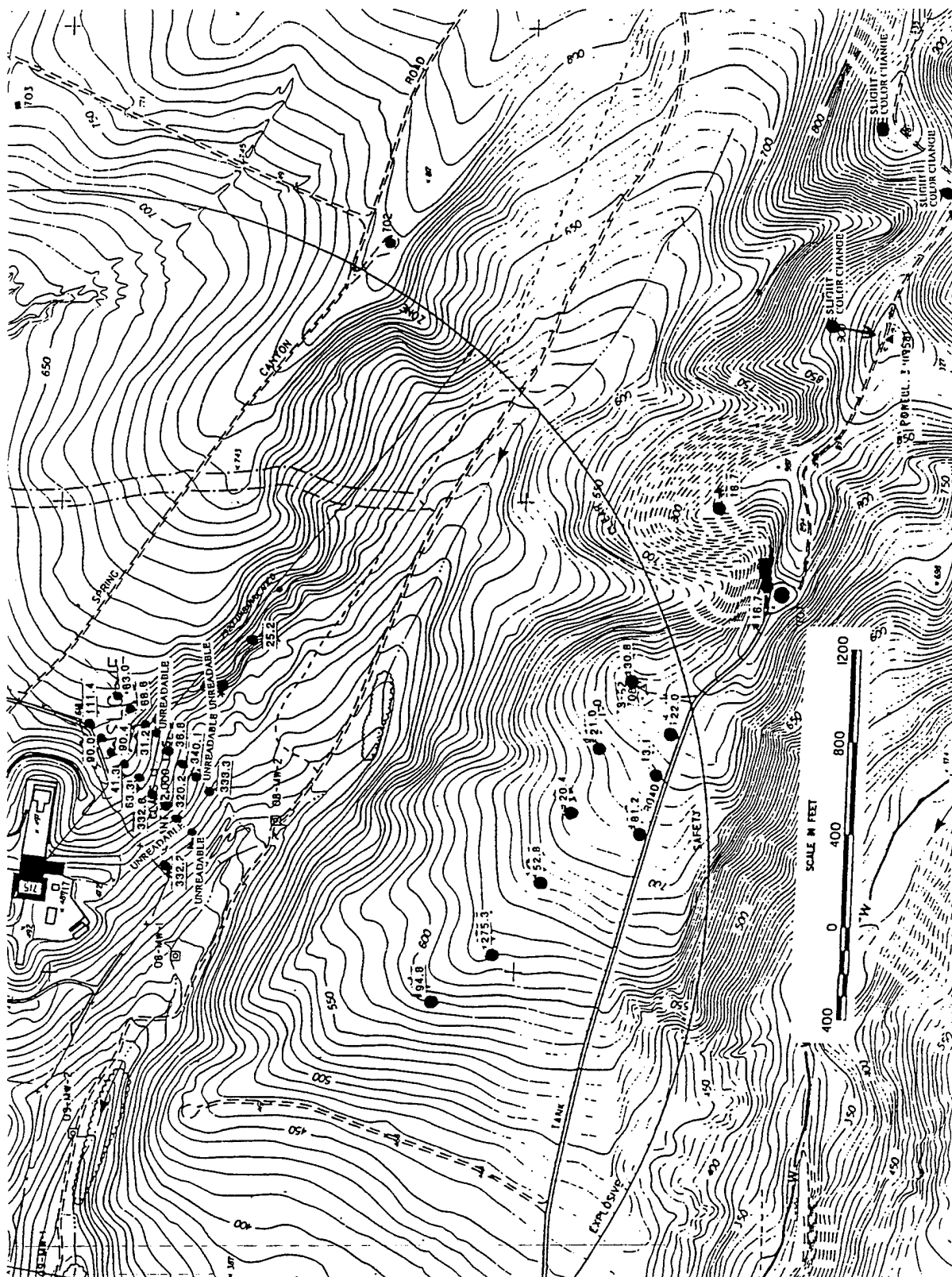


Figure 33. Location of dosimeters for #K15 launch.

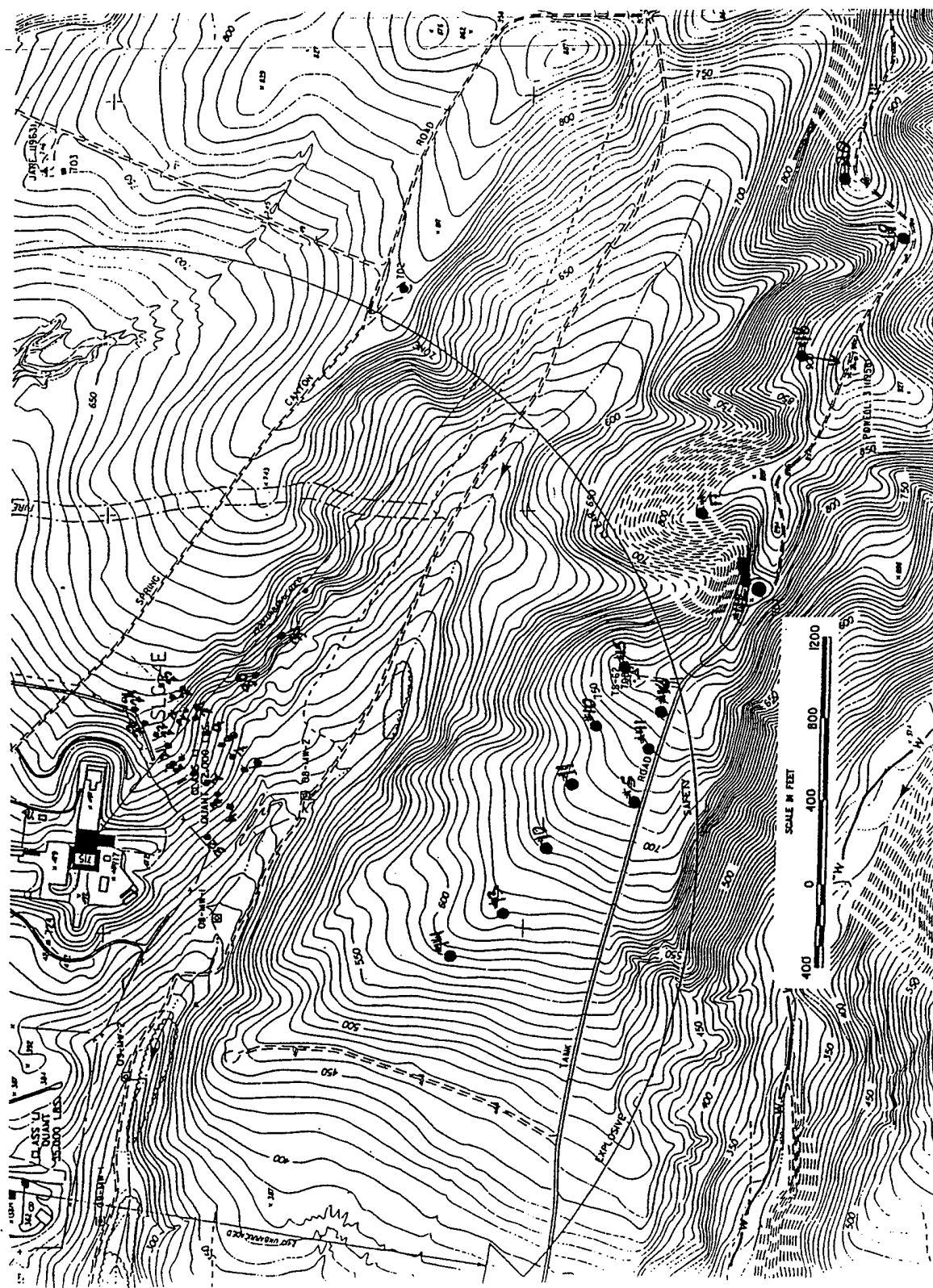


Figure 34. #K15 launch dosage levels (ppm min).

Appendix A—REEDM Code Calculations of Cloud Stabilization Heights and Ground-Level HCl Exposure Doses

[Provided by Dr. Robert Abernathy, The Aerospace Corporation - Environmental Monitoring & Technology Department.]

**Cloud Stabilization Heights Calculated
from T-0.25 h Rawinsonde Data**

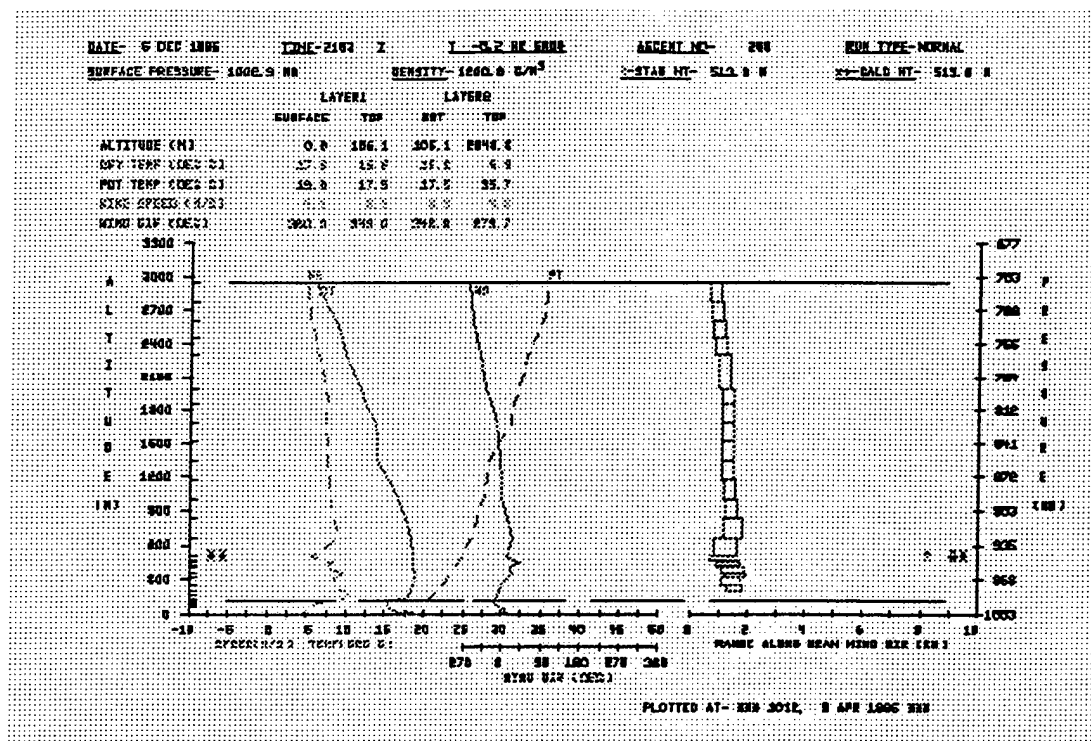


Figure 1: K-15 REEDM Meteorological Data from T-0.25h Rawinsonde Sounding.

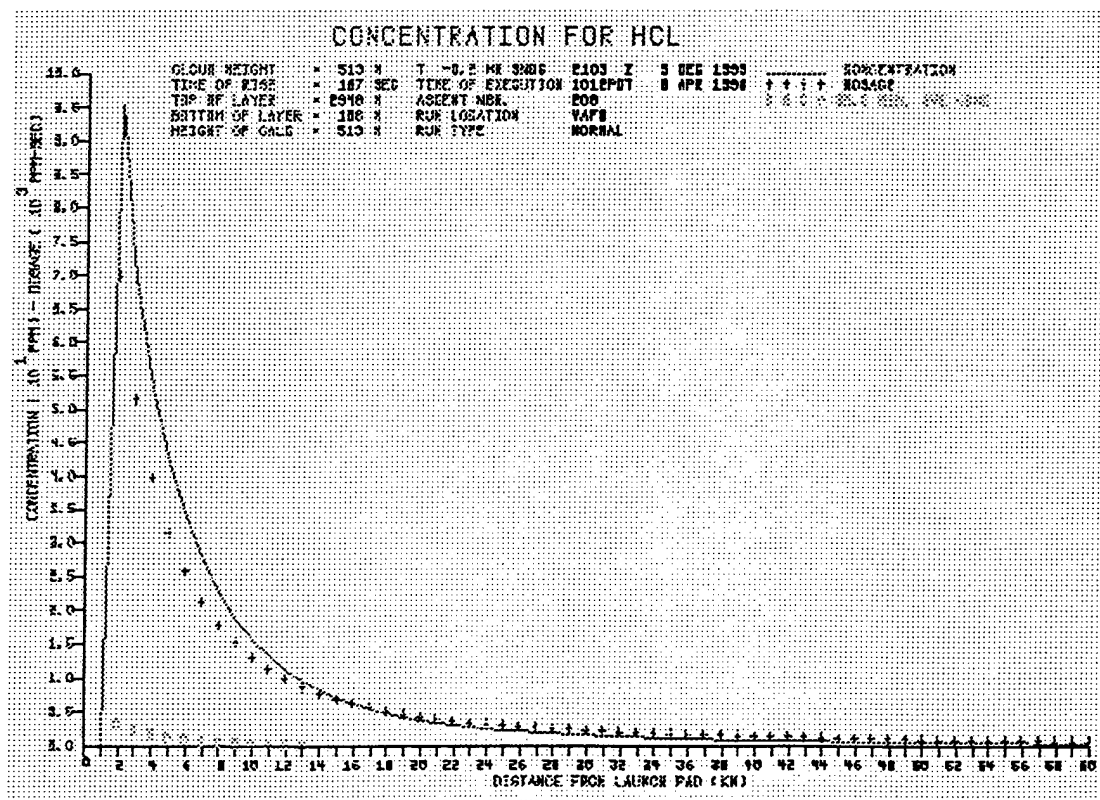


Figure 2: K-15 REEDM Version 7.05 Concentration Predictions for the Predicted Stabilization Height (514 m) Based upon the T-0.25h Rawinsonde.

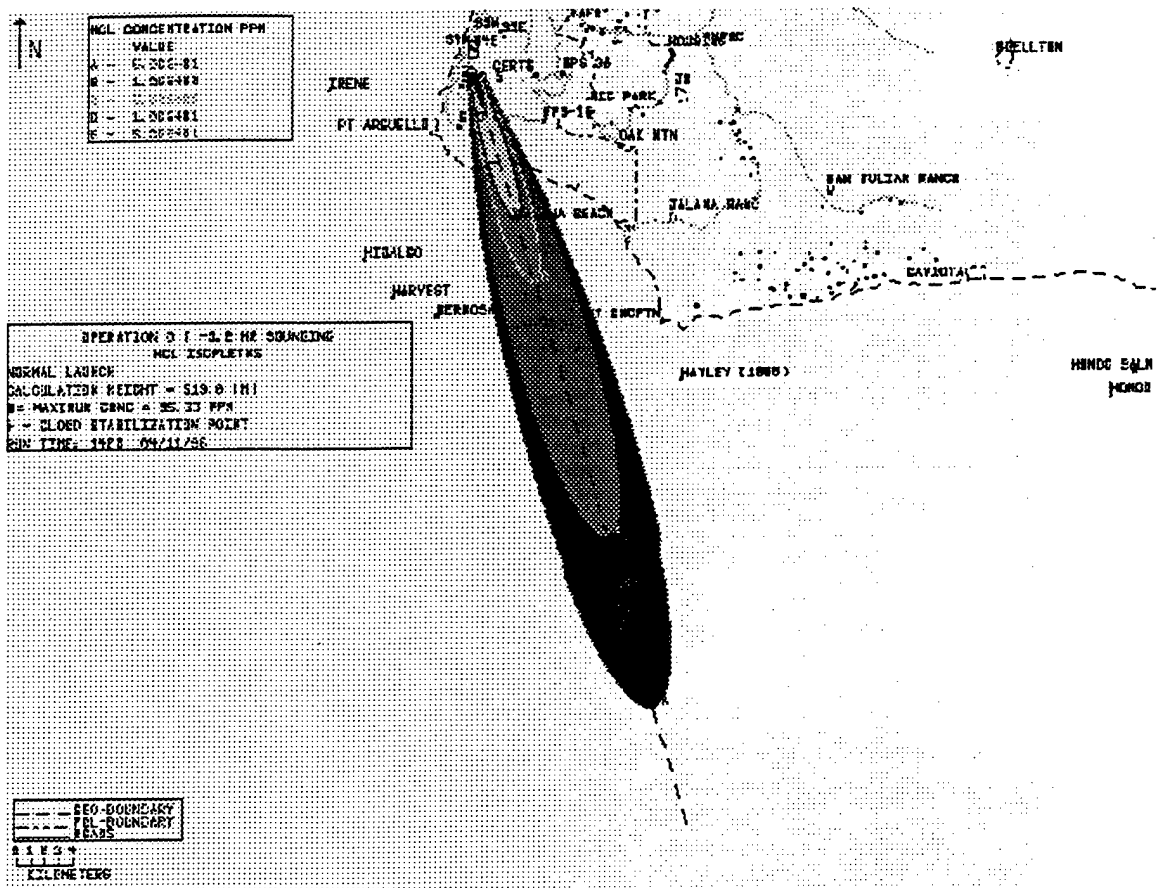


Figure 3: K-15 REEDM Version 7.05 Isopleth Predictions for the Predicted Stabilization Height (514 m) Based upon the T-0.25h Rawinsonde.

1*****

ROCKET EXHAUST EFFLUENT DIFFUSION MODEL REEDM PAGE 2

VERSION 7.05 AT VAFB

1420 PDT 11 APR 1996

launch time: 1318 PST 05 DEC 1995

RAWINSONDE ASCENT NUMBER 208,2103 Z 5 DEC 1995 T -0.2 HR

----- PROGRAM OPTIONS -----

MODEL	CONCENTRATION	
RUN TYPE	OPERATIONAL	
WIND-FIELD TERRAIN EFFECTS MODEL		NONE
LAUNCH VEHICLE	TITAN IV	
LAUNCH TYPE	NORMAL	
LAUNCH COMPLEX NUMBER	4E	
TURBULENCE PARAMETERS ARE DETERMINED FROM		DOPPLER & TOWER
DATA		
SPECIES	HCL	
CLOUD SHAPE	ELLIPTICAL	
CALCULATION HEIGHT	STABILIZATION	
PROPELLANT TEMPERATURE (DEG. C)		13.00
CONCENTRATION AVERAGING TIME (SEC.)		1800.00
DECAY COEFFICIENT	0.0000	
ABSORPTION COEFFICIENT (RNG- 0 TO 1,NO ABSORPTION=0)		0.0000
DIFFUSION COEFFICIENTS	LATERAL	1.0000
	VERTICAL	1.0000
VEHICLE AIR ENTRAINMENT PARAMETER	GAMMAE	0.6400
DOWNWIND EXPANSION DISTANCE (METERS)	LATERAL	100.00
	VERTICAL	100.00

----- DATA FILES -----

INPUT FILES

RAWINSONDE FILE	k15_2103.raw
DATA BASE FILE	RDMBASE

OUTPUT FILES

PRINT FILE	k15_2103.stb
PLOT FILE	k15_2103.stp

1*****

ROCKET EXHAUST EFFLUENT DIFFUSION MODEL REEDM PAGE 3

VERSION 7.05 AT VAFB

1420 PDT 11 APR 1996

launch time: 1318 PST 05 DEC 1995

RAWINSONDE ASCENT NUMBER 208,2103 Z 5 DEC 1995 T -0.2 HR

----- METEOROLOGICAL RAWINSONDE DATA -----

RAWINSONDE MSS/WIN

TIME- 2103 Z DATE- 05 DEC 1995

ASCENT NUMBER 208

----- T -0.2 HR SOUNDING -----

MET. NO.	ALTITUDE MSL (FT)	WIND GND (M)	WIND DIR (DEG)	WIND SPEED (M/S)	AIR TEMP (DEG C)	AIR PTEMP (MB)	AIR DPTMP (%)	PRESS MERP	RH	H INT-		
1	368	0.0	0.0	0	4.1	8.0	17.8	19.0	11.2	1002.9	65.0	
2	422	54.0	16.5	13	5.1	10.0	16.9	18.3	11.0	1001.0	68.0	
3	458	89.5	27.3	10	4.9	9.6	16.4	17.8	10.9	999.7	70.1	**
4	493	125.0	38.1	7	4.7	9.2	15.8	17.4	10.8	998.5	72.0	
5	533	164.5	50.1	3	4.9	9.6	15.7	17.4	11.0	997.0	73.6	**
6	572	204.0	62.2	358	5.1	10.0	15.6	17.4	11.2	995.6	74.8	
7	620	252.0	76.8	350	5.9	11.5	15.5	17.5	11.4	993.9	76.8	**
8	668	300.0	91.4	341	6.7	13.0	15.3	17.5	11.6	992.2	78.3	
9	716	348.0	106.1	346	8.3	16.1	15.2	17.5	11.8	990.5	80.0	*
10	821	453.0	138.1	346	10.8	20.9	17.9	20.8	13.4	986.8	75.0	
11	923	554.5	169.0	350	10.3	20.0	18.0	21.2	13.1	983.2	72.9	**
12	1024	656.0	199.9	353	9.9	19.2	18.2	21.6	12.8	979.7	71.1	
13	1188	820.0	249.9	0	8.4	16.3	18.5	22.4	12.4	974.0	67.9	
14	1393	1025.0	312.4	17	8.5	16.6	18.8	23.2	11.8	967.0	63.9	
15	1516	1148.0	349.9	25	10.2	19.8	18.7	23.5	11.7	962.8	63.6	
16	1680	1312.0	399.9	17	7.3	14.2	18.6	23.9	11.5	957.2	63.1	
17	1762	1394.0	424.9	29	7.8	15.2	18.6	24.1	11.4	954.4	63.0	**
18	1844	1476.0	449.9	41	8.4	16.3	18.6	24.4	11.3	951.7	62.6	
19	1926	1558.0	474.9	26	7.0	13.7	18.5	24.6	11.2	948.9	62.4	**
20	2008	1640.0	499.9	11	5.7	11.1	18.5	24.8	11.1	946.1	62.2	
21	2518	2150.0	655.3	26	8.9	17.3	18.2	26.0	10.5	929.2	60.7	
22	3074	2705.5	824.6	13	8.4	16.4	17.5	26.8	8.8	911.0	57.1	**
23	3629	3261.0	994.0	360	8.0	15.5	16.7	27.6	7.1	893.1	53.2	
24	4198	3830.5	1167.5	358	7.8	15.2	15.4	27.9	6.3	875.1	55.0	**
25	4768	4400.0	1341.1	356	7.7	14.9	14.0	28.2	5.4	857.4	55.9	
26	5326	4958.0	1511.2	351	7.5	14.6	13.8	29.6	3.6	840.3	50.7	**

27	5884	5516.0	1681.3	346	7.4	14.3	13.6	31.1	1.8	823.5	44.6
28	6470	6102.0	1859.9	332	7.5	14.6	12.1	31.4	2.6	806.2	52.0
29	6927	6559.0	1999.2	319	7.4	14.4	11.7	32.1	-2.5	793.0	37.0
30	7889	7521.0	2292.4	307	6.4	12.5	9.9	33.2	-4.6	765.6	35.6
31	8405	8037.0	2449.7	298	5.9	11.4	9.3	34.2	-5.1	751.2	36.8 **
32	8921	8553.0	2607.0	290	5.3	10.3	8.6	35.1	-5.6	737.1	35.9
33	9481	9113.0	2777.6	285	5.1	9.8	7.2	35.4	-5.6	722.0	40.6 **
34	10041	9673.0	2948.3	280	4.8	9.4	5.8	35.7	-5.7	707.2	43.4

* - INDICATES THE CALCULATED TOP OF THE SURFACE MIXING LAYER

** - INDICATES THAT DATA IS LINEARLY INTERPOLATED FROM INPUT
METEOROLOGY

1 *****

ROCKET EXHAUST EFFLUENT DIFFUSION MODEL REEDM PAGE 4

VERSION 7.05 AT VAFB

1420 PDT 11 APR 1996

launch time: 1318 PST 05 DEC 1995

RAWINSONDE ASCENT NUMBER 208,2103 Z 5 DEC 1995 T -0.2 HR

----- METEOROLOGICAL RAWINSONDE DATA -----

SURFACE AIR DENSITY (GM/M**3)	1200.82	
DEFAULT CALCULATED MIXING LAYER HEIGHT (M)		106.07
CLOUD COVER IN TENTHS OF CELESTIAL DOME		0.0
CLOUD CEILING (M)	9999.0	

***REEDM WARNING 09, END OF FILE READ, DATA MAY BE TRUNCATED, FILE =
k15_2103.raw
THE ERROR OCCURRED AT RECORD 35.00

***REEDM ERROR 09, INCOMPLETE DATA - DOPPLER
THE ERROR OCCURRED AT RECORD 35.00

***REEDM WARNING 09, END OF FILE READ, DATA MAY BE TRUNCATED, FILE =
k15_2103.raw
THE ERROR OCCURRED AT RECORD 35.00

***REEDM ERROR 09, INCOMPLETE DATA - TOWER
THE ERROR OCCURRED AT RECORD 35.00
----- PLUME RISE DATA -----

EXHAUST RATE OF MATERIAL-	(GRAMS/SEC)	4.12749E+06
TOTAL MATERIAL OUTPUT-	(GRAMS)	5.36146E+08
HEAT OUTPUT PER GRAM-	(CALORIES)	1555.5800
VEHICLE RISE TIME PARAMETERS-	(TK=(A*Z**B)+C) A=	0.8678
	B=	0.4500
	C=	0.0000

1*****

ROCKET EXHAUST EFFLUENT DIFFUSION MODEL REEDM PAGE 5

VERSION 7.05 AT VAFB

1420 PDT 11 APR 1996

launch time: 1318 PST 05 DEC 1995

RAWINSONDE ASCENT NUMBER 208,2103 Z 5 DEC 1995 T -0.2 HR

----- EXHAUST CLOUD -----

MET. TOP CLOUD CLOUD CLOUD STABILIZED STABILIZED
LAYER OF LAYER RISE TIME RISE RANGE RISE BEARING CLOUD RANGE CLOUD
BEARING

NO. (METERS) (SECONDS) (METERS) (DEGREES) (METERS) (DEGREES)

1	16.5	2.9	6.3	183.8	0.0	0.0
2	27.3	4.0	16.2	188.1	0.0	0.0
3	38.1	5.1	21.8	188.6	0.0	0.0
4	50.1	6.4	27.4	188.3	0.0	0.0
5	62.2	7.6	33.5	187.2	0.0	0.0
6	76.8	9.2	40.9	185.4	0.0	0.0
7	91.4	10.9	50.3	182.3	0.0	0.0
8	106.1	12.8	61.7	178.5	0.0	0.0
9	138.1	17.1	87.8	174.7	0.0	0.0
10	169.0	21.9	135.0	171.8	0.0	0.0
11	199.9	27.3	187.5	171.2	0.0	0.0
12	249.9	37.3	262.0	171.9	1454.2	175.7
13	312.4	52.3	367.1	174.7	1338.6	184.6
14	349.9	62.9	471.6	179.4	1433.7	193.9
15	399.9	79.5	593.1	184.5	1352.9	193.9
16	424.9	89.5	693.6	186.8	1275.5	194.3
17	449.9	101.1	772.2	189.2	1282.6	199.8
18	474.9	115.6	866.3	192.6	1252.4	199.2
19	499.9	136.5	985.8	194.2	1186.4	194.9
20	655.3	168.0 *	1232.8	193.9	1232.8	193.9
21	824.6	168.0 *	1232.8	193.9	1232.8	193.9
22	994.0	168.0 *	1232.8	193.9	1232.8	193.9
23	1167.5	168.0 *	1232.8	193.9	1232.8	193.9
24	1341.1	168.0 *	1232.8	193.9	1232.8	193.9
25	1511.2	168.0 *	1232.8	193.9	1232.8	193.9
26	1681.3	168.0 *	1232.8	193.9	1232.8	193.9
27	1859.9	168.0 *	1232.8	193.9	1232.8	193.9
28	1999.2	168.0 *	1232.8	193.9	1232.8	193.9
29	2292.4	168.0 *	1232.8	193.9	1232.8	193.9
30	2449.7	168.0 *	1232.8	193.9	1232.8	193.9

31	2607.0	168.0 *	1232.8	193.9	1232.8	193.9
32	2777.6	168.0 *	1232.8	193.9	1232.8	193.9
33	2948.3	168.0 *	1232.8	193.9	1232.8	193.9

* - INDICATES CLOUD STABILIZATION TIME WAS USED

1*****

ROCKET EXHAUST EFFLUENT DIFFUSION MODEL REEDM PAGE 6

VERSION 7.05 AT VAFB

1420 PDT 11 APR 1996

launch time: 1318 PST 05 DEC 1995

RAWINSONDE ASCENT NUMBER 208,2103 Z 5 DEC 1995 T -0.2 HR

----- EXHAUST CLOUD -----

LAYER CLOUD

MET. TOP SOURCE UPDRAFT CLOUD STD. DEVIATION MATERIAL DIST.
LAYER OF LAYER STRENGTH VELOCITY RADIUS ALONGWIND CROSSWIND
NO. (METERS) (GRAMS) (M/S) (METERS) (METERS) (METERS)

1	16.5	0.00000E+00	8.9	0.0	0.0	0.0
2	27.3	0.00000E+00	9.7	0.0	0.0	0.0
3	38.1	0.00000E+00	9.9	0.0	0.0	0.0
4	50.1	0.00000E+00	9.7	0.0	0.0	0.0
5	62.2	0.00000E+00	9.3	0.0	0.0	0.0
6	76.8	0.00000E+00	8.9	0.0	0.0	0.0
7	91.4	0.00000E+00	8.3	0.0	0.0	0.0
8	106.1	0.00000E+00	7.9	0.0	0.0	0.0
9	138.1	0.00000E+00	6.9	0.0	0.0	0.0
10	169.0	0.00000E+00	6.1	0.0	0.0	0.0
11	199.9	0.00000E+00	5.4	0.0	0.0	0.0
12	249.9	1.51631E+06	4.6	277.0	129.1	129.1
13	312.4	4.19581E+06	3.8	325.6	151.7	151.7
14	349.9	3.50821E+06	3.3	356.1	165.9	165.9
15	399.9	5.55795E+06	2.7	375.3	174.9	174.9
16	424.9	3.06769E+06	2.3	387.1	180.4	180.4
17	449.9	3.20769E+06	2.0	392.8	183.0	183.0
18	474.9	3.30833E+06	1.5	396.9	184.9	184.9
19	499.9	3.36961E+06	0.9	399.3	186.1	186.1
20	655.3	* 2.67853E+07	0.0	395.1	184.1	184.1
21	824.6	* 1.87791E+07	0.0	330.1	153.8	153.8
22	994.0	* 6.44320E+06	0.0	199.9	93.2	93.2
23	1167.5	* 6.00496E+06	0.0	199.9	93.2	93.2
24	1341.1	* 5.53129E+06	0.0	199.9	93.2	93.2
25	1511.2	* 5.04919E+06	0.0	199.9	93.2	93.2
26	1681.3	* 4.74531E+06	0.0	199.9	93.2	93.2
27	1859.9	* 4.70703E+06	0.0	199.9	93.2	93.2
28	1999.2	* 3.50068E+06	0.0	199.9	93.2	93.2
29	2292.4	* 6.95415E+06	0.0	199.9	93.2	93.2
30	2449.7	* 3.52901E+06	0.0	199.9	93.2	93.2
31	2607.0	* 3.40645E+06	0.0	199.9	93.2	93.2

32	2777.6 * 3.57134E+06	0.0	199.9	93.2	93.2
33	2948.3 * 3.45255E+06	0.0	199.9	93.2	93.2

* - INDICATES CLOUD STABILIZATION TIME WAS USED

1*****
 ROCKET EXHAUST EFFLUENT DIFFUSION MODEL REEDM PAGE 7
 VERSION 7.05 AT VAFB
 1420 PDT 11 APR 1996
 launch time: 1318 PST 05 DEC 1995
 RAWINSONDE ASCENT NUMBER 208,2103 Z 5 DEC 1995 T -0.2 HR

----- CLOUD STABILIZATION -----

CALCULATION HEIGHT	(METERS)	513.79
STABILIZATION HEIGHT	(METERS)	513.79
STABILIZATION TIME	(SECS)	167.98
FIRST MIXING LAYER HEIGHT-	(METERS)	TOP = 106.07
	BASE=	0.00
SECOND SELECTED LAYER HEIGHT-	(METERS)	TOP = 2948.33
	BASE=	106.07
SIGMAR(AZ) AT THE SURFACE	(DEGREES)	11.1214
SIGMER(EL) AT THE SURFACE	(DEGREES)	3.4690

MET. LAYER NO.	WIND SPEED (M/SEC)	WIND SPEED (M/SEC)	WIND SPEED (M/SEC)	WIND DIRECTION (DEG)	SIGMA OF AZI ANG (DEG)	SIGMA OF ELE ANG (DEG)
1	4.83	1.03	6.50	13.00	9.7279	4.4120
2	5.04	0.21	11.52	-2.95	8.1230	5.5730
3	4.84	0.21	8.57	-2.95	7.7779	5.9450
4	4.84	0.21	4.82	-4.55	7.5375	6.2315
5	5.04	0.21	0.27	-4.55	7.3495	6.4720
6	5.53	0.77	353.75	-8.50	7.1898	6.6895
7	6.30	0.77	345.25	-8.50	7.0484	6.8922
8	7.49	1.59	343.50	5.00	3.9926	3.9926
9	9.52	2.47	346.00	0.00	1.0000	1.0000
10	10.53	-0.44	347.75	3.50	1.0000	1.0000
11	10.10	-0.44	351.25	3.50	1.0000	1.0000
12	9.13	-1.49	356.50	7.00	1.0000	1.0000
13	8.46	0.15	8.35	16.70	1.0000	1.0000
14	9.36	1.65	20.85	8.30	1.0000	1.0000
15	8.75	-2.88	21.00	-8.00	1.0000	1.0000
16	7.58	0.54	23.00	12.00	1.0000	1.0000
17	8.12	0.54	35.00	12.00	1.0000	1.0000
18	7.72	-1.34	33.50	-15.00	1.0000	1.0000
19	6.38	-1.34	18.50	-15.00	1.0000	1.0000
20	7.31	3.19	18.35	14.70	1.0000	1.0000
21	8.67	-0.46	19.27	-12.85	1.0000	1.0000
22	8.21	-0.46	6.42	-12.85	1.0000	1.0000

23	7.90	-0.15	358.88	-2.25	1.0000	1.0000
24	7.74	-0.15	356.63	-2.25	1.0000	1.0000
25	7.59	-0.15	353.20	-4.60	1.0000	1.0000
26	7.43	-0.15	348.60	-4.60	1.0000	1.0000
27	7.43	0.15	338.90	-14.80	1.0000	1.0000
28	7.46	-0.10	325.00	-13.00	1.0000	1.0000
29	6.92	-0.98	312.70	-11.60	1.0000	1.0000
30	6.15	-0.57	302.60	-8.60	1.0000	1.0000

```

1 *****
  ROCKET EXHAUST EFFLUENT DIFFUSION MODEL REEDM    PAGE  8
    VERSION 7.05 AT VAFB
    1420 PDT 11 APR 1996
    launch time: 1318 PST 05 DEC 1995
  RAWINSONDE ASCENT NUMBER  208,2103  Z 5 DEC 1995  T -0.2 HR
  *****

```

----- CALCULATED METEOROLOGICAL LAYER PARAMETERS -----

MET. LAYER NO.	WIND WIND SPEED (M/SEC)	WIND SPEED SHEAR (M/SEC)	WIND DIRECTION (DEG)	WIND DIRECTION SHEAR (DEG)	SIGMA OF AZI ANG (DEG)	SIGMA OF ELE ANG (DEG)
31	5.58	-0.57	294.00	-8.60	1.0000	1.0000
32	5.18	-0.23	287.20	-5.00	1.0000	1.0000
33	4.95	-0.23	282.20	-5.00	1.0000	1.0000

TRANSITION LAYER NUMBER- 1

VALUE AT (METERS)	HEIGHT (METERS)	TEMP. (DEG K)	WIND SPEED (M/SEC)	WIND SHEAR (M/SEC)	WIND DIR. (DEG)	SIGMA SHEAR (DEG)	SIGMA AZI (DEG)	SIGMA ELE (DEG)
TOP-	106.07	290.68	8.28	346.00	1.0000	1.0000		
LAYER-		5.46	0.89	356.90	8.13	7.3132	5.7381	
BOTTOM-	0.00	292.17	4.12	360.00	11.1214	3.4690		

TRANSITION LAYER NUMBER- 2

VALUE AT (METERS)	HEIGHT (METERS)	TEMP. (DEG K)	WIND SPEED (M/SEC)	WIND SHEAR (M/SEC)	WIND DIR. (DEG)	SIGMA SHEAR (DEG)	SIGMA AZI (DEG)	SIGMA ELE (DEG)
TOP-	2948.33	308.88	4.84	279.70	1.0000	1.0000		
LAYER-		6.27	1.36	344.13	21.34	1.0000	1.0000	
BOTTOM-	106.07	290.68	8.28	346.00	1.0000	1.0000		

```

1 *****
  ROCKET EXHAUST EFFLUENT DIFFUSION MODEL REEDM    PAGE  9
    VERSION 7.05 AT VAFB
    1420 PDT 11 APR 1996
    launch time: 1318 PST 05 DEC 1995
  RAWINSONDE ASCENT NUMBER  208,2103  Z 5 DEC 1995  T -0.2 HR
  *****

```

----- MAXIMUM CENTERLINE CALCULATIONS -----

CONCENTRATION OF HCL AT A HEIGHT OF 513.8 METERS
DOWNWIND FROM A TITAN IV NORMAL LAUNCH
CALCULATIONS APPLY TO THE LAYER BETWEEN 106.1 AND 2948.3 METERS

RANGE FROM PAD (METERS)	PEAK BEARING FROM PAD (DEGREES)	CLOUD CONCEN- TRATION (PPM)	CLOUD ARRIVAL TIME (MIN)	DEPARTURE TIME (MIN)
2000.218	182.016	95.331	2.416	5.656
3000.037	176.005	69.792	3.423	8.346
4000.011	173.281	53.208	4.707	11.004
5000.003	171.396	41.853	6.533	13.664
6000.001	170.262	33.621	8.346	16.316
7000.000	169.214	27.392	10.156	18.977
8000.000	168.783	22.576	11.952	21.627
9000.000	168.176	18.749	13.751	24.289
10000.000	167.690	15.669	15.545	26.953
11000.000	167.293	13.174	17.335	29.619
12000.000	166.962	11.147	19.123	32.287
13000.000	167.054	9.502	20.901	34.946
14000.000	166.816	8.155	22.685	37.617
15000.000	166.610	7.049	24.467	40.290
16000.000	166.430	6.137	26.248	44.585
17000.000	166.270	5.381	28.011	51.894
18000.000	166.129	4.751	29.749	54.967
19000.000	166.002	4.221	31.485	62.289
20000.000	165.888	3.774	33.221	68.535
21000.000	165.785	3.393	34.956	72.000
22000.000	165.691	3.067	36.690	75.466
23000.000	165.606	2.785	38.424	78.931
24000.000	165.527	2.540	40.157	82.397
25000.000	165.455	2.326	41.890	85.863
26000.000	165.389	2.137	43.622	89.329
27000.000	165.327	1.970	45.353	92.796
28000.000	165.270	1.822	47.085	96.262
29000.000	165.216	1.689	48.816	99.729
30000.000	165.167	1.569	50.546	103.196
31000.000	165.120	1.461	52.277	106.662
32000.000	165.076	1.364	54.007	110.129
33000.000	165.035	1.275	55.737	113.596
34000.000	164.997	1.194	57.466	117.063
35000.000	164.960	1.120	59.196	120.530
36000.000	164.926	1.052	60.925	123.998
37000.000	164.894	0.990	62.654	127.465

38000.000	164.863	0.933	64.383	130.932
39000.000	165.227	0.880	66.104	134.385
40000.000	165.200	0.832	67.833	137.852
41000.000	165.173	0.786	69.561	141.320
42000.000	165.148	0.744	71.290	144.787

1 *****

ROCKET EXHAUST EFFLUENT DIFFUSION MODEL REEDM PAGE 10

VERSION 7.05 AT VAFB

1420 PDT 11 APR 1996

launch time: 1318 PST 05 DEC 1995

RAWINSONDE ASCENT NUMBER 208,2103 Z 5 DEC 1995 T -0.2 HR

----- MAXIMUM CENTERLINE CALCULATIONS -----

CONCENTRATION OF HCL AT A HEIGHT OF 513.8 METERS
DOWNWIND FROM A TITAN IV NORMAL LAUNCH
CALCULATIONS APPLY TO THE LAYER BETWEEN 106.1 AND 2948.3 METERS

RANGE FROM PAD (METERS)	PEAK BEARING FROM PAD (DEGREES)	CLOUD CONCEN- TRATION (PPM)	CLOUD ARRIVAL TIME (MIN)	DEPARTURE TIME (MIN)
43000.000	165.125	0.706	73.018	148.255
44000.000	165.102	0.669	74.746	151.722
45000.000	165.080	0.636	76.474	155.190
46000.000	165.060	0.604	78.202	158.658
47000.000	165.040	0.575	79.930	162.125
48000.000	165.021	0.547	81.658	165.593
49000.000	165.003	0.521	83.386	169.061
50000.000	164.985	0.497	85.114	172.529
51000.000	164.968	0.475	86.841	175.996
52000.000	164.952	0.453	88.569	179.464
53000.000	164.937	0.433	90.296	182.932
54000.000	164.922	0.415	92.024	186.400
55000.000	164.907	0.397	93.751	189.868
56000.000	164.893	0.380	95.479	193.336
57000.000	164.880	0.364	97.206	196.803
58000.000	164.867	0.350	98.933	200.271
59000.000	164.854	0.335	100.660	203.739
60000.000	164.842	0.322	102.387	207.207

RANGE BEARING

95.331 IS THE MAXIMUM PEAK CONCENTRATION

2000.2 182.0

1 *****
 ROCKET EXHAUST EFFLUENT DIFFUSION MODEL REEDM PAGE 11
 VERSION 7.05 AT VAFB
 1420 PDT 11 APR 1996
 launch time: 1318 PST 05 DEC 1995
 RAWINSONDE ASCENT NUMBER 208,2103 Z 5 DEC 1995 T -0.2 HR

----- MAXIMUM CENTERLINE CALCULATIONS -----

CONCENTRATION OF HCL AT A HEIGHT OF 513.8 METERS
 DOWNWIND FROM A TITAN IV NORMAL LAUNCH
 CALCULATIONS APPLY TO THE LAYER BETWEEN 106.1 AND 2948.3 METERS

30.0 MIN.				
RANGE	MEAN	CLOUD	CLOUD	
FROM PAD	BEARING	CONCEN-	ARRIVAL	DEPARTURE
(METERS)	FROM PAD	TRATION	TIME	TIME
	(DEGREES)	(PPM)	(MIN)	(MIN)
2000.218	182.016	3.910	2.416	5.656
3000.037	176.005	2.888	3.423	8.346
4000.011	173.281	2.229	4.707	11.004
5000.003	171.396	1.779	6.533	13.664
6000.001	170.262	1.453	8.346	16.316
7000.000	169.214	1.209	10.156	18.977
8000.000	168.783	1.021	11.952	21.627
9000.000	168.176	0.873	13.751	24.289
10000.000	167.690	0.753	15.545	26.953
11000.000	167.293	0.655	17.335	29.619
12000.000	166.962	0.575	19.123	32.287
13000.000	167.054	0.509	20.901	34.946
14000.000	166.816	0.454	22.685	37.617
15000.000	166.610	0.408	24.467	40.290
16000.000	166.430	0.369	26.248	44.585
17000.000	166.270	0.336	28.011	51.894
18000.000	166.129	0.308	29.749	54.967
19000.000	166.002	0.285	31.485	62.289
20000.000	165.888	0.264	33.221	68.535
21000.000	165.785	0.247	34.956	72.000
22000.000	165.691	0.231	36.690	75.466
23000.000	165.606	0.217	38.424	78.931
24000.000	165.527	0.205	40.157	82.397
25000.000	165.455	0.194	41.890	85.863
26000.000	165.389	0.185	43.622	89.329
27000.000	165.327	0.176	45.353	92.796
28000.000	165.270	0.168	47.085	96.262
29000.000	165.216	0.160	48.816	99.729

30000.000	165.167	0.153	50.546	103.196
31000.000	165.120	0.147	52.277	106.662
32000.000	165.076	0.141	54.007	110.129
33000.000	165.035	0.136	55.737	113.596
34000.000	164.997	0.131	57.466	117.063
35000.000	164.960	0.126	59.196	120.530
36000.000	164.926	0.121	60.925	123.998
37000.000	164.894	0.117	62.654	127.465
38000.000	164.863	0.113	64.383	130.932
39000.000	165.227	0.109	66.104	134.385
40000.000	165.200	0.106	67.833	137.852
41000.000	165.173	0.102	69.561	141.320

1 *****
 ROCKET EXHAUST EFFLUENT DIFFUSION MODEL REEDM PAGE 12
 VERSION 7.05 AT VAFB
 1420 PDT 11 APR 1996
 launch time: 1318 PST 05 DEC 1995
 RAWINSONDE ASCENT NUMBER 208,2103 Z 5 DEC 1995 T -0.2 HR

----- MAXIMUM CENTERLINE CALCULATIONS -----

CONCENTRATION OF HCL AT A HEIGHT OF 513.8 METERS
 DOWNWIND FROM A TITAN IV NORMAL LAUNCH
 CALCULATIONS APPLY TO THE LAYER BETWEEN 106.1 AND 2948.3 METERS

30.0 MIN.				
RANGE	MEAN	CLOUD	CLOUD	
FROM PAD	BEARING	CONCEN-	ARRIVAL	DEPARTURE
(METERS)	FROM PAD	TRATION	TIME	TIME
	(DEGREES)	(PPM)	(MIN)	(MIN)
42000.000	165.148	0.099	71.290	144.787
43000.000	165.125	0.096	73.018	148.255
44000.000	165.102	0.093	74.746	151.722
45000.000	165.080	0.090	76.474	155.190
46000.000	165.060	0.088	78.202	158.658
47000.000	165.040	0.085	79.930	162.125
48000.000	165.021	0.083	81.658	165.593
49000.000	165.003	0.081	83.386	169.061
50000.000	164.985	0.078	85.114	172.529
51000.000	164.968	0.076	86.841	175.996
52000.000	164.952	0.074	88.569	179.464
53000.000	164.937	0.072	90.296	182.932
54000.000	164.922	0.070	92.024	186.400
55000.000	164.907	0.069	93.751	189.868
56000.000	164.893	0.067	95.479	193.336
57000.000	164.880	0.065	97.206	196.803
58000.000	164.867	0.064	98.933	200.271
59000.000	164.854	0.062	100.660	203.739
60000.000	164.842	0.061	102.387	207.207

RANGE BEARING

 3.910 IS THE MAXIMUM 30.0 MIN. MEAN CONCENTRATION 2000.2 182.0

**Ground-Level HCl Exposure Doses Calculated
from T-0.25 h Rawinsonde Data**

ROCKET EXHAUST EFFLUENT DIFFUSION MODEL REEDM

PAGE 2

VERSION 7.07 AT VAFB

0932 PDT 16 AUG 1996

launch time: 1318 PST 05 DEC 1995

RAWINSONDE ASCENT NUMBER 208, 2103 Z 5 DEC 1995 T -0.2 HR

----- PROGRAM OPTIONS -----

MODEL	CONCENTRATION
RUN TYPE	OPERATIONAL
WIND-FIELD TERRAIN EFFECTS MODEL	NONE
LAUNCH VEHICLE	TITAN IV
LAUNCH TYPE	NORMAL
LAUNCH COMPLEX NUMBER	4E
TURBULENCE PARAMETERS ARE DETERMINED FROM	DOPPLER & TOWER DATA
SURFACE CHEMISTRY MODEL	absorption coefficient
SPECIES SURFACE FACTOR	HCL 0.000
CLOUD SHAPE	ELLIPTICAL
CALCULATION HEIGHT	SURFACE
PROPELLANT TEMPERATURE (DEG. C)	13.00
CONCENTRATION AVERAGING TIME (SEC.)	1800.00
mixing layer reflection coefficient (RNG- 0 TO 1,no reflection=0)	1.0000
DIFFUSION COEFFICIENTS	LATERAL 1.0000
	VERTICAL 1.0000
VEHICLE AIR ENTRAINMENT PARAMETER	GAMMAE 0.6400
WNWIND EXPANSION DISTANCE (METERS)	LATERAL 100.00
	VERTICAL 100.00

----- DATA FILES -----

INPUT FILES

RAWINSONDE FILE	k15.raw
DATA BASE FILE	rdmbase.vaf

OUTPUT FILES

PRINT FILE	k157_raw.sur
PLOT FILE	k157_raw.sup

 ROCKET EXHAUST EFFLUENT DIFFUSION MODEL REEDM PAGE 3
 VERSION 7.07 AT VAFB
 0932 PDT 16 AUG 1996
 launch time: 1318 PST 05 DEC 1995
 RAWINSONDE ASCENT NUMBER 208, 2103 Z 5 DEC 1995 T -0.2 HR

----- METEOROLOGICAL RAWINSONDE DATA -----

TEST NBR SITE: 900 OP NO: W3999 ASC NO: 208
 RAWINSONDE MSS/WIN
 TIME- 2103 Z DATE- 05 DEC 1995
 ASCENT NUMBER 208

----- T -0.2 HR SOUNDING -----

MET. LEV. NO.	MSL (FT)	ALTITUDE GND (FT)	GND (M)	WIND DIR (DEG)	WIND SPEED (M/S)	WIND (KTS)	AIR TEMP (DEG C)	AIR PTEMP (DEG C)	AIR DPTMP	AIR PRESS (MB)	AIR RH (%)	H M	INT- ERP
1	368	0.0	0.0	0	4.1	8.0	17.8	19.0	11.2	1002.9	65.0		
2	422	54.0	16.5	13	5.1	10.0	16.9	18.3	11.0	1001.0	68.0		
3	458	89.5	27.3	10	4.9	9.6	16.4	17.8	10.9	999.7	70.1	**	
4	493	125.0	38.1	7	4.7	9.2	15.8	17.4	10.8	998.5	72.0		
5	533	164.5	50.1	3	4.9	9.6	15.7	17.4	11.0	997.0	73.6	**	
6	572	204.0	62.2	358	5.1	10.0	15.6	17.4	11.2	995.6	74.8		
	620	252.0	76.8	350	5.9	11.5	15.5	17.5	11.4	993.9	76.8	**	
8	668	300.0	91.4	341	6.7	13.0	15.3	17.5	11.6	992.2	78.3		
9	716	348.0	106.1	346	8.3	16.1	15.2	17.5	11.8	990.5	80.0	*	
10	821	453.0	138.1	346	10.8	20.9	17.9	20.8	13.4	986.8	75.0		
11	923	554.5	169.0	350	10.3	20.0	18.0	21.2	13.1	983.2	72.9	**	
12	1024	656.0	199.9	353	9.9	19.2	18.2	21.6	12.8	979.7	71.1		
13	1188	820.0	249.9	0	8.4	16.3	18.5	22.4	12.4	974.0	67.9		
14	1393	1025.0	312.4	17	8.5	16.6	18.8	23.2	11.8	967.0	63.9		
15	1516	1148.0	349.9	25	10.2	19.8	18.7	23.5	11.7	962.8	63.6		
16	1680	1312.0	399.9	17	7.3	14.2	18.6	23.9	11.5	957.2	63.1		
17	1762	1394.0	424.9	29	7.8	15.2	18.6	24.1	11.4	954.4	63.0	**	
18	1844	1476.0	449.9	41	8.4	16.3	18.6	24.4	11.3	951.7	62.6		
19	1926	1558.0	474.9	26	7.0	13.7	18.5	24.6	11.2	948.9	62.4	**	
20	2008	1640.0	499.9	11	5.7	11.1	18.5	24.8	11.1	946.1	62.2		
21	2518	2150.0	655.3	26	8.9	17.3	18.2	26.0	10.5	929.2	60.7		
22	3074	2705.5	824.6	13	8.4	16.4	17.5	26.8	8.8	911.0	57.1	**	
23	3629	3261.0	994.0	360	8.0	15.5	16.7	27.6	7.1	893.1	53.2		
24	4198	3830.5	1167.5	358	7.8	15.2	15.4	27.9	6.3	875.1	55.0	**	
25	4768	4400.0	1341.1	356	7.7	14.9	14.0	28.2	5.4	857.4	55.9		
26	5326	4958.0	1511.2	351	7.5	14.6	13.8	29.6	3.6	840.3	50.7	**	
27	5884	5516.0	1681.3	346	7.4	14.3	13.6	31.1	1.8	823.5	44.6		
28	6470	6102.0	1859.9	332	7.5	14.6	12.1	31.4	2.6	806.2	52.0		
29	6927	6559.0	1999.2	319	7.4	14.4	11.7	32.1	-2.5	793.0	37.0		
30	7889	7521.0	2292.4	307	6.4	12.5	9.9	33.2	-4.6	765.6	35.6		
31	8405	8037.0	2449.7	298	5.9	11.4	9.3	34.2	-5.1	751.2	36.8	**	
	8921	8553.0	2607.0	290	5.3	10.3	8.6	35.1	-5.6	737.1	35.9		
	9481	9113.0	2777.6	285	5.1	9.8	7.2	35.4	-5.6	722.0	40.6	**	
34	10041	9673.0	2948.3	280	4.8	9.4	5.8	35.7	-5.7	707.2	43.4		

* - INDICATES THE CALCULATED TOP OF THE SURFACE MIXING LAYER

** - INDICATES THAT DATA IS LINEARLY INTERPOLATED FROM INPUT METEOROLOGY

ROCKET EXHAUST EFFLUENT DIFFUSION MODEL REEDM

PAGE 4

VERSION 7.07 AT VAFB

0932 PDT 16 AUG 1996

launch time: 1318 PST 05 DEC 1995

RAWINSONDE ASCENT NUMBER 208, 2103 Z 5 DEC 1995 T -0.2 HR

----- METEOROLOGICAL RAWINSONDE DATA -----

SURFACE AIR DENSITY (GM/M**3)	1200.82
DEFAULT CALCULATED MIXING LAYER HEIGHT (M)	106.07
CLOUD COVER IN TENTHS OF CELESTIAL DOME	0.0
CLOUD CEILING (M)	9999.0

***REEDM WARNING 09, END OF FILE READ, DATA MAY BE TRUNCATED, FILE =
k15.raw

THE ERROR OCCURRED AT RECORD 64.00

***REEDM ERROR 09, INCOMPLETE DATA - DOPPLER

THE ERROR OCCURRED AT RECORD 64.00

----- PLUME RISE DATA -----

EXHAUST RATE OF MATERIAL INTO GRN CLD-	(GRAMS/SEC)		4.14271E+06
TOTAL GROUND CLD MATERIAL-	(GRAMS)		3.89920E+07
HEAT OUTPUT PER GRAM-	(CALORIES)		1555.6
ICL RISE HEIGHT DEFINING GROUND CLD-	(M)		199.9
VEHICLE RISE TIME PARAMETERS-	(TK=(A*Z**B)+C)	A=	0.8677
		B=	0.4500
		C=	0.0000.
EXHAUST RATE OF MATERIAL INTO CONTRAIL-	(GRAMS/SEC)		4.14271E+06
CONTRAIL HEAT OUTPUT PER GRAM-	(CALORIES)		1555.6

1*****
ROCKET EXHAUST EFFLUENT DIFFUSION MODEL REEDM PAGE 5
VERSION 7.07 AT VAFB
0932 PDT 16 AUG 1996
launch time: 1318 PST 05 DEC 1995
RAWINSONDE ASCENT NUMBER 208, 2103 Z 5 DEC 1995 T -0.2 HR

----- EXHAUST CLOUD -----

MET. LAYER NO.	TOP OF LAYER (METERS)	CLOUD RISE TIME (SECONDS)	CLOUD RISE RANGE (METERS)	CLOUD RISE BEARING (DEGREES)	STABILIZED CLOUD RANGE (METERS)	STABILIZED CLOUD BEARING (DEGREES)
1	16.5	2.9	6.3	183.8	0.0	0.0
2	27.3	4.0	16.2	188.1	0.0	0.0
3	38.1	5.1	21.8	188.6	0.0	0.0
4	50.1	6.4	27.3	188.3	0.0	0.0
5	62.2	7.6	33.4	187.2	0.0	0.0
6	76.8	9.2	40.8	185.4	0.0	0.0
7	91.4	10.9	50.3	182.3	0.0	0.0
8	106.1	12.7	61.6	178.5	0.0	0.0
9	138.1	17.1	87.6	174.7	0.0	0.0
10	169.0	21.9	134.8	171.8	0.0	0.0
11	199.9	27.3	187.1	171.2	1609.0	171.2
	249.9	37.3	261.5	171.9	1455.4	175.7
13	312.4	52.2	366.4	174.7	1339.8	184.6
14	349.9	62.7	470.6	179.4	1435.1	194.0
15	399.9	79.3	591.7	184.5	1354.2	193.9
16	424.9	89.2	691.9	186.8	1276.4	194.3
17	449.9	100.8	770.0	189.2	1283.7	199.9
18	474.9	115.2	863.5	192.5	1253.5	199.2
19	499.9	135.7	981.5	194.2	1187.6	194.9
20	655.3	168.1 *	1232.8	193.9	1232.8	193.9
21	824.6	168.1 *	1232.8	193.9	1232.8	193.9
22	994.0	168.1 *	1232.8	193.9	1232.8	193.9
23	1167.5	168.1 *	1232.8	193.9	1232.8	193.9
24	1341.1	168.1 *	1232.8	193.9	1232.8	193.9
25	1511.2	168.1 *	1232.8	193.9	1232.8	193.9
26	1681.3	168.1 *	1232.8	193.9	1232.8	193.9
27	1859.9	168.1 *	1232.8	193.9	1232.8	193.9
28	1999.2	168.1 *	1232.8	193.9	1232.8	193.9
29	2292.4	168.1 *	1232.8	193.9	1232.8	193.9
30	2449.7	168.1 *	1232.8	193.9	1232.8	193.9
31	2607.0	168.1 *	1232.8	193.9	1232.8	193.9
32	2777.6	168.1 *	1232.8	193.9	1232.8	193.9
33	2948.3	168.1 *	1232.8	193.9	1232.8	193.9

* - INDICATES CLOUD STABILIZATION TIME WAS USED

ROCKET EXHAUST EFFLUENT DIFFUSION MODEL REEDM

PAGE 6

VERSION 7.07 AT VAFB

0932 PDT 16 AUG 1996

launch time: 1318 PST 05 DEC 1995

RAWINSONDE ASCENT NUMBER 208, 2103 Z 5 DEC 1995 T -0.2 HR

----- EXHAUST CLOUD -----

CHEMICAL SPECIES = HCL

MET. LAYER NO.	TOP OF LAYER (METERS)	LAYER SOURCE STRENGTH (GRAMS)	CLOUD UPDRAFT VELOCITY (M/S)	CLOUD RADIUS (METERS)	STD. DEVIATION ALONGWIND (METERS)	MATERIAL DIST. CROSSWIND (METERS)
1	16.5	0.000000E+00	8.9	0.0	0.0	0.0
2	27.3	0.000000E+00	9.8	0.0	0.0	0.0
3	38.1	0.000000E+00	9.9	0.0	0.0	0.0
4	50.1	0.000000E+00	9.7	0.0	0.0	0.0
5	62.2	0.000000E+00	9.4	0.0	0.0	0.0
6	76.8	0.000000E+00	8.9	0.0	0.0	0.0
7	91.4	0.000000E+00	8.4	0.0	0.0	0.0
8	106.1	0.000000E+00	7.9	0.0	0.0	0.0
9	138.1	0.000000E+00	6.9	0.0	0.0	0.0
10	169.0	0.000000E+00	6.1	0.0	0.0	0.0
11	199.9	1.59923E+04	5.4	37.0	17.2	17.2
12	249.9	2.98378E+05	4.6	189.5	88.3	88.3
13	312.4	8.29241E+05	3.8	282.1	131.5	131.5
14	349.9	6.94183E+05	3.3	332.5	154.9	154.9
15	399.9	1.10050E+06	2.7	362.7	169.0	169.0
16	424.9	6.07703E+05	2.3	380.8	177.5	177.5
17	449.9	6.35626E+05	2.0	389.5	181.5	181.5
18	474.9	6.55765E+05	1.5	395.6	184.3	184.3
19	499.9	6.68119E+05	0.9	399.3	186.1	186.1
20	655.3 *	5.31054E+06	0.0	393.2	183.2	183.2
21	824.6 *	3.74712E+06	0.0	291.6	135.9	135.9
22	994.0 *	1.30680E+06	0.0	132.8	61.9	61.9
23	1167.5 *	1.19205E+06	0.0	199.9	93.2	93.2
24	1341.1 *	1.09802E+06	0.0	199.9	93.2	93.2
25	1511.2 *	1.00232E+06	0.0	199.9	93.2	93.2
26	1681.3 *	9.41992E+05	0.0	199.9	93.2	93.2
27	1859.9 *	9.34395E+05	0.0	199.9	93.2	93.2
28	1999.2 *	6.94922E+05	0.0	199.9	93.2	93.2
29	2292.4 *	1.38047E+06	0.0	199.9	93.2	93.2
30	2449.7 *	7.00545E+05	0.0	199.9	93.2	93.2
31	2607.0 *	6.76216E+05	0.0	199.9	93.2	93.2
32	2777.6 *	7.08949E+05	0.0	199.9	93.2	93.2
33	2948.3 *	6.85368E+05	0.0	199.9	93.2	93.2

* - INDICATES CLOUD STABILIZATION TIME WAS USED

1*****
ROCKET EXHAUST EFFLUENT DIFFUSION MODEL REEDM PAGE 7
VERSION 7.07 AT VAFB
0932 PDT 16 AUG 1996
launch time: 1318 PST 05 DEC 1995
RAWINSONDE ASCENT NUMBER 208, 2103 Z 5 DEC 1995 T -0.2 HR

----- CLOUD STABILIZATION -----

CALCULATION HEIGHT	(METERS)	0.00
STABILIZATION HEIGHT	(METERS)	514.55
STABILIZATION TIME	(SECS)	168.10
FIRST MIXING LAYER HEIGHT-	(METERS)	TOP = 106.07
		BASE= 0.00
SECOND SELECTED LAYER HEIGHT-	(METERS)	TOP = 2948.33
		BASE= 106.07
SIGMAR(AZ) AT THE SURFACE	(DEGREES)	8.9304
SIGMER(EL) AT THE SURFACE	(DEGREES)	1.1549

MET. LAYER NO.	WIND SPEED (M/SEC)	WIND SPEED SHEAR (M/SEC)	WIND DIRECTION (DEG)	WIND DIRECTION SHEAR (DEG)	SIGMA OF AZI ANG (DEG)	SIGMA OF ELE ANG (DEG)
1	4.83	1.03	6.50	13.00	8.2255	2.8775
2	5.04	0.21	11.52	-2.95	7.6369	5.7750
3	4.84	0.21	8.57	-2.95	8.5266	8.1250
4	4.84	0.21	4.82	-4.55	9.6250	9.6250
5	5.04	0.21	0.27	-4.55	10.2750	10.2750
6	5.53	0.77	353.75	-8.50	9.8250	9.8250
7	6.30	0.77	345.25	-8.50	8.2750	8.2750
8	7.49	1.59	343.50	5.00	4.2500	4.2500
9	9.52	2.47	346.00	0.00	1.0000	1.0000
10	10.53	-0.44	347.75	3.50	1.0000	1.0000
11	10.10	-0.44	351.25	3.50	1.0000	1.0000
12	9.13	-1.49	356.50	7.00	1.0000	1.0000
13	8.46	0.15	8.35	16.70	1.0000	1.0000
14	9.36	1.65	20.85	8.30	1.0000	1.0000
15	8.75	-2.88	21.00	-8.00	1.0000	1.0000
16	7.58	0.54	23.00	12.00	1.0000	1.0000
17	8.12	0.54	35.00	12.00	1.0000	1.0000
18	7.72	-1.34	33.50	-15.00	1.0000	1.0000
19	6.38	-1.34	18.50	-15.00	1.0000	1.0000
20	7.31	3.19	18.35	14.70	1.0000	1.0000
21	8.67	-0.46	19.27	-12.85	1.0000	1.0000
22	8.21	-0.46	6.42	-12.85	1.0000	1.0000
23	7.90	-0.15	358.88	-2.25	1.0000	1.0000
24	7.74	-0.15	356.63	-2.25	1.0000	1.0000
25	7.59	-0.15	353.20	-4.60	1.0000	1.0000
26	7.43	-0.15	348.60	-4.60	1.0000	1.0000
27	7.43	0.15	338.90	-14.80	1.0000	1.0000
28	7.46	-0.10	325.00	-13.00	1.0000	1.0000
29	6.92	-0.98	312.70	-11.60	1.0000	1.0000
30	6.15	-0.57	302.60	-8.60	1.0000	1.0000

ROCKET EXHAUST EFFLUENT DIFFUSION MODEL REEDM

PAGE 8

VERSION 7.07 AT VAFB

0932 PDT 16 AUG 1996

launch time: 1318 PST 05 DEC 1995

RAWINSONDE ASCENT NUMBER 208, 2103 Z 5 DEC 1995 T -0.2 HR

----- CALCULATED METEOROLOGICAL LAYER PARAMETERS -----

MET. LAYER NO.	WIND SPEED (M/SEC)	WIND SPEED SHEAR (M/SEC)	WIND DIRECTION (DEG)	WIND DIRECTION SHEAR (DEG)	SIGMA OF AZI ANG (DEG)	SIGMA OF ELE ANG (DEG)
31	5.58	-0.57	294.00	-8.60	1.0000	1.0000
32	5.18	-0.23	287.20	-5.00	1.0000	1.0000
33	4.95	-0.23	282.20	-5.00	1.0000	1.0000

ALTITUDE RANGE USED IN COMPUTING TRANSITION LAYER AVERAGES
IS 0.0 TO 994.0 METERS.

TRANSITION LAYER NUMBER- 1

VALUE AT	HEIGHT (METERS)	TEMP. (DEG K)	WIND SPEED (M/SEC)	WIND SPEED SHEAR (M/SEC)	WIND DIR. (DEG)	WIND DIR. SHEAR (DEG)	SIGMA AZI. (DEG)	SIGMA ELE. (DEG)
TOP-	106.07	290.68	8.28		346.00		1.0000	1.0000
LAYER-			5.46	0.89	356.90	8.13	8.2672	7.2472
BOTTOM-	0.00	292.17	4.12		360.00		8.9304	1.1549

TRANSITION LAYER NUMBER- 2

VALUE AT	HEIGHT (METERS)	TEMP. (DEG K)	WIND SPEED (M/SEC)	WIND SPEED SHEAR (M/SEC)	WIND DIR. (DEG)	WIND DIR. SHEAR (DEG)	SIGMA AZI. (DEG)	SIGMA ELE. (DEG)
TOP-	2948.33	308.88	4.84		279.70		1.0000	1.0000
LAYER-			8.21	0.70	11.76	9.60	1.0000	1.0000
BOTTOM-	106.07	290.68	8.28		346.00		1.0000	1.0000

```

1*****
ROCKET EXHAUST EFFLUENT DIFFUSION MODEL REEDM          PAGE    9
VERSION 7.07 AT VAFB
0932 PDT 16 AUG 1996
launch time: 1318 PST 05 DEC 1995
RAWINSONDE ASCENT NUMBER    208, 2103    Z    5 DEC 1995    T    -0.2 HR
*****

```

----- MAXIMUM CENTERLINE CALCULATIONS -----

** DECAY COEFFICIENT (1/SEC) = 0.00000E+00 **

CONCENTRATION OF HCL AT A HEIGHT OF 0.0 METERS
DOWNWIND FROM A TITAN IV NORMAL LAUNCH
CALCULATIONS APPLY TO THE LAYER BETWEEN 0.0 AND 106.1 METERS

RANGE FROM PAD (METERS)	BEARING FROM PAD (DEGREES)	PEAK CONCEN- TRATION (PPM)	CLOUD ARRIVAL TIME (MIN)	CLOUD DEPARTURE TIME (MIN)

** NO HCL			FOUND **	

 ROCKET EXHAUST EFFLUENT DIFFUSION MODEL REEDM

PAGE . 10

VERSION 7.07 AT VAFB

0932 PDT 16 AUG 1996

launch time: 1318 PST 05 DEC 1995

RAWINSONDE ASCENT NUMBER 208, 2103 Z 5 DEC 1995 T -0.2 HR

 ----- MAXIMUM CENTERLINE CALCULATIONS -----

** DECAY COEFFICIENT (1/SEC) = 0.00000E+00 **

CONCENTRATION OF HCL AT A HEIGHT OF 0.0 METERS

DOWNWIND FROM A TITAN IV NORMAL LAUNCH

CALCULATIONS APPLY TO THE LAYER BETWEEN 0.0 AND 106.1 METERS

RANGE FROM PAD (METERS)	BEARING FROM PAD (DEGREES)	TOTAL DOSAGE (PPM SEC)	CLOUD ARRIVAL TIME (MIN)	CLOUD DEPARTURE TIME (MIN)

** NO HCL

FOUND **

```

1*****
      ROCKET EXHAUST EFFLUENT DIFFUSION MODEL REEDM          PAGE  11
      VERSION 7.07 AT VAFB
      0932 PDT 16 AUG 1996
      launch time: 1318 PST 05 DEC 1995
      RAWINSONDE ASCENT NUMBER 208, 2103  Z  5 DEC 1995  T  -0.2 HR
*****

```

----- MAXIMUM CENTERLINE CALCULATIONS -----

** DECAY COEFFICIENT (1/SEC) = 0.00000E+00 **

CONCENTRATION OF HCL AT A HEIGHT OF 0.0 METERS
 DOWNWIND FROM A TITAN IV NORMAL LAUNCH
 CALCULATIONS APPLY TO THE LAYER BETWEEN 0.0 AND 106.1 METERS

		30.0 MIN.		
RANGE	BEARING	MEAN	CLOUD	CLOUD
FROM PAD	FROM PAD	CONCEN-	ARRIVAL	DEPARTURE
(METERS)	(DEGREES)	TRATION	TIME	TIME
		(PPM)	(MIN)	(MIN)

 ** NO HCL FOUND **

***REEDM WARNING 04, CONCENTRATION IS ZERO FOR CENTERLINE PLOTS.

Appendix B—Meteorological Data

[Provided by Steven Sambol, Staff Meteorologist, 30th Space Wing (AFSPACECOM), Vandenberg AFB, CA.]

Meteorological data were measured at a number of VAFB monitoring locations prior to launch and during development and dispersion of the launch cloud. Representative data of three different types are tabulated here. Data are first presented for meteorological measurements performed at numerous meteorological towers at various base elevations in feet above mean sea level. Note that the #K15 launch occurred at 2118 Zulu time (Zulu time is PST + 8 h), and data are provided shortly before and after launch. Data are presented on the wind direction in degrees azimuth, the mean wind speed in knots, and the ambient and dew point temperatures in degrees Rankine at these locations. See Vandenberg Wind Tower Network at the end of these tables for locations, instrument height, measurements and base elevations of the towers.

Doppler Acoustic Sounder System (DASS) data are presented second. These data were determined at the four locations on base noted. Included in the tabulated data are measurement height above instrument, H, horizontal wind direction azimuth, DIR, horizontal and vertical wind speed, HSPD and VSPD, standard deviation of the horizontal direction, HDEV, standard deviation of horizontal speed, HSDV, and standard deviation of vertical speed, VSDV. Vertical speed may be negative but all other values are positive.

Composite data collected at T-15 min are presented last, with the measurements in the units noted. This data is a combination of what is considered to be the most accurate data measurements from tower, DASS and Rawinsonde data at the T-15 min time.

Meteorological Tower Data at 2055Z 5 Dec 95 (T-23 min)—Atmospheric Pressure at Tower 60–1012 mmHg

Tower #	Level (ft)	Dir (deg)	Mean Speed (kt)	Mean Temp (°F)	Dew Pt. (°F)	Max Gust (kt)	Mean Deviation
4	12	359	13	-	-	18	43
5	12	330	10	-	-	16	60
7	12	309	10	-	-	15	50
8	12	357	8	-	-	14	78
14	12	9	5	-	-	5	0
15	6	-	-	71.2	-	-	-
15	12	310	6			11	97
17	12	305	8			12	152
18	12	299	11			16	54
20	12	319	5			13	203
50	12	315	12			18	15
51	12	324	10			16	58
51	54	317	15	66.2	-	18	31
52	12	326	11			17	63
52	54	330	14	65.3		19	43
53	6			75.8			
53	12	336	16			25	36
53	54	344	20	71.5		27	34
54	6			63.0			
54	12	341	8			14	76
54	54	328	9	61.1		16	54
55	6			65.0			
55	12	276	17	62.4		25	67
56	6	626					
56	12	43	23			33	15
57	6			62.8			
57	12	301	6			11	66
57	54	303	8	61.5		14	48
58	6			72.8			
58	12	323	11			16	35
58	54	317	13	69.5		18	35
60	6			69.0			
60	12	319	13			18	30
60	54	322	15	65.8	49.0	20	16
64	6			63.0			
64	12	348	10			16	35
64	54	335	12	61.6		16	39
65	6			63.6			
65	12	338	15			23	29
65	54	337	20	63.0		25	24
66	6			67.8	58.2		
66	12	281	10			14	40
66	54	332	12	65.7		15	1
101	6			63.0			
101	12	332	10			14	59
101	54	343	11	61.6		16	48

Tower #	Level (ft)	Dir (deg)	Mean Speed (kt)	Mean Temp (°F)	Dew Pt. (°F)	Max Gust (kt)	Mean Deviation
102	6			62.2			
102	12	327	10			14	40
102	54	327	11	60.0		15	23
102	102	329	12			17	19
200	6			73.6			
200	12	351	11			18	112
200	54	360	14	64.7		18	76
200	102	0	15			22	118
200	204	359	10	64.9		18	84
300	6			61.6			
300	12	9	8			13	89
300	54	24	9	59.5		13	70
300	102	12	9	60.5		15	76
300	108	21	9			13	77
300	204	6	10	59.6		17	71
300	300	348	11	59.5		18	57
301	6			65.0	53.0		
301	12	357	14			21	46
301	54	356	18	64.5	57.0	22	35
301	102	1	19	62.3	53.2	23	33
301	204	350	1	61.8	54.0	4	150
301	300	0	0	63.5	53.0	1	

Meteorological Tower Data at 2120Z 5 Dec 95 (T+2 min)—Atmospheric Pressure at Tower 60—1012.04 mmHg

Tower #	Level (ft)	Dir (deg)	Mean Speed (kt)	Mean Temp (°F)	Dew Pt. (°F)	Max Gust (kt)	Mean Deviation
4	12	1	13	-	-	19	41
5	12	322	12	-	-	16	53
7	12	307	8	-	-	15	49
8	6	-	-	78.5	-	-	-
8	12	355	9	-	-	14	68
14	12	9	5	-	-	5	0
15	6	-	-	71.8	-	-	-
15	12	315	8	-	-	13	108
17	12	296	8	-	-	12	147
18	12	303	12	-	-	15	164
20	6	-	-	73.6	-	-	-
20	12	334	4	-	-	10	205
50	6	-	-	65.0	-	-	-
50	12	321	12	-	-	18	39
50	54	334	11	66.2	-	20	168
51	6	-	-	67.4	-	-	-
51	12	334	8	-	-	14	68
51	54	328	11	66.3	-	18	47
52	6	-	-	73.0	-	-	-
52	12	333	12	-	-	17	60
52	54	336	15	65.3	-	19	43
53	6	-	-	73.0	-	-	-
53	12	335	20	-	-	26	57
53	54	342	24	69.6	-	30	42
54	6	-	-	61.2	-	-	-
54	12	333	8	-	-	13	62
54	54	322	10	59.4	-	15	47
55	6	-	-	63.4	-	-	-
55	12	267	19	61.5	-	25	92
56	6	-	-	60.0	-	-	-
56	12	42	23	-	-	33	22
57	6	-	-	63.0	-	-	-
57	12	313	6	-	-	12	86
57	54	317	7	62.1	-	13	72
58	6	-	-	71.6	49.0	-	-
58	12	328	13	-	-	21	57
58	54	321	16	68.1	-	22	54
60	6	-	-	67.2	52.6	-	-
60	12	325	14	-	-	18	38
60	54	326	17	63.8	49.0	21	31
64	6	-	-	62.0	-	-	-
64	12	349	11	-	-	16	27
64	54	339	13	60.9	-	18	34
65	6	-	-	63.2	-	-	-
65	12	339	15	-	-	23	17
65	54	340	20	62.8	-	24	17

Tower #	Level (ft)	Dir (deg)	Mean Speed (kt)	Mean Temp (°F)	Dew Pt. (°F)	Max Gust (kt)	Mean Deviation
66	6	-	-	66.0	58.0	-	-
66	12	285	12	-	-	16	49
66	54	334	13	63.8	-	17	19
101	6	-	-	63.0	-	-	-
101	12	337	10	-	-	15	57
101	54	343	12	61.9	-	16	54
102	6	-	-	62.0	-	-	-
102	12	335	11	-	-	16	45
102	54	335	13	59.8	-	18	32
102	102	335	14	-	-	19	26
200	6	-	-	72.8	-	-	-
200	12	1	6	-	-	12	105
200	54	13	8	64.7	-	13	87
200	102	28	9	-	-	15	139
200	108	15	2	64.6	-	11	99
300	6	-	-	61.4	-	-	-
300	12	4	7	-	-	13	76
300	54	16	9	59.1	-	14	72
300	102	3	8	60.2	-	12	68
300	108	11	8	-	-	13	65
300	204	0	9	59.1	-	14	57
300	300	344	12	58.7	-	19	43
301	6	-	-	64.4	53.4	-	-
301	12	4	11	-	-	17	55
301	54	2	14	63.9	57.0	19	57
301	102	5	16	61.7	54.0	21	47
301	204	350	2	60.8	54.0	4	39
301	300	0	0	63.5	54.0	1	-

Vandenberg Wind Tower Network

Tower #	Lat N x Lon W	Location/Bldg	Elevation (ft)	Inst. Ht. (ft)	Readouts
004	34.31.51 120.33.55	Agena Tank Farm/B1180	395	12	Direction & Speed
005	34.45.13 120.34.16	Upper Air Observatory/B1764	330	12	Direction & Speed
007	34.43.57 120.32.01	Motor Pool/B10004	445	12	Direction & Speed
008	34.49.32 120.30.30	Vandenberg Tracking Station/B23251	920	6 12	Temperature, Direction, Spd
014	34.36.31 120.31.31	Freq. Interference Control/ B440 SVAFB	1450	12	Direction, speed
015	34.46.16 120.31.51	Base Weather Station/B21150	570	6 12	Temperature, Direction, Spd.
017	34.52.56 120.38.12	LF-06 B1980	125	12	Direction, speed
018	34.50.42 120 34 57	LF-02	300	12	Direction & Speed
020	34.36.27 120 27 52	Miguelito Canyon (Off Base) (SVAFB)	309	20	Temperature, Direction, Spd.
050	34.48.02 120 35 55	Bomarc	135	54	Temp, Delta temp, direction and speed
051	34.42.36 120 33 55	STS V21/V19, OMCF	400	54	Temp, Delta temp, direction and speed
052	34.44.09 120 35 43	Pad 395C	200	54	Temp, Delta temp, direction and speed
053	34.33.24 120 36 42	Boathouse (SVAFB)	55	54	Temp, Delta temp, direction and speed
054	34.38.31 120 35 28	SLC-3 (SVAFB)	450	54	Temp, Delta temp, direction and speed
055	34.35.14 120 35 39	Remote Radar Site (SVAFB)	1530	54	Temp, Delta temp, direction and speed
056	34.34.59 120 33 40	Tranquillon Radar (SVAFB)	2140	54	Temperature, direction & spd
057	34.40.01 120 35 21	HSSF (SVAFB)	296	54	temp, Delta temp, dir. spd.
058	34.41.50 120 32 17	Titan Tank Farm	375	54	temp, Delta temp, direction and speed
059	34.48.08 120 34 52	MAB	226	54	temp, dew pt, barometer, direction & spd
060	34.50.59 120 35 57	LF-08	121	54	temp, dew pt, barometer, delta temp, direction & spd
061	34.38.33 120 33 21	UHF Road (SVAFB)	504	54	temp, delta temp, direction & speed
064	34.36.50 120 33 03	Motr Bore Site (SVAFB)	1200	54	temp, delta temp, direction & speed
065	34.33.59 120 29 59	Oak Mountain Telemetry (SVAFB)	2053	54	temp, delta temp, direction & speed
066	34.39.54 120 33 17	NASA	27	54	temp, dew pt, delta temp, direction & spd
101	34.36.38 120 33 58	Range Ops (SVAFB)	1080	102	temp, delta temp. direction & speed
102	34.45.30 120 37 18	SLC-2	215	102	temp, delta temp, direction & speed

Tower #	Lat N x Lon W	Location/Bldg	Elevation (ft)	Inst. Ht. (ft)	Readouts
200	34.36.28 120 37 35	SLC-5 (SVAFB)	310	204	temp, delta temp, direction & speed
300	34.38.01 120 36 50	SLC-4 (SVAFB)	385	300	temp, delta temp, direction & speed
301	34.34.48 120 37 57	SLC-6 (SVAFB)	380	300	temp, dew pt, barometer, rain gauge, visiometer, short & long wave rad, direction & spd

Doppler Acoustic Sounder System (DASS) Data at 2055Z 5 Dec 95 (T-23 min)

DASS#1

Inversion Layer measured at 180m

Location: Bldg. 900 at 34 39 49.95 N Latitude x 120 34 43.75 W Latitude

Elevation: 367 ft above Mean Sea Level

H (m)	DIR °	HSPD m/s	VSPD m/s	HDEV °	HSDV m/s	VSDV m/s
0	321	9.8	6.9	1.8	2	1
50	312	6.5	-3	3.7	4	2
150	324	9.3	-3	3.4	4	2
200	333	9.3	-1	3.7	5	3
250	336	8.3	-2	3.9	4	2
300	342	8.2	-4	4.6	6	2
350	348	8.1	-3	4.7	6	2
400	357	8.3	-2	4.8	7	2
450	358	6.4	-4	4.3	3	2
500	3	8.7	-5	4.7	7	2
550	6	8.5	-3	3.6	4	2
650	NO DATA	NO DATA	NO DATA	NO DATA	NO DATA	NO DATA
700	581	3.1	-9	2.3	4	4
750	491	3.5	-3	2.0	3	2
800	8	9.8	-10	4.4	8	8
850	43	8.0	-2.3	4.1	5	11
900	26	5.6	-4.0	87	10	6
950	25	7.5	-3.8	6.8	11	21

DASS #2

Inversion Layer measured at 100m

Location: Space Launch Complex 4 at 34 38 9.15 N Latitude x 120 36 56.05 W Longitude

Elevation: 307 ft above Mean Sea Level

H (m)	DIR °	HSPD m/s	VSPD m/s	HDEV °	HSDV m/s	VSDV m/s
0	291	4.9	4	6.9	9	1
50	314	5.8	1	6.9	1.9	1.0
100	327	10.2	1.3	3.2	5.0	1.2
150	330	12.7	10.3	3.1	4.9	1.4
200	348	11.2	7.6	4.6	5.6	1.2
250	100	13.1	-1.0	4.2	4.1	0.9
300	55	7.4	5.9	9.9	1	9
350	010	12.0	4.6	0.6	5.9	1.0
400	053	22.7	3.0	NO DATA	NO DATA	1.0
450	097	17.0	7.3	5.6	6.2	1.4
500	061	22.8	6.9	NO DATA	NO DATA	1.4
550	102	16.0	6.3	6.7	6.6	1.2
600	012	5.3	6.9	NO DATA	NO DATA	1.3
650	071	8.4	0.4	8.9	4	8
700	113	10.7	2.9	NO DATA	NO DATA	7
750	068	10.6	1.2	4.3	1.2	1.4
800	112	14.1	NO DATA	NO DATA	NO DATA	1.6
850	111	14.0	2.6	NO DATA	NO DATA	2.1
900	118	14.4	2.1	NO DATA	NO DATA	2.3

DASS #3 Inversion layer measured at 150m
 Location: Bldg. 1764 at 34 45 15.61 N Latitude x 120 34 18.94 W Longitude
 Elevation: 322 ft. above Mean Sea Level

H (m)	DIR °	HSPD m/s	VSPD m/s	HDEV °	HSDV m/s	VSDV m/s
0	349	3.0	0	9.5	9	3
50	9	4.5	-6	227	2.0	3.7
100	349	7.4	-4	107	2.6	3.9
150	356	9.3	6	184	4.1	4.6
200	92	5.5	1	177	2.3	4.7
250	14	6.8	2.0	609	3.3	6.7
300	169	4.2	1.8	304	3.6	6.3
350	72	7.1	2.0	201	3.3	8.0
400	34	6.2	2.7	544	3.1	6.5
450	48	4.9	2.9	269	3.7	6.2
500	74	5.2	9.0	267	2.7	5.4
550	52	8.5	6.0	390	4.2	6.7
600	55	8.0	-6	520	3.5	5.6
650	74	8.7	2.3	505	2.8	6.1
700	98	11.1	-7	352	7.6	7.6
750	81	10.6	0	379	7.4	7.3
800	128	20.5	2.3	197	11.4	6.2
850	110	12.8	3	211	8.5	8.5
900	92	11.3	5	252	9.1	7.5
950	109	14.9	7.6	223	7.9	5.5
1000	105	17.0	3.8	245	7.3	8.4

DASS #4 Inversion layer measured at 112m
 Location: LF-03 at 34 50 44.42 N Latitude x 120 34 53.58 W Longitude
 Elevation: 301 ft. above Mean Sea Level

H (m)	DIR °	HSPD m/s	VSPD m/s	HDEV °	HSDV m/s	VSDV m/s
0	298	2.5	2	20	2.9	9.9
50	304	7.2	-5	54	5	3
100	314	6.9	-4	45	4.0	2.0
150	336	5.6	-4	57	5.0	3.0
200	357	6.0	-5	59	5.0	3.0
250	2	6.6	-4	53	5.0	4.0
300	14	7.3	-4	49	6.0	4.0
350	25	7.6	-5	43	5.0	2.0
400	28	7.6	-3	42	4.0	3.0
450	34	8.0	-3	38	4.0	3.0
500	43	8.1	-4	37	4.0	5.0
550	45	8.5	-4	35	4.0	4.0
600	46	9.6	-4	28	3.0	2.0
650	NO DATA	NO DATA	NO DATA	NO DATA	NO DATA	NO DATA
700	722	6.1	-3	13	5	2
750	441	1.6	-3	31	6	2
800	431	9.0	-3	28	4	3
850	45	9.8	-6	30	4	3
900	47	10.2	-9	35	5	6
950	NO DATA	NO DATA	NO DATA	NO DATA	NO DATA	NO DATA

Doppler Acoustic Sounder System (DASS) Data at 2120Z 5 Dec 95 (T+2 min)

DASS#1 Inversion Layer measured at 180m
 Location: Bldg. 900 at 34 39 49.95 N Latitude x 120 34 43.75 W Longitude
 Elevation: 367 ft. above Mean Sea Level

H (m)	DIR °	HSPD m/s	VSPD m/s	HDEV °	HSDV m/s	VSDV m/s
0	323	1.01	6.9	1.7	3	1
50	312	8.8	-6	3.3	6	4
100	322	10.8	-4	3.3	6	4
150	326	11.7	-3	3.1	6	3
200	333	10.9	-2	3.2	5	4
250	338	10.0	-2	3.6	6	4
300	344	9.0	-3	3.8	5	3
350	348	8.6	-3	3.9	5	4
400	351	7.7	-6	4.2	4	5
450	1	8.4	-4	4.3	6	3
600	381	1.0	-10	5.0	13	2
650	421	1.7	-15	4.4	12	8
800	391	2.7	-14	4.0	11	5
850	441	4.3	-9	3.2	9	6
950	412	0.8	2.3	2.6	13	21

DASS#2 Inversion layer measured at 800m
Location: Space Launch Complex 4 at 34 38 9.15 N Latitude x 120 36 56.05 W Longitude
Elevation: 307 ft. above Mean Sea Level

H (m)	DIR °	HSPD m/s	VSPD m/s	HDEV °	HSDV m/s	VSDV m/s
0	302	5.7	5	4.0	11	2
50	321	8.8	0	5.8	24	10
100	327	11.7	0	10.6	26	12
150	332	11.7	1.6	6.3	18	15
200	335	10.5	8	1.9	9	8
250	NO DATA	NO DATA	3	NO DATA	NO DATA	6
300	305	7.6	3.6	0.3	34	6
350	355	6.6	5	1.5	2	4
400	NO DATA	NO DATA	-4	NO DATA	NO DATA	4
450	NO DATA	NO DATA	NO DATA	NO DATA	NO DATA	3
500	NO DATA	NO DATA	2	NO DATA	NO DATA	3
550	91	6.7	4.9	7.7	24	6
600	27	7.2	0	3.5	14	7
650	21	9.3	5	1.5	5	7
700	25	7.9	4	3.7	6	3
750	23	8.6	2	NO DATA	NO DATA	2
800	NO DATA	NO DATA	3	NO DATA	NO DATA	NO DATA

DASS#3 Inversion layer measured at 150m
Location: Bldg. 1764 at 34 45 15.61 N Latitude x 120 34 18.94 W Longitude
Elevation: 322 ft. above Mean Sea Level

H (m)	DIR °	HSPD m/s	VSPD m/s	HDEV °	HSDV m/s	VSDV m/s
0	344	3.6	-1	5.3	11	3
50	1	4.8	2.1	6.7	26	10
100	346	7.8	5.1	7.6	31	9
150	346	11.7	7	5.1	24	12
200	353	9.9	6	6.0	18	9
250	0	8.4	6.1	9.0	31	7
300	14	8.0	4.5	6.9	23	9
350	25	10.2	7.6	9.7	5	7
400	17	7.3	3.3	2.3	25	6
450	41	8.4	4.4	5.6	32	5
500	11	5.7	1.0	2.0	13	8
550	39	10.5	-14	1.3	13	8
600	49	9.6	4.5	6.4	26	8
650	21	9.4	2	NO DATA	NO DATA	5
700	64	4.8	3.0	NO DATA	NO DATA	6
750	NO DATA	NO DATA	NO DATA	NO DATA	NO DATA	2
800	63	5.9	2.0	1.0	4	2
850	NO DATA	NO DATA	-1.0	NO DATA	NO DATA	NO DATA
950	NO DATA	NO DATA	4.0	NO DATA	NO DATA	NO DATA
1000	NO DATA	NO DATA	-4	NO DATA	NO DATA	10

DASS#4 Inversion layer measured at 375m
 Location: LF-03 at 34 50 44.42 N Latitude x 120 34 53.58 W Longitude
 Elevation: 301 ft. above Mean Sea Level

H (m)	DIR °	HSPD m/s	VSPD m/s	HDEV °	HSDV m/s	VSDV m/s
0	313	2.8	1.0	9.0	1	NO DATA
50	325	78	-2	4.1	5	3
100	333	7.1	-1	4.9	5	4
150	352	8.7	-3	4.1	5	3
200	358	9.1	-4	3.7	5	3
250	358	9.1	-4	3.7	5	3
300	16	9.5	-7	3.4	5	3
350	27	9.9	-7	3.2	4	2
400	27	9.2	-6	3.2	4	2
450	40	9.7	-9	3.6	5	5
500	49	10.4	-11	3.2	5	7
550	53	11.1	-12	3.4	6	6
600	46	11.6	-9	3.3	6	3
650	53	12.2	-13	3.0	6	7
700	56	12.1	-12	3.3	7	8
750	54	11.6	-11	3.1	6	6
800	51	10.5	-12	3.2	5	6
850	52	1.06	-14	3.7	6	8
900	35	9.5	-10	3.5	5	5
950	45	10.8	-14	2.7	4	9

Composite Atmospheric Data

Date/Time: 5 Dec 95, 2103Z (T-15 minutes)
Site: Bldg. 900, Vandenberg AFB

ALT Geom ft. & source	DIR (deg)	SPEED (kts)	TEMP (°C)	DEWPT (°C)	ATM PRESS (millibars)	REL HUM (%)	DENSITY (gm/M³)
368 T	360	8.0	17.8	11.2	1002.90	65.0	1200.82
422 T	13.0	10.0	16.9	11.0	1000.97	68.0	1199.56
493 T	7.1	9.2	15.8	10.8	998.45	72.0	1197.90
572 T	358.0	10.0	15.6	11.2	995.63	74.8	1195.23
668 T	341.0	13.0	15.3	11.6	992.21	78.3	1191.99
716 D	346.0	16.1	15.2	11.8	990.50	80.0	1190.37
821 D	346.0	20.9	17.9	13.4	986.77	75.0	1174.16
1024 D	353.0	19.2	18.2	12.8	979.71	71.1	1164.67
1188 D	0.0	16.3	18.5	12.4	974.03	67.9	1157.06
1393 D	16.7	16.6	18.8	11.8	966.99	63.9	1147.62
1516 D	25.0	19.8	18.7	11.7	962.78	63.6	1142.92
1680 D	17.0	14.2	18.6	11.5	957.20	63.1	1136.67
1844 D	41.0	16.3	18.6	11.3	951.65	62.6	1130.46
2008 D	11.0	11.1	18.5	11.1	946.13	62.2	1124.29
2518 D	25.7	17.3	18.2	10.5	929.18	60.7	1105.31
3629 R	360.0	15.5	16.7	7.1	893.14	53.2	1068.88
4768 R	355.5	14.9	14.0	5.4	857.38	55.9	1036.09
5884 R	346.3	14.3	13.6	1.8	823.55	44.6	997.35
6470 R	331.5	14.6	12.1	2.6	806.24	52.0	981.27
6927 R	318.5	14.4	11.7	-2.5	792.98	37.0	967.48
7889 R	306.9	12.5	9.9	-4.6	765.60	35.6	940.28
8921 R	289.7	10.3	8.6	-5.6	737.13	35.9	909.58
10041R	279.7	9.4	5.8	-5.7	707.24	43.4	881.37

NOTE: Sources are T= Met. tower 300
D=DASS#2 (SLC-4)
R=Bldg. 900 rawinsonde

Appendix C—Description of Sampling Aircraft

Cloud sampling was performed using a Piper Seminole aircraft, Model PA-44-180. The following pages present a photo of this model, with performance specification data, downloaded from the New Piper Aircraft Inc. Internet Web page and used by permission. Also presented are sketches of the installation of the Geomet instrument probe and the Spectral Sciences instrument. These sketches were prepared to document the external aircraft modifications for FAA approval.

Also included herein is a test report on a wipe sample taken from the wing of the aircraft after the fly-through mission. As would be expected, the sample contained principally aluminum oxide from the solid rocket exhaust, with small amounts of chlorine probably from HCl or its reaction products. Traces of boron, silicon, calcium and iron were also present, possibly from airborne dust in the cloud aerosol.

Piper Seminole



Piper Seminole - PA-44-180

Performance Specifications

Engine

Manufacturer: Lycoming

Model: O-360-A1H6/LO-360-A1H6

Horsepower: 180 hp

Weights

Gross Weight: 3800 lbs/1724 kgs

Standard Empty/Equipped Weight (*b,c): 2586 lbs/1173 kgs

Standard Useful Load (*a): 1230 lbs/558 kgs

Dimensions

Wing Span: 38.6 feet/11.8 meters

Length: 27.6 feet/8.4 meters

Height: 8.5 feet/2.6 meters

Wing Area: 183.8 square feet/17.08 square meters

Fuel Capacity

Usable Fuel: 108 gallons/409 litres

Maximum Speed

TAS at Gross Weight: 168 kts/311 kmh

Cruising Speeds

Normal Cruise Speed: 162 kts/300 kmh

Cruising Range

Cruising Range: 610 nm/1130 km
(45 minute reserves at 75% power)

Stall Speed

Flaps Down Full 40 degrees: IAS 55 kts/IAS 102 kmh

Service Ceiling

Twin Engine (100 fpm): 15,000 feet/4572 meters
Single Engine (50 fpm): 3,800 feet/1158 meters

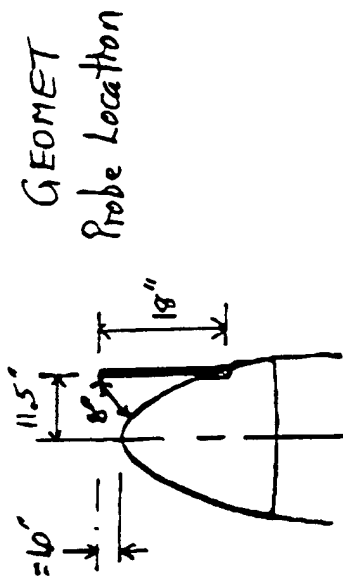
Take-Off Distance

Total over 50-foot obstacle: 2200 feet/671 meters

Landing Distance

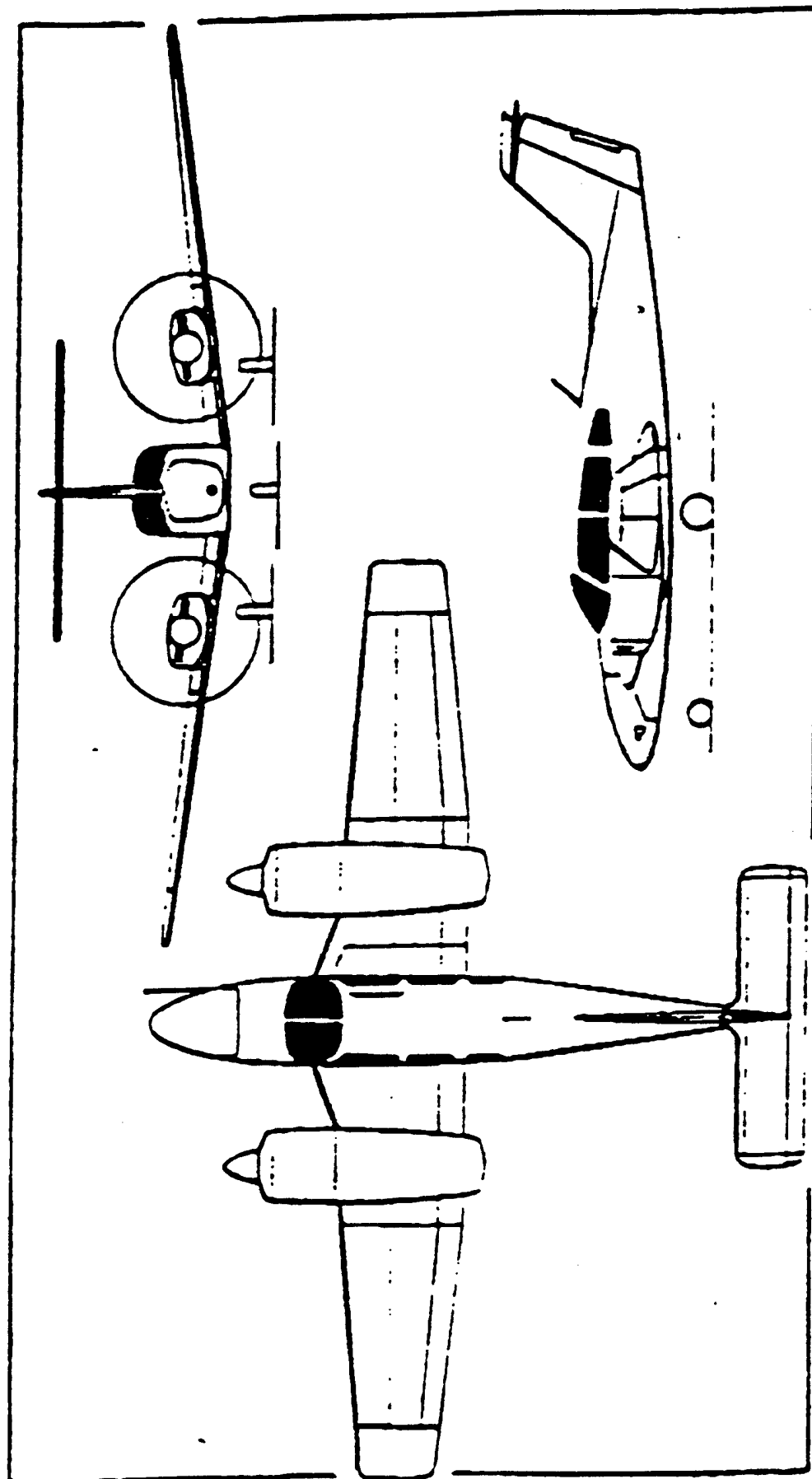
Total over 50-foot obstacle: 1490 feet/454 meters

- *a. Standard Useful load is ramp weight minus standard equipped weight.
- *b. The standard empty weight and standard equipped weight are the same.
- *c. Standard aircraft per marketing.

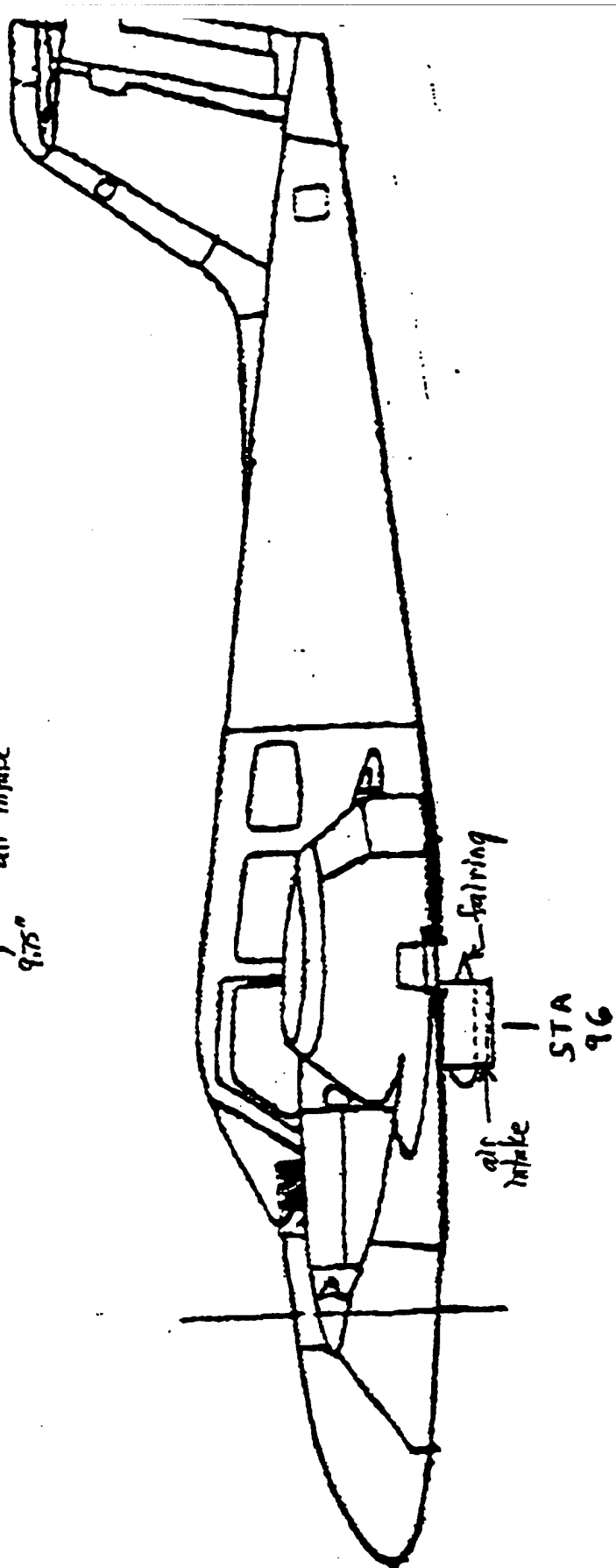
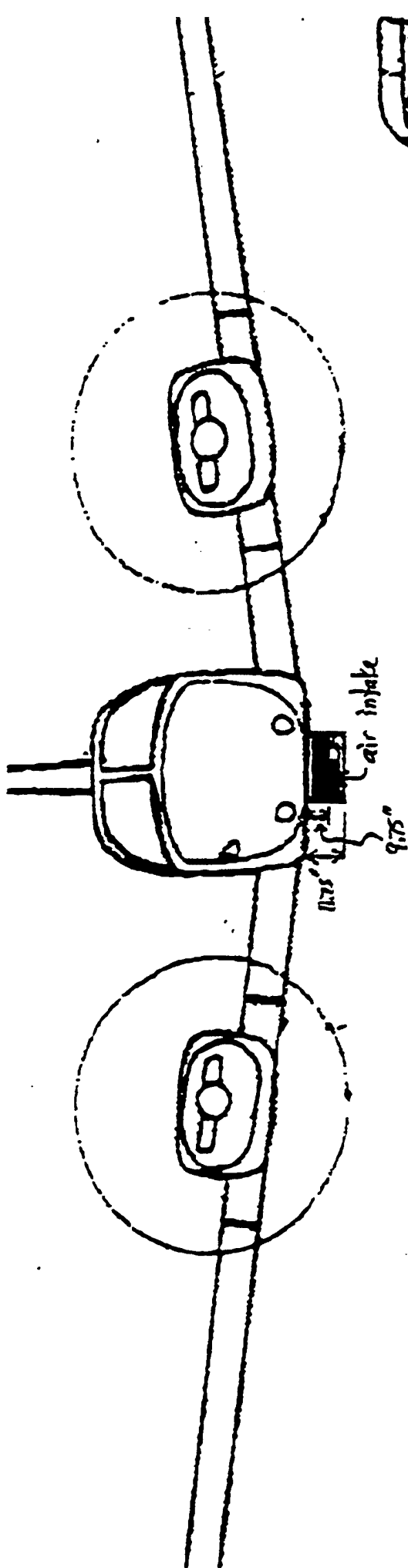


GEOMET
Probe Location

PIPER — AIRCRAFT: USA 441

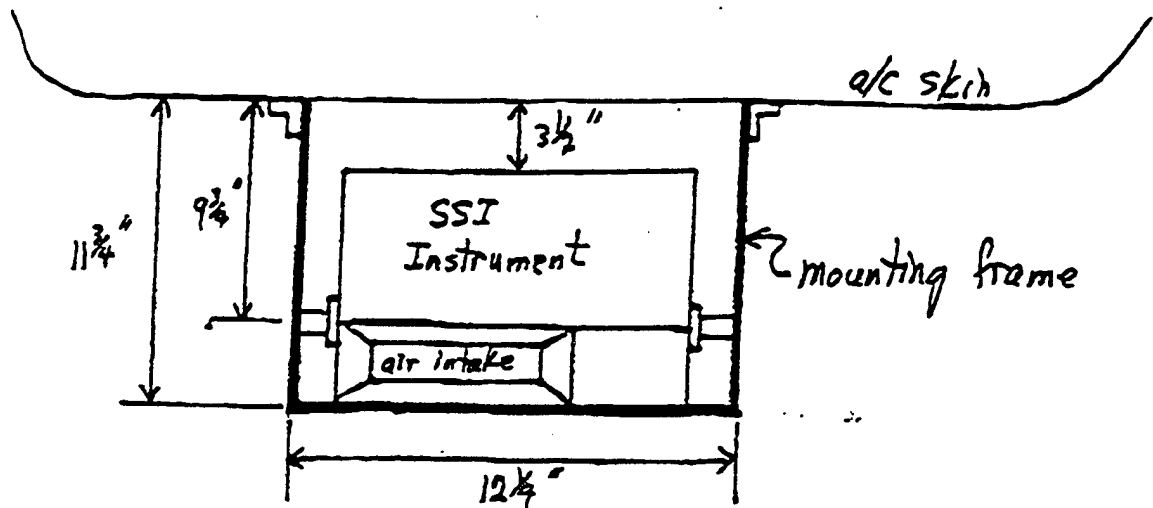


Piper Seminole lightweight twin-engined four-seat cabin monoplane (Pitts Press)

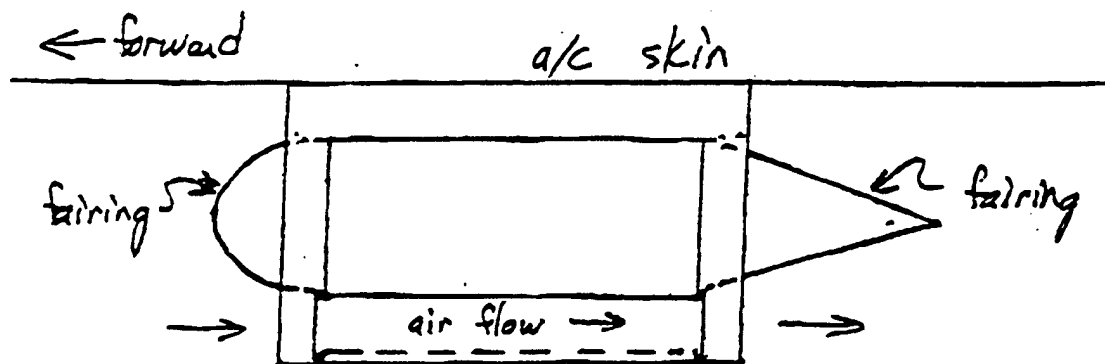


*Spectral Sciences Instrument
Installation*

Spectral Sciences Instrument



Front View



side view

AEROSPACE TECHNICAL MEMORANDUM

ATM NO.: 96(1410-02)-2

TO: Noble Dowling

FROM: MMTC

TITLE: SEM/EDS Analysis of Flight Debris

DATE: 30 January 1996

AUTHOR(S): J.C. Uht

DIVISION: Technology Ops.

FILING SUBJECT(S): SEM Analysis

CCC: 5652

PROJECT OR PROGRAM: Titan Environmental

PAGES: 4

ABSTRACT/SUMMARY

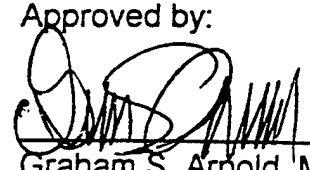
It was observed that after a small plane had flown through a plume of rocket exhaust, a deposit of light brown grit adhered to the leading edge of the plane's wings. A sample of the deposit was wiped off of the wing and the wipe was submitted for SEM and EDS analysis. EDS shows the deposit to be primarily aluminum oxide with trace amounts of Boron, Silicon, Chlorine, Calcium and Iron.

Written by:



Joseph C. Uht
Spacecraft Phenomena
Surface Science

Approved by:



Graham S. Arnold, Manager
Spacecraft Phenomena
Surface Science

It was observed that after a small plane had flown through a plume of rocket exhaust, a deposit of light brown grit adhered to the leading edge of the plane's wings. A sample of the deposit was wiped off of the wing and the wipe was submitted for SEM and EDS analysis. Visually the sample appeared both gritty and oily.

The samples were scraped from the wiper onto a carbon stub. They were then examined in a JEOL 840 SEM using a beam voltage of 15KV. X-ray data were taken using an EDAX 9900 EDS system, with a windowless detector, which is attached to the JEOL SEM.

SEM micrographs 4197 and 4198 as seen in figure 1 show the constituents of the grit to be spheres that range in size from submicron to twenty microns in diameter. The spheres appear to have been melted and resolidified.

EDS spectra as seen in figure 2 indicate that the spheres are primarily aluminum oxide with trace amounts of B, Si, Cl, Ca and Fe. Al_2O_3 is consistent with the deposit arising from the solid rocket plume. The chlorine is probably a remnant of HCL. The reason for the light brown color cannot be given based on these findings.

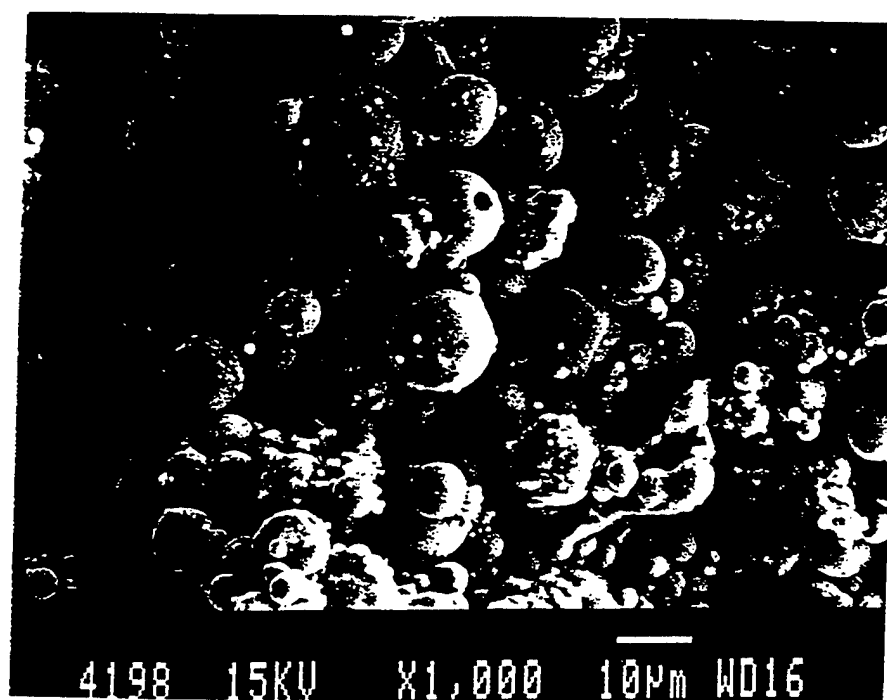
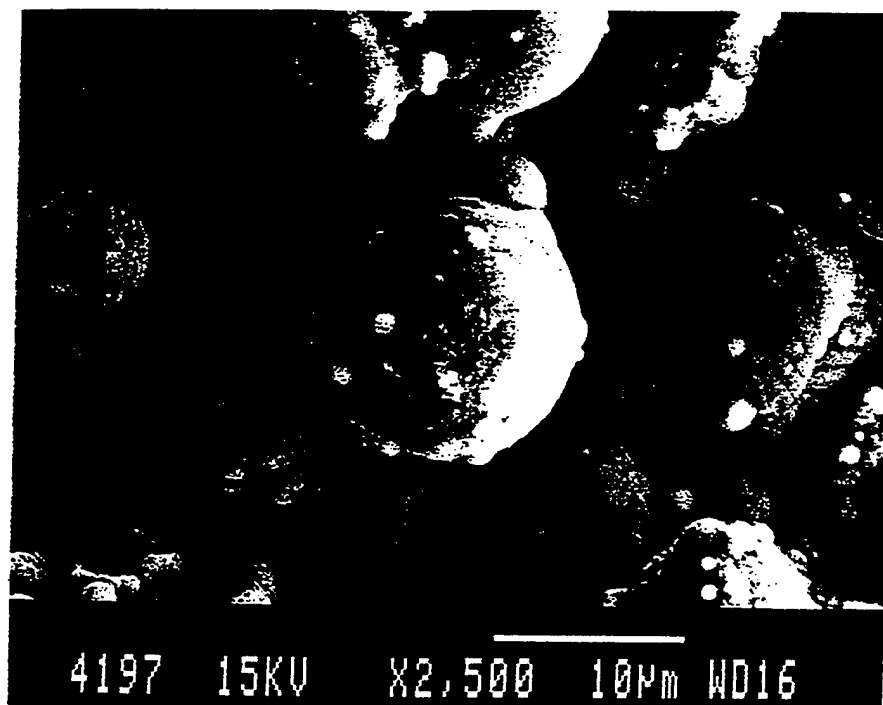
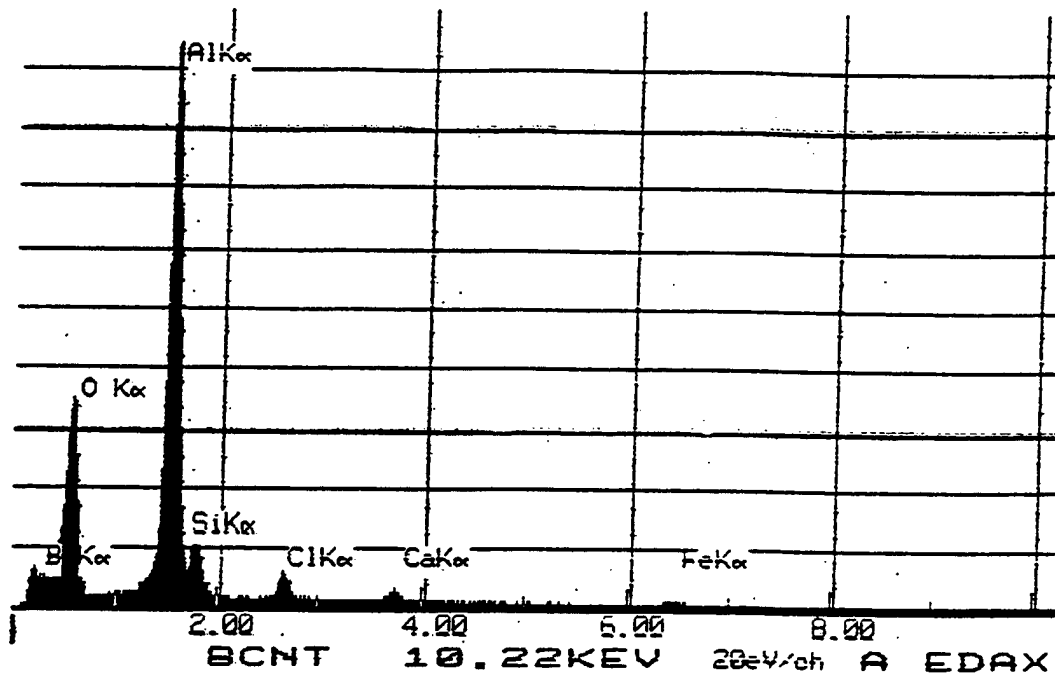


Figure 1

16-JAN-96 14:33:18 EDAX READY
 RATE= 1534CPS TIME= 95LSEC
 FS= 5383CNT PRST= 100CSEC
 A =



16-JAN-96 14:36:14 EDAX READY
 RATE= 0CPS TIME= 95LSEC
 FS= 1345CNT PRST= 100CSEC
 A =

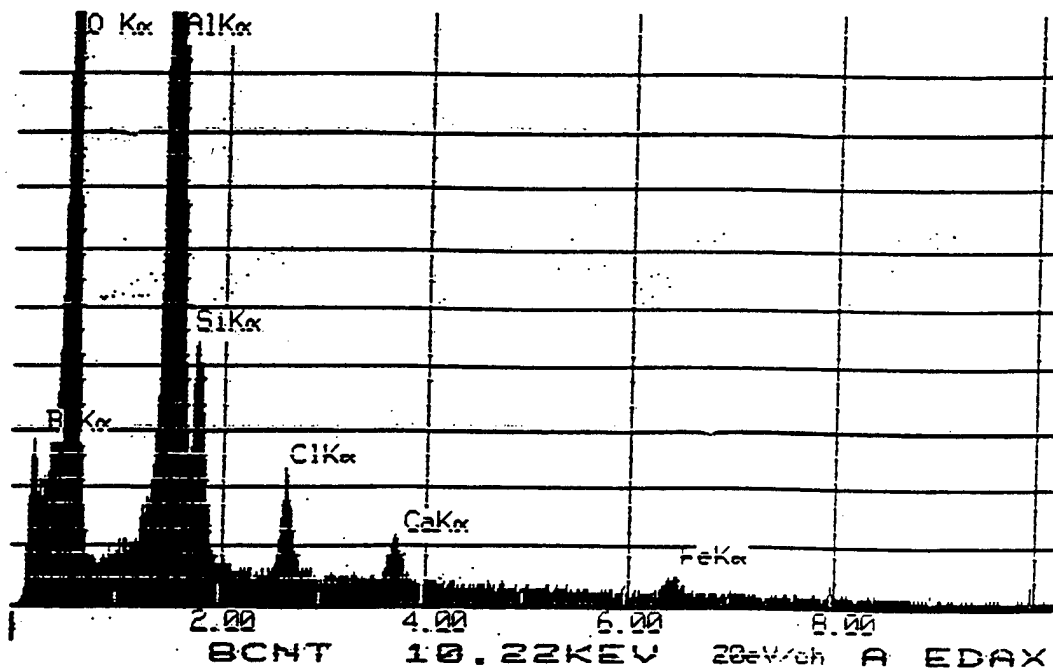


Figure 2

Appendix D—Spectral Sciences Inc. Report SSI-TR-274
“Measurement of Gas Phase Hydrogen Chloride
in the Exhaust Cloud of a Titan Rocket”

MEASUREMENT OF GAS PHASE HYDROGEN CHLORIDE IN THE EXHAUST CLOUD OF A TITAN ROCKET

**Prepared by
Steven Richtsmeier, Fritz Bien, Michael W. Matthew, and Lawrence S. Bernstein
Spectral Sciences, Inc.
99 South Bedford Street, #7
Burlington, MA 01803-5169**

**Prepared for
Mr. Marvin Becker
SRS Technologies
425 Titan III Road (CCAS)
Cape Canaveral Air Station
Patrick AFB, FL 32925-1902**

Under P.O. Nos. SDDNB-1067 and SDDNB-1097

April 1996

TABLE OF CONTENTS

1. INTRODUCTION	1
2. INSTRUMENT OPERATION	2
3. INSTRUMENT CALIBRATION AND PERFORMANCE	4
4. RESULTS	8
4.1 Carbon Monoxide	9
4.2 Hydrogen Chloride	11
4.3 Ambient Temperature Measurement	18
4.4 Experimental Difficulties	20
5. COMPARISON TO PREDICTED HCL CONCENTRATIONS	21
6. SUMMARY	23
7. REFERENCES	24
APPENDIX A: FLOPPY DISK CONTENTS	A-1

LIST OF FIGURES

Figure 1.	Signal from a 57 ppm HCl/N ₂ Calibration Gas Mixture.	6
Figure 2.	Signal from a 500 ppm HCl/N ₂ Calibration Gas Mixture.	6
Figure 3.	CO Instrument Response to an 18 ppm CO/N ₂ Calibration Gas Mixture.	7
Figure 4.	CO Instrument Response to 18 and 120 ppm CO/N ₂ Gas Mixtures.	7
Figure 5.	CO Lamp Relative Intensity.	10
Figure 6.	CO Instrument Lamp Temperature.	10
Figure 7.	HCl Lamp Temperature.	12
Figure 8.	HCl Source Lamp Intensity.	12
Figure 9.	HCl Source Lamp Intensity During Cloud Sampling.	13
Figure 10.	HCl Lamp Intensity During Exhaust Cloud Encounter 2.	13
Figure 11.	HCl Concentration (No Averaging).	14
Figure 12.	HCl Concentration (3.85 sec Averaging).	15
Figure 13.	HCl Concentration (No Averaging) for Cloud Encounter 2.	16
Figure 14.	HCl Concentration (3.85 sec Averaging) for Cloud Encounter 2.	16
Figure 15.	Integrated [HCl] as a Function of Time.	17
Figure 16.	Air Temperature - HCl Instrument.	18
Figure 17.	Air Temperature During Early Cloud Encounters.	19
Figure 18.	Air Temperature During Cloud Encounter 2.	19

LIST OF TABLES

Table 1.	Event Time Line	8
----------	-----------------------	---

1. INTRODUCTION

This report describes measurements made on the exhaust cloud of a Titan rocket launched 5 December 1995. The principal objective of this program was to monitor the evolution of gas phase hydrochloric acid (HCl), a major component of the exhaust of aluminized solid propellant rocket motors. An instrument package was mounted to the underside of a small piloted airplane. This package contained sensors for HCl, carbon monoxide (CO), and ambient air temperature, and information was recorded continuously as a function of time on a 3 Hz time scale as the airplane repeatedly traversed the exhaust cloud.

Though the airplane attempted to follow the Titan exhaust cloud for nearly two hours, a combination of problems resulted in only 10 minutes of HCl data and no CO data being acquired. A single short-duration flight test prior to the Titan launch would have uncovered these problems and enabled their correction. The instrument package has been refurbished and is now operational. The problems encountered during the Titan measurements, their correction, and recommendation for future measurements are discussed in detail in a later section. The HCl instrument did record average HCl concentrations ranging from 10 - 32 ppm over the course of 8 encounters with the rocket exhaust cloud, and these data are temporally correlated with features in the recorded ambient air temperature profiles.

While not without its problems, this first in-flight test of the Spectral Sciences, Inc. HCl/CO sensor package demonstrated the capability to perform rapid and sensitive in-situ trace species measurements of rocket exhaust plumes. With the lessons learned from this flight, it is anticipated that in future flights: (1) both the CO and HCl sensors will be operational, (2) improvements to the in-flight signal levels will result in improved sensitivity and time response, and (3) improvements to the sample flow geometry will result in a much longer sensor lifetime due to reduced deposition of aluminum oxide onto mirror surfaces.

In this report, we briefly describe the operating principles of the HCl and CO instruments, describe instrument calibration and performance, and discuss difficulties encountered during the flight test. The HCl concentration information that we were able to gather is presented and compared with theoretical estimates of the expected concentrations. The HCl concentration as a function of time along with air temperature information is included on a floppy disk along with this report.

2. INSTRUMENT OPERATION

The HCl and CO instruments were originally built to be flown on small remotely-piloted aircraft.^{1,2} The original design requirements for HCl monitoring from an aircraft, namely, fast (1 second or less) response, sensitivity over the 1 ppmv to several hundred ppmv range, small size and low weight, suggested the use of a non-dispersive IR absorption (NDIR) sensor.^{3,4} The sensor design is based on an adaptation of recent designs^{5,6} that utilize a gas-filled molecular line lamp.⁷ Unobstructed sampling of the air stream is provided by using an open optical cavity. The entire instrument measures 25 cm x 19 cm x 13 cm and weighs about 4 kg. For the current project, the instruments are suspended, one in front of the other, within a U-bracket on rubber shock mounts, and the whole of the bracket assembly is bolted to the bottom of a piloted airplane. Sample air flow is perpendicular to the instrument optical axis.

The HCl instrument operation is summarized as follows. Light from a lamp, which is emitted preferentially at the wavelengths of HCl spectral lines, is focused through a rotating gas filter wheel and directed through a White-type multi-pass cavity that has a 6-m-long absorption path. Light exiting the cavity is directed onto a photo detector fitted with a narrow band filter. The photo detector signal is digitized by an on-board data logging system (Onset Computer Corp. Tattletale Model 2B), summed for a period of time, and sent via an RS-232 serial line to a laptop computer where raw data is recorded for post-flight processing. The filter wheel holds two pairs of gas cells. One pair contains pure N₂, which transmits all of the light from the lamp; the other pair contains a high concentration of HCl. Comparison of the light intensities transmitted through each of the gas cells provides a direct measure of the concentration of HCl in the sample path. The CO instrument is identical to the HCl instrument with the exceptions that the lamp and filter cells are filled with CO rather than HCl, and the transmission of the band pass filter is centered about the CO fundamental rather than the HCl fundamental. The requested data rate for this project was 3 Hz. The standard deviation in the concentration baseline is about 4 ppmv on this time scale for [HCl], and about 2 ppmv for [CO]. For a plane speed of 54 m/s, the corresponding spatial resolution of the concentration data is 19 m.

In addition to the gas sensor, each instrument monitors ambient air temperature in the flow channel as well as the temperature within the instrument package. The air temperature measurement, from a fast (0.1 s response time) thermistor, serves as a second indicator of the presence of the exhaust cloud. Another thermocouple mounted in the lamp wrapping monitors the lamp temperature. These data are logged along with the concentration data for diagnostic purposes.

3. INSTRUMENT CALIBRATION AND PERFORMANCE

The quantity of HCl in the sample volume is derived by comparing the intensities of the light transmitted through the sample volume and each of the gas filter cells. We define the quantity R

$$R = \frac{(I_{N_2} - I_{HCl})}{I_{HCl}} \quad (1)$$

where I is the transmitted light intensity through the sample volume and the gas in the specific filter cell denoted by the subscript. The magnitude of R is a maximum when there is no HCl in the sample volume and is denoted R_0 . The presence of HCl in the sample volume reduces I_{N_2} while I_{HCl} remains essentially constant, thereby reducing R. The degree by which R is reduced is directly related to the concentration of gas in the sample volume. The instrument is calibrated by introducing known quantities of HCl into the sample volume and measuring R. The measurements are then fit to a functional form, and the function and its parameters are applied during post-processing of the data. The quantity A as defined by

$$A = -\log \left(\frac{R}{R_0} \right) \quad (2)$$

is a convenient form in which to treat R because it is roughly proportional to [HCl] at low concentrations (tens of ppmv) and is zero valued when the HCl concentration is zero. Use of a third order polynomial in A as the fitting function allows the instrument to be calibrated for concentrations spanning a range from a few ppmv to hundreds of ppmv, i.e.,

$$[HCl] = C_1 A + C_3 A^3 \quad (3)$$

where C_1 and C_3 are adjustable coefficients. The cubic term in Equation (4) compensates for the non-Beer's Law behavior of higher concentration HCl samples. The same procedure is followed in calibrating the CO instrument.

Figures 1 - 4 illustrate instrument response to several calibration gas standards. During calibration, a steel shroud is fitted, though not tightly sealed, around the sample volume and a gas mixture of known composition is flowed through the shroud. In Figure 1, a flow of a 57 ppm HCl/N₂ mixture is started at time = 62400 sec and turned off at time = 62600 sec. Data points are spaced 0.35 sec apart, and the corresponding standard deviation in the [HCl] baseline is about 4 ppm. After the flow is turned on, a minute or so is required before the apparent concentration actually reaches 57 ppm. This is due to the fact that HCl is readily adsorbed onto surfaces and time is required to passivate the surfaces of the flow system. There is no passivation time associated in the regular measurement configuration because the instrument samples the free air stream flow. Figure 2 shows instrument response to a 500 ppm HCl/N₂ calibration gas mixture. As in Figure 1, there is a finite passivation time before the concentration reaches 500 ppm. The extended tail in the concentration drop from 86360 to 86385 sec in the figure was caused by stopping gas flow without pumping out the sample volume, allowing the gas to slowly escape around the end of the calibration shroud.

The CO measurement is inherently less noisy than the HCl measurement because a greater fraction of the lamp emission falls at the wavelengths of the CO absorption lines. The standard deviation in the CO baseline is about 2 ppm for 0.35 sec sampling. Figure 3 illustrates the response of the CO instrument to an 18 ppm CO/N₂ calibration gas mixture. Since CO is less readily adsorbed to surfaces, there are no passivation effects apparent in the concentration profile. The concentration immediately reaches 18 ppm and stays there as long as the gas flows. Figure 4 shows the concentration profile as the 18 ppm mixture is turned on and then pumped out of the sample volume three successive times, followed by introduction of a 120 ppm mixture.

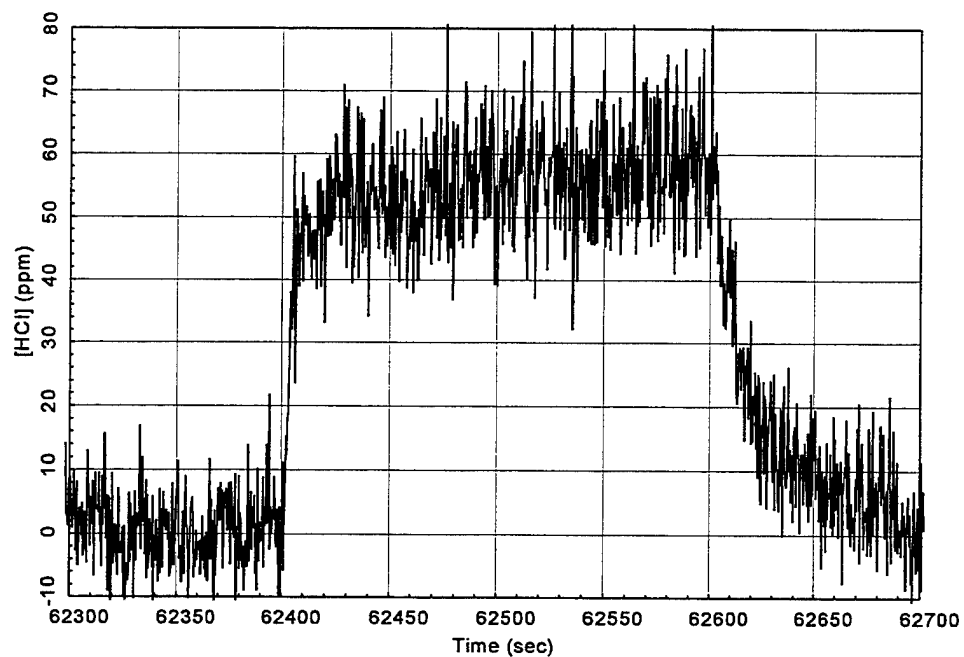


Figure 1. Signal from a 57 ppm HCl/N₂ Calibration Gas Mixture.

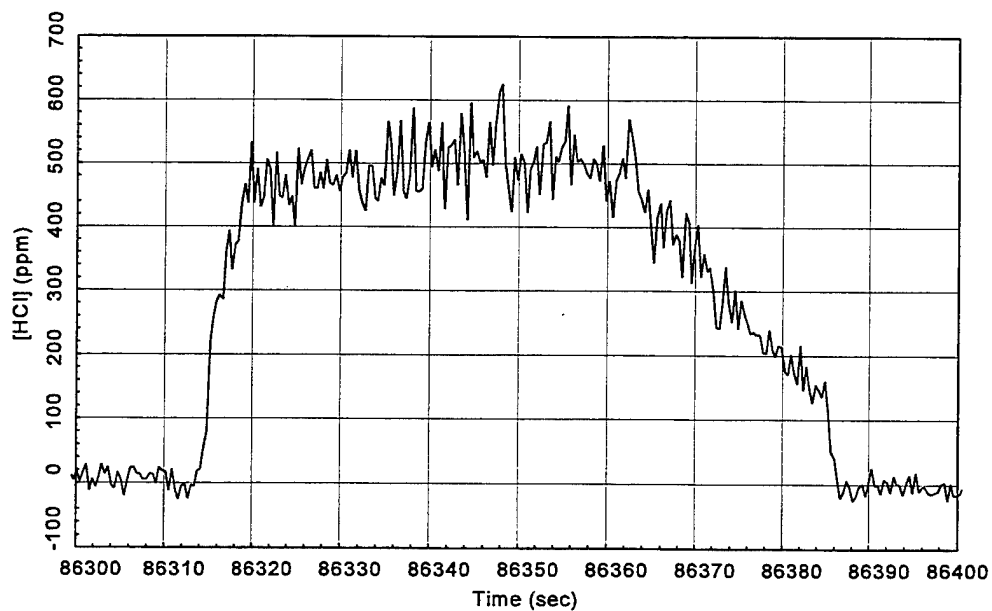


Figure 2. Signal from a 500 ppm HCl/N₂ Calibration Gas Mixture.

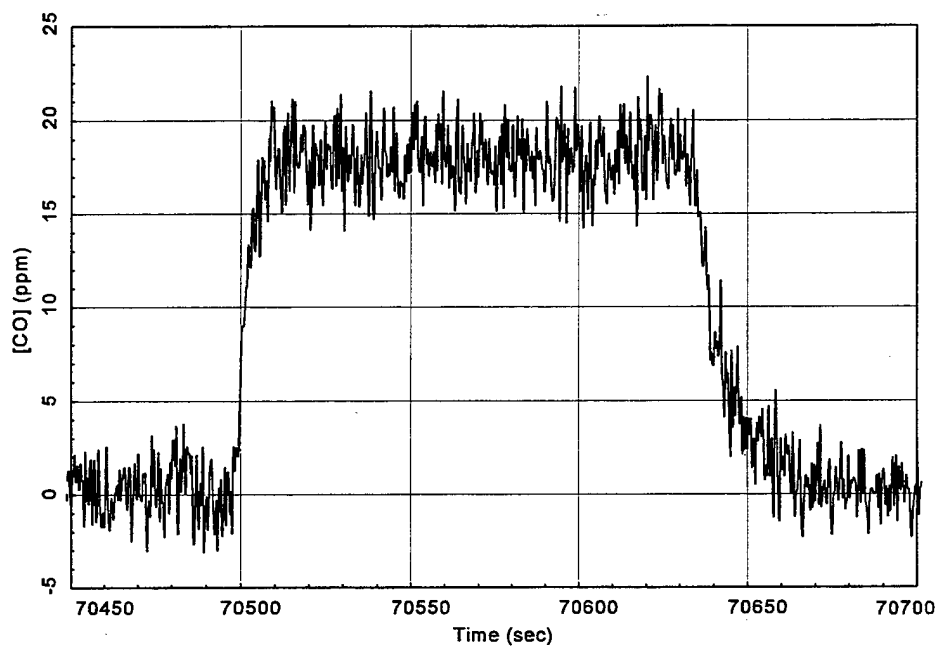


Figure 3. CO Instrument Response to an 18 ppm CO/N₂ Calibration Gas Mixture.

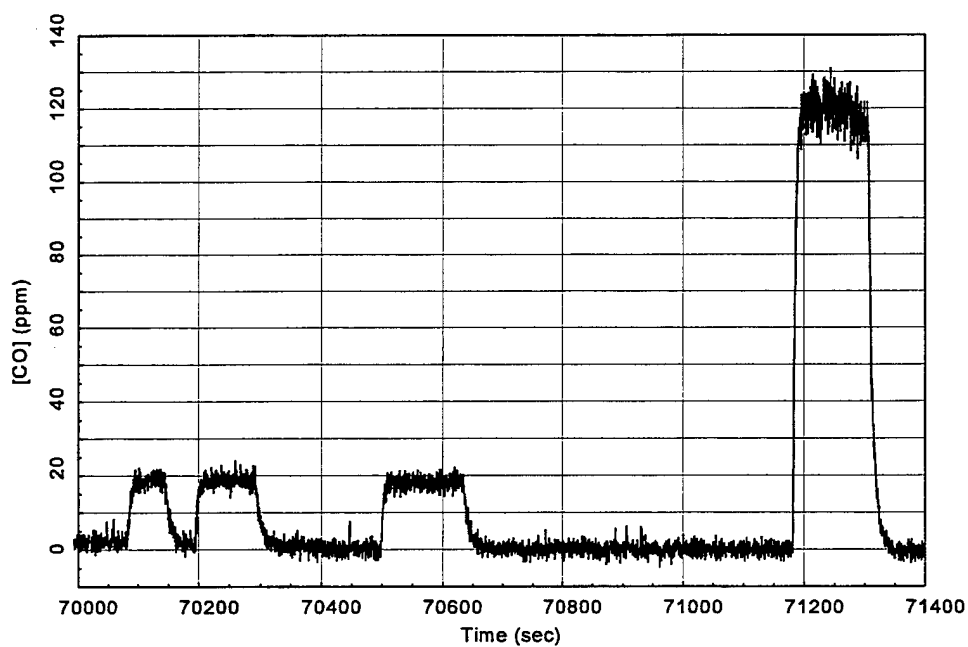


Figure 4. CO Instrument Response to 18 and 120 ppm CO/N₂ Gas Mixtures.

4. RESULTS

The HCl instrument successfully recorded average HCl concentrations ranging from 10 - 32 ppm over the course of 8 encounters with the rocket exhaust cloud. These data are temporally correlated with features in the recorded ambient air temperature profiles. Table 1 contains a time line of events associated with the measurement, along with the average HCl concentrations extracted from the data for the exhaust cloud encounters.

Table 1. Event Time Line

Event	Start (sec)	Start (hh:mm:ss)	End (sec)	End (hh:mm:ss)	Duration (sec)	Avg. [HCl] (ppm)
start CO file	45766	12:42:46 pm				
start HCl file	45799	12:43:19 pm				
CO lamp intensity anomaly	45935	12:45:35 pm	45990	12:46:30 pm	55	
HCl lamp intensity anomaly	45943	12:45:43 pm	45990	12:46:30 pm	47	
CO drops	46443	12:54:03 pm				
HCl drops again	46450	12:54:10 pm				
CO monitor dead	46470	12:54:30 pm				
Airplane takeoff (from air temp. monitors)	46480	12:54:40 pm				
Titan launch	47940	1:19:00 pm				
Encounter 1	48110	1:21:50 pm	48121	1:22:01 pm	11	10
Encounter 2	48174	1:22:54 pm	48192	1:23:12 pm	18	26
Encounter 3	48240	1:24:00 pm	48252	1:24:12 pm	12	32
Encounter 4	48290	1:24:50 pm	48307	1:25:07 pm	17	20
Encounter 5	48353	1:25:53 pm	48375	1:26:15 pm	22	15
Encounter 6	48428	1:27:08 pm	48465	1:27:45 pm	37	22
Encounter 7	48470	1:27:50 pm	48495	1:28:15 pm	25	17
Encounter 8	48510	1:28:30 pm	48530	1:28:50 pm	20	15
Encounter 9	48570	1:29:30 pm	48590	1:29:50 pm	20	
Encounter 10	48655	1:30:55 pm				
Encounter 11	48703	1:31:43 pm				
Encounter 12	48750	1:32:30 pm				
Encounter 13	48790	1:33:10 pm				
End HCl file	55544	3:25:44 pm				

A combination of problems limited the useful information collected to ten minutes of HCl data, and no CO data. The difficulties encountered include:

- (1) the instrument mounting bracket does not leave enough clearance for the instruments to move on their shock mounts without bottoming out in the mounting bracket,
- (2) air flowing over the ends of the instruments cools the source lamps excessively, resulting in lost source intensity,
- (3) aluminum oxide (Al_2O_3) particulates in the rocket exhaust cloud tend to deposit on the sample cell mirrors with each successive pass through the exhaust cloud, resulting in lost source intensity.

These items would have to be addressed before the instruments are flown again.

4.1 Carbon Monoxide

Item (1) above likely contributed to the failure of the CO instrument. The instrument mounting bracket built by F.I.T. requires modification. The instruments are held in place by rubber shock mounts, and post-flight inspection showed that the instruments actually bottomed out in the bracket during flight. The bracket was designed too small, and F.I.T. even had to mill out a portion of the bracket just to provide enough clearance to fit the instruments, but there is not enough room to allow for the instruments to move. This not only introduces noise into the gas measurements, but the shock of striking the bracket could potentially damage the instruments. Figure 5 shows relative intensity of the CO lamp source as a function of time. The first anomaly in the curve occurs at 45935 sec and lasts for 55 sec, about the time when the plane was taxiing from the hanger area to the runway. The apparent CO lamp intensity begins to decline again at 46443 sec, and then becomes completely unstable at 46470 sec, and remains unusable for the duration of the flight. This time corresponds to airplane takeoff. The loss of source intensity was not due to computer failure or burnout of the lamp. The data acquisition computer continued to collect temperature information, and the lamp temperature was maintained at about 695 C throughout the course of the flight (see Figure 6). Note however that the CO lamp temperature did decrease by 30 - 40 C after takeoff due to air flow over the instrument. This decrease would not have significantly affected lamp output on its own. However, the temperature decrease observed for the HCl lamp did have a more serious effect on the performance of the HCl instrument (see below).

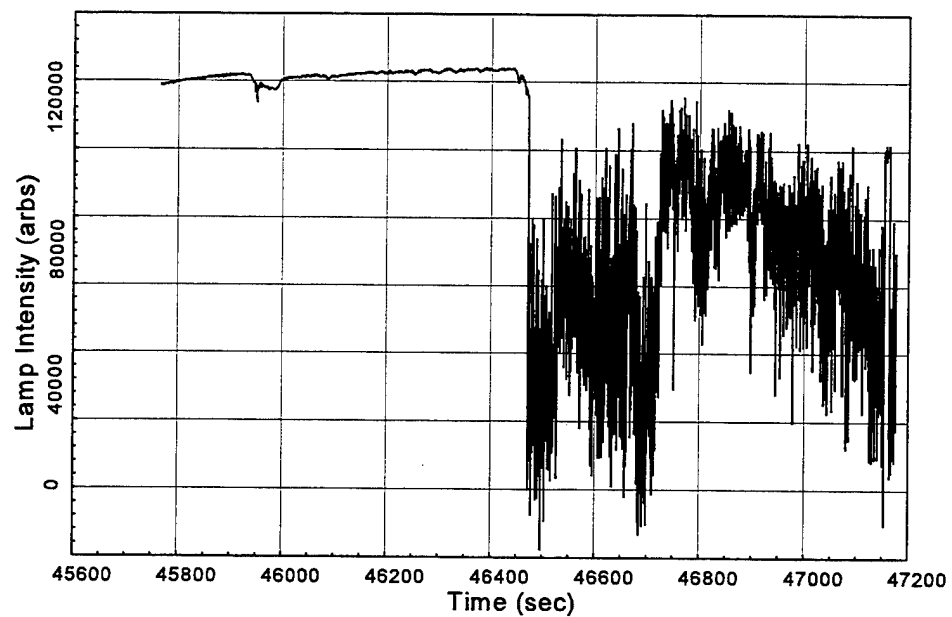


Figure 5. CO Lamp Relative Intensity.

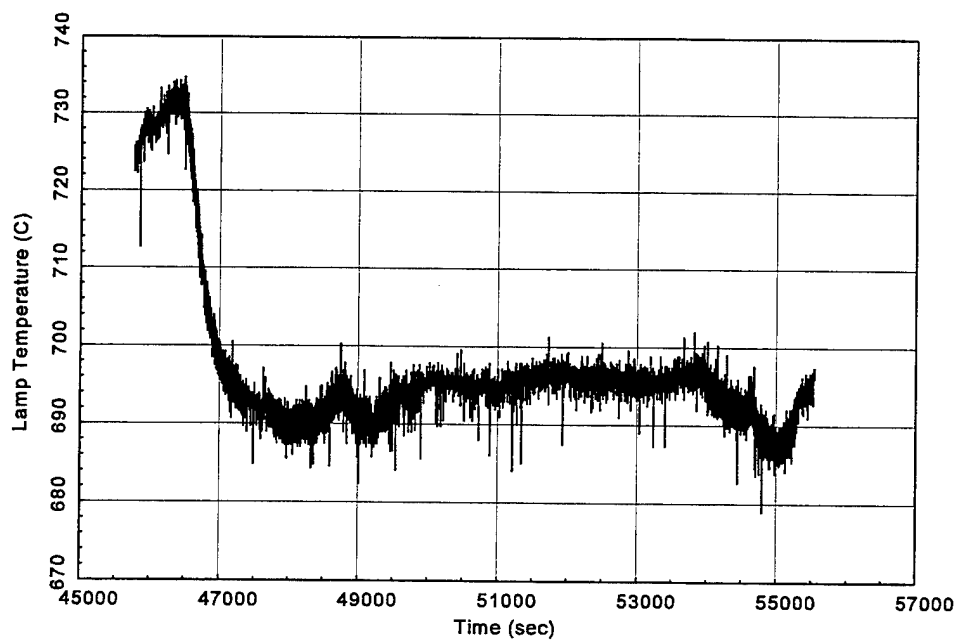


Figure 6. CO Instrument Lamp Temperature.

4.2 Hydrogen Chloride

The HCl instrument functioned properly for the duration of the experiment, but the combination of lamp cooling due to air flow over the instrument and light loss due to deposition of particulates on the instrument mirrors limited the collection of useful concentration data to 10 minutes after launch. Figure 7 plots the HCl source lamp temperature as a function of time. The lamp temperature decreased from about 840 C while on the ground to about 725 C while in flight. This is a much stronger cooling effect than the CO instrument suffered, likely due to the fact that the CO instrument was mounted behind the HCl instrument and so was more shielded from the air flow. As a result, 60 % of the HCl lamp source intensity was lost before the plane reached the Titan exhaust cloud (see Figure 8).

The second cause of light loss was deposition of Al_2O_3 particulates on the sample cell mirrors. Figure 9 shows HCl source lamp intensity as a function of time during the period when the plane made its first several passes through the exhaust cloud. The lamp intensity appears similar to a step function with at least 13 steps of decreasing intensity over the period 48000 - 48800 sec. Each step corresponds to a single pass of the plane through the exhaust cloud. Particulate deposition during a pass slightly reduces mirror reflectivity and gives a reduced source intensity at the completion of the pass. Figure 10 shows the lamp intensity associated with a single pass through the cloud. The lamp intensity is relatively constant until a sharp drop-off at 48174 sec. After 18 sec, the intensity recovers to a new, lower baseline. The light intensity previous to 48192 sec is less than this new baseline due to absorption by HCl and scattering by particulates in the sample volume.

The presence of Al_2O_3 particulates in the sample volume and on the mirrors does not interfere with the calibration of the concentration measurement. The gas correlation technique used here has a built-in normalization which discriminates against spectrally uncorrelated absorbers, be they particulates or other gaseous species. However, the consequence of the gradual loss of source light is a corresponding increase in the noise floor of the measurement, until apparent concentrations can no longer be distinguished from noise. On the other hand, a benefit (though one gladly traded for full source intensity) of the particulate deposition is that it allows unambiguous determination of the particulate cloud entrance and exit times. These were determined from examination of data in the form of Figure 10 and are presented in Table 1.

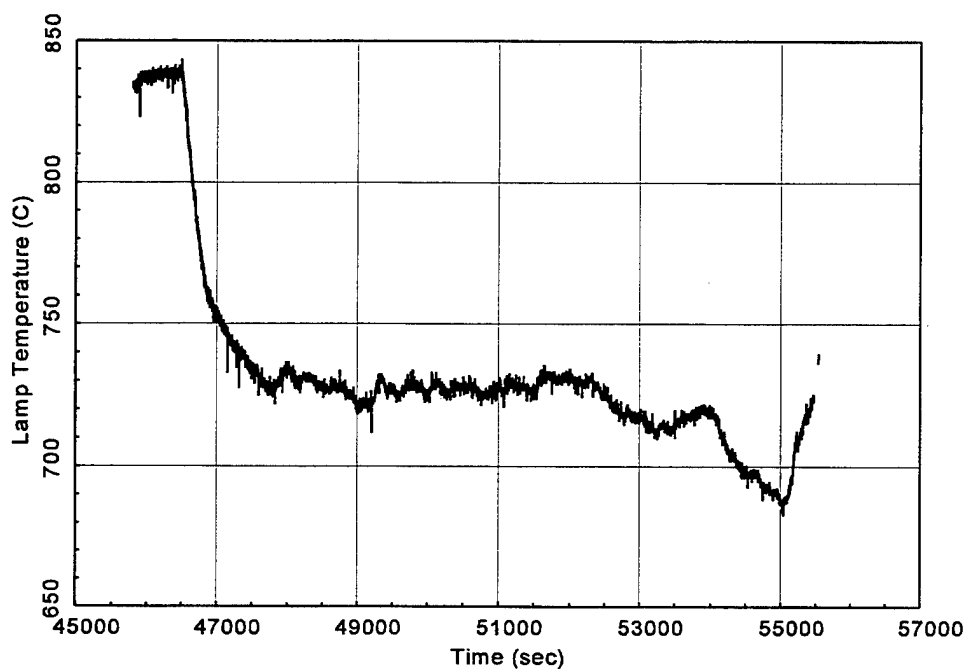


Figure 8. HCl Lamp Temperature.

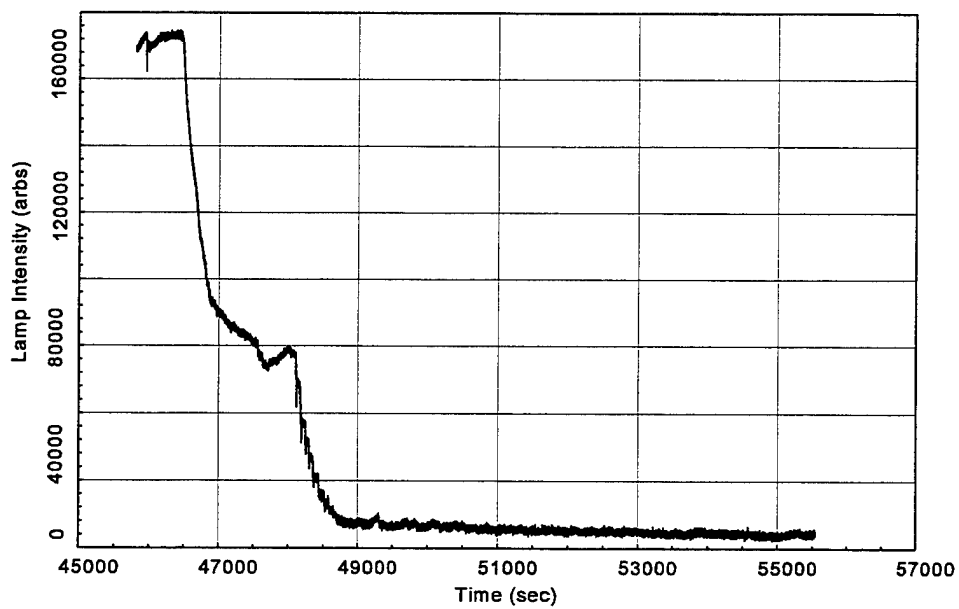


Figure 7. HCl Source Lamp Intensity.

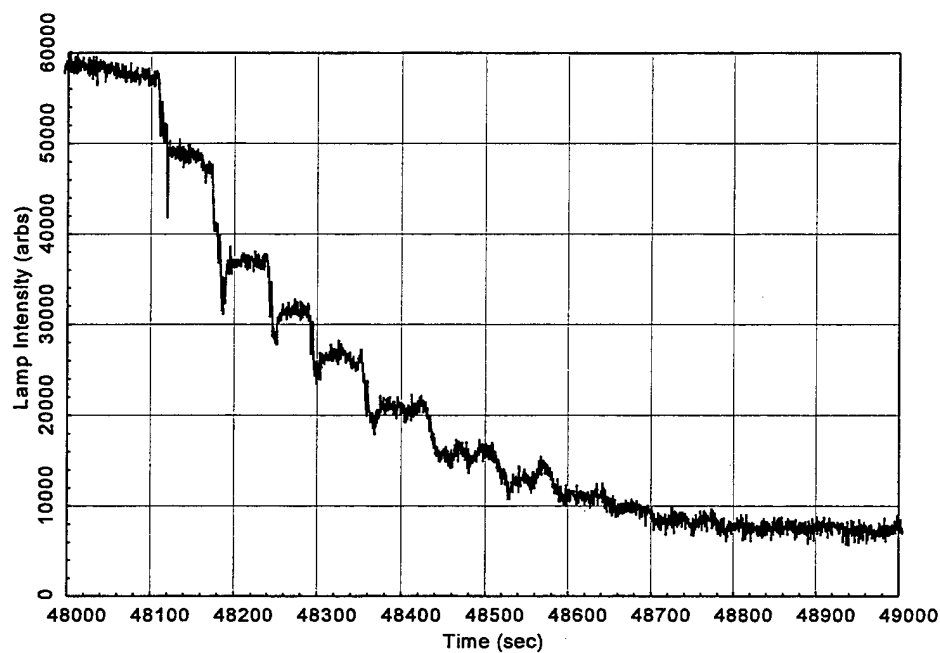


Figure 9. HCl Source Lamp Intensity During Cloud Sampling.

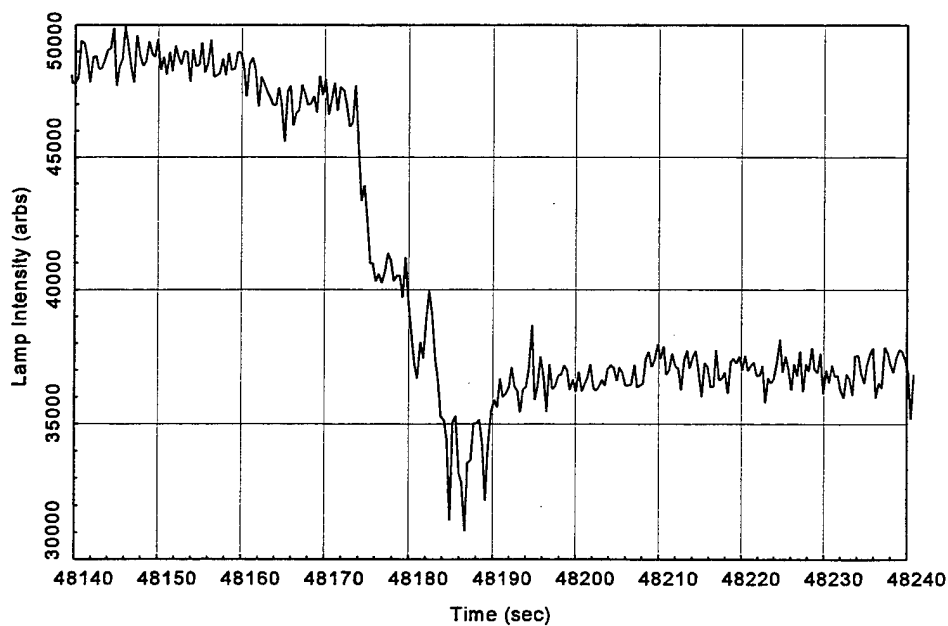


Figure 10. HCl Lamp Intensity During Exhaust Cloud Encounter 2.

Figure 11 displays HCl concentration as a function of time over the period of the first nine exhaust cloud encounters. Each data point corresponds to 0.35 sec of sampling. Assuming a plane velocity of 54 m/s (120 mph) the spatial resolution of the measurement is 19 m. On this scale, the apparent HCl concentration can reach hundreds of parts per million. The dotted-line boxes in Figure 11 mark exhaust cloud entrance and exit times of the particulate cloud. For the most part, it appears that HCl events occur while the plane is in the particulate cloud, implying that exhaust gases and particulates travel together on this time scale. This is more clear in Figure 12 where a 3.85 sec averaging window has been applied to the data. As would be expected, the noise in the concentration baseline, and thus the minimum detectable HCl concentration, appears to increase with time because of loss of source light. By 48550 sec, [HCl] excursions from the zero baseline while the instruments are out of the exhaust cloud are comparable to those while in the cloud, and the [HCl] data are unusable.

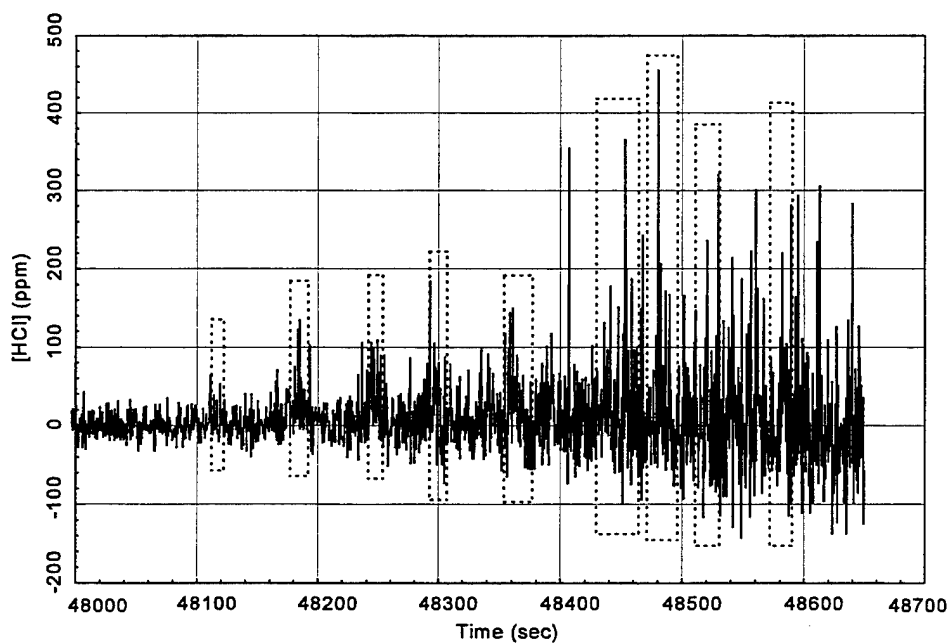


Figure 11. HCl Concentration (No Averaging).

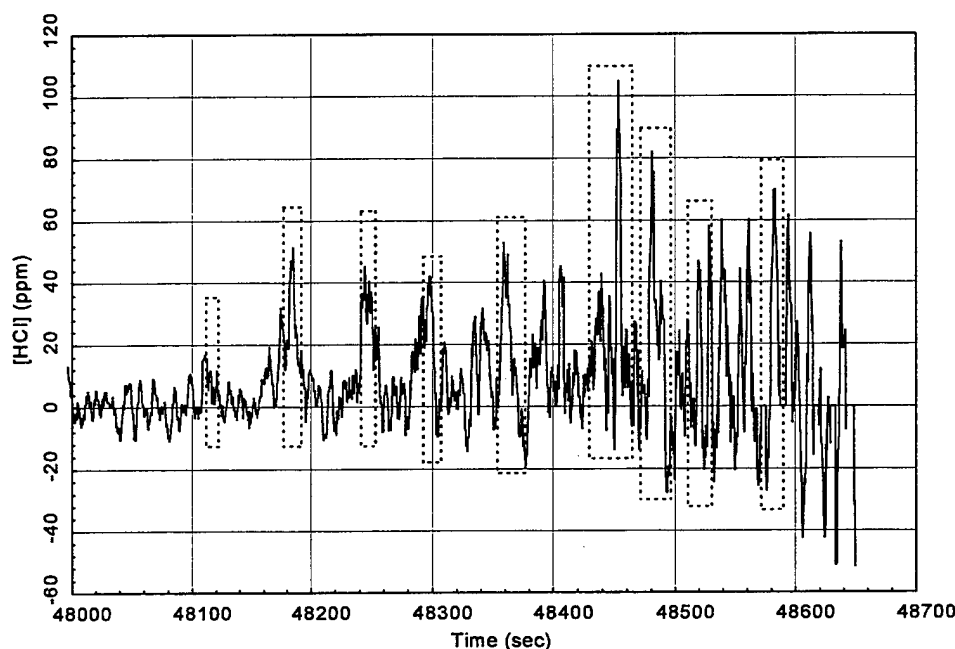


Figure 12. HCl Concentration (3.85 sec Averaging).

Figures 13 and 14 examine the HCl data on a finer time scale for unaveraged and averaged data, respectively, for the second exhaust cloud encounter. Again, the dotted-line boxes indicate when the instruments were in the particulate cloud, and HCl events are temporally correlated with the particulate cloud. In Figure 13, excursions in the zero baseline were typically about 20 ppm, while concentrations in the cloud sometimes exceeded 100 ppm. In Figure 14, the HCl observed during the period 48174 - 48192 sec is clearly above the zero baseline.

Another form in which to present the concentration is as accumulated or integrated [HCl]. Figure 15 presents integrated [HCl] as a function of time as determined by

$$\text{Integrated [HCl]} = \int_{t_1 = 48000}^t [\text{HCl}] dt \quad . \quad (4)$$

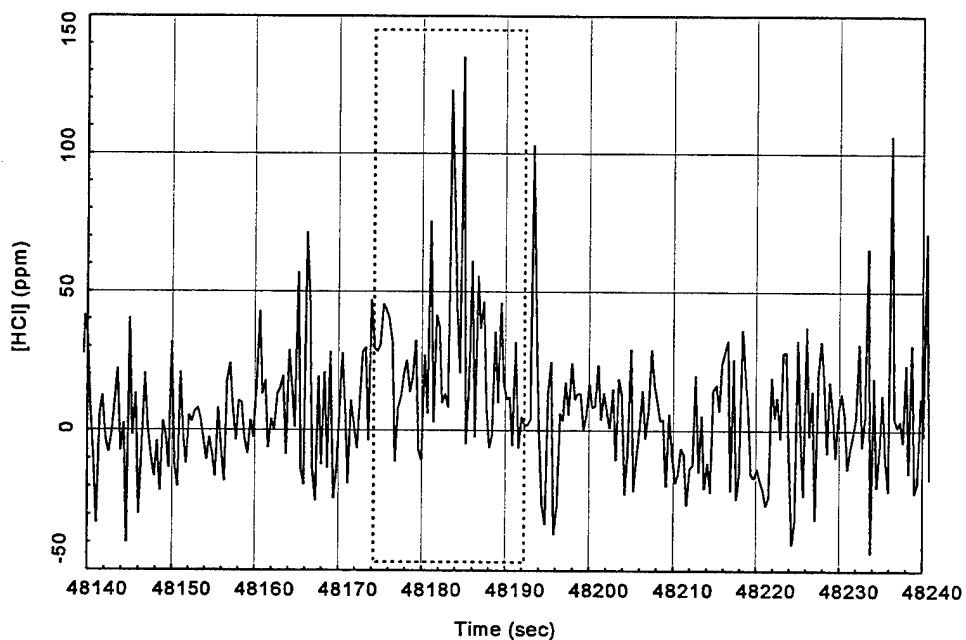


Figure 13. HCl Concentration (No Averaging) for Cloud Encounter 2.

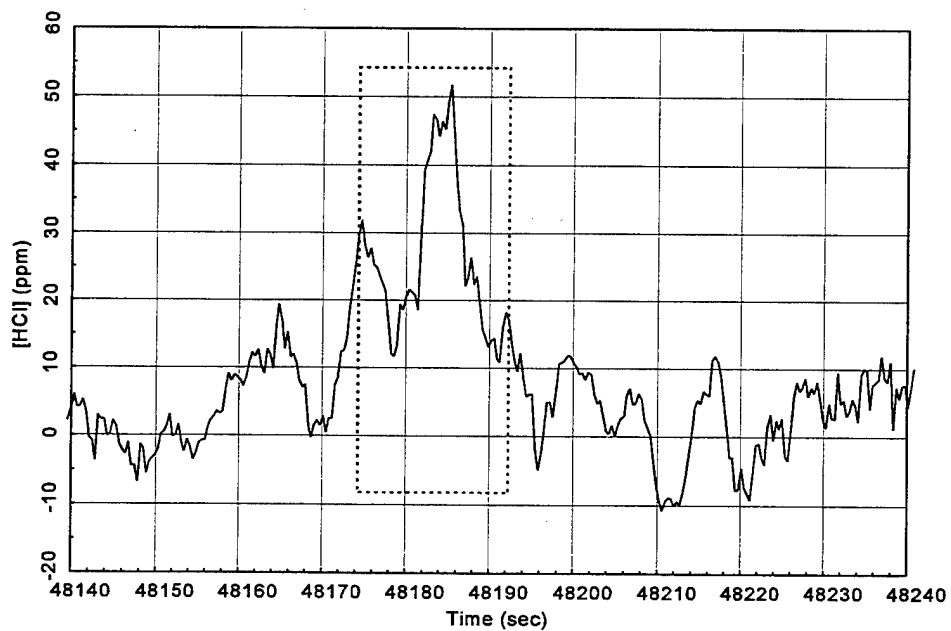


Figure 14. HCl Concentration (3.85 sec Averaging) for Cloud Encounter 2.

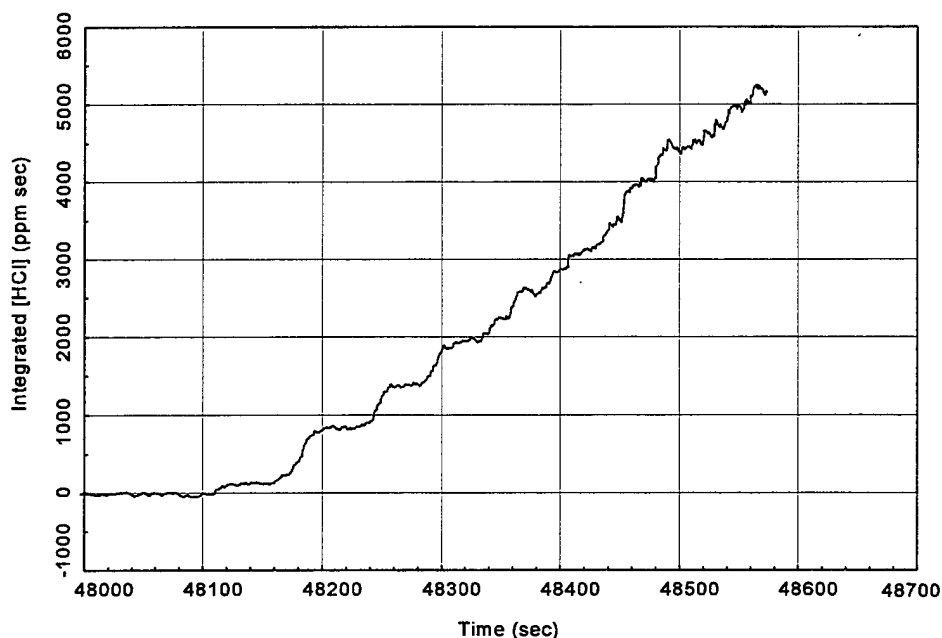


Figure 15. Integrated [HCl] as a Function of Time.

Each step in the accumulated concentration occurs as HCl is encountered. The curve is flat between passes through the cloud. The average concentration along any interval is given by

$$[HCl]_{avg} = \frac{\int_{t_1}^{t_2} [HCl] dt}{t_2 - t_1} \quad (5)$$

$[HCl]_{avg}$ for the first eight cloud encounters are tabulated in Table 1. The average concentration measured over the first 10 min after launch ranged from 10 to 32 ppm. In general, the higher concentrations were observed during the early passes (encounter 1 excepted) with the concentration diminishing with time. We have no physical knowledge of the nature of the first pass through the exhaust cloud, but judging from the relatively low concentration (10 ppm) and the fact that the percentage of light lost due to particulate deposition was lower for this pass than for subsequent passes, the implications are that perhaps only the cloud edge and not the heart of the cloud was sampled.

4.3 Ambient Temperature Measurement

Both instruments incorporated fast thermistors protruding into the sample volume for measurement of ambient air temperatures. Figures 16 - 18 show air temperature on various time scales as measured by the HCl instrument. The dotted lines in the figures mark the times when the instrument was in the exhaust cloud as determined by the effects of particulate deposition on source lamp intensity. For the early encounters, a decrease in the measured temperature was observed at the cloud edges compared to the temperature on either side, and the inside of the cloud was warmer than the edges. Temperature features measured by the CO instrument exhibited similar detail.

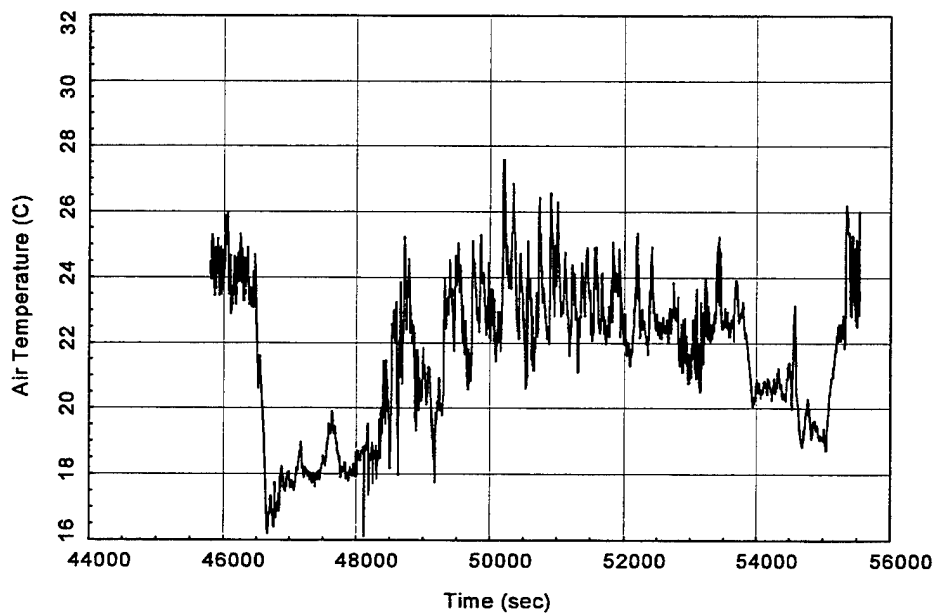


Figure 16. Air Temperature - HCl Instrument.

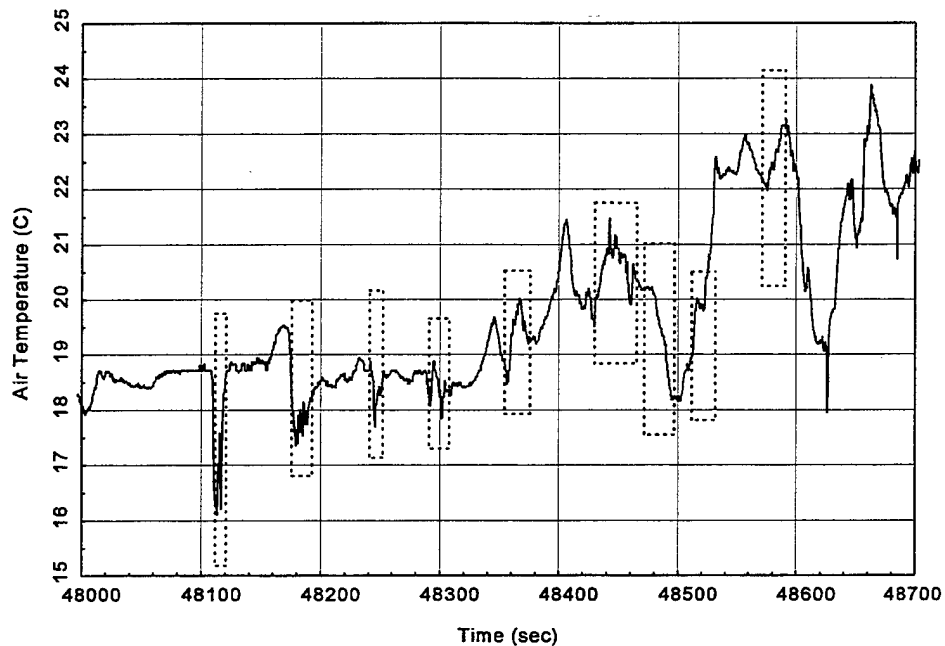


Figure 17. Air Temperature During Early Cloud Encounters.

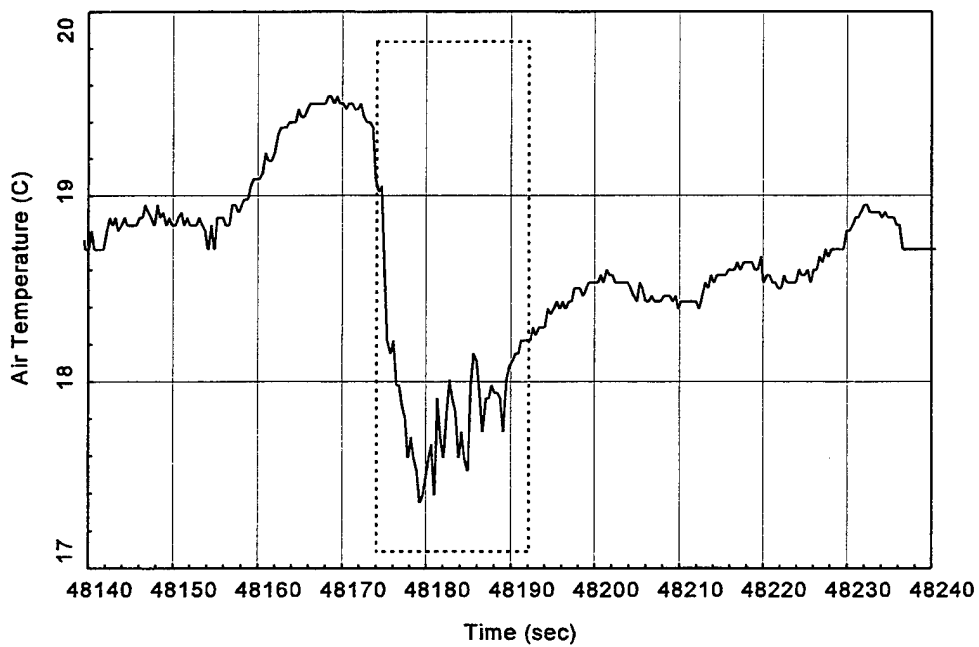


Figure 18. Air Temperature During Cloud Encounter 2.

4.4 Experimental Difficulties

There were a number of difficulties encountered during December's flight test which should be addressed if these instruments are to be flown again. First, the instrument mounting bracket built by F.I.T. is too small and requires modification. The instruments are held in place by rubber shock mounts, and post-flight inspection showed that the instruments actually bottomed out in the bracket during flight. The bracket was designed too small, as evidenced by the fact that F.I.T. had to mill out a portion of the bracket just to provide enough clearance to fit the instruments, and there is not enough room to allow for the instruments to move. This not only potentially introduces noise into the concentration measurements, but the shock of striking the bracket could potentially damage the instruments and perhaps contributed to the in-flight failure of the CO instrument.

A second mounting modification is necessary to shield the instruments from ambient air flow. At the plane velocities of the last flight test, the temperature of the lamp sources was reduced much more than anticipated, resulting in the loss of 60% of instrument source light before any gas sampling took place. We would like to modify the instrument mounting bracket with a baffle to redirect air flow away from the sides of the instruments to prevent instrument heat loss.

Finally, each pass of the instruments through the Titan exhaust cloud resulted in signal loss as particulates were deposited on the sample cell mirrors. It will be necessary to modify the sample flow vent to protect the mirrors from direct impingement by particulates and prevent the resulting gradual loss of signal. Another way to avoid particulate deposition, if it fits within measurement objectives, might be to avoid sampling the cloud during the first several minutes after launch when the particulate cloud is most dense.

5. COMPARISON TO PREDICTED HCL CONCENTRATIONS

An estimate of the expected altitude-dependent HCl concentration profile can be established directly from the HCl deposition profile due to the Titan launch along with an estimate of the effective radius of the missile exhaust trail. The total rate of mass ejection from the missile is given by

$$\frac{dm}{dt} = \frac{F}{u_e} \quad , \quad (6)$$

where F is thrust and u_e is the exhaust exit velocity. For the Titan $F = 7.1 \times 10^6$ N for the solid propellant boosters, and $u_e = 3,000$ m/s, thus, $dm/dt = 2.4 \times 10^3$ kg/s. Taking the average molecular weight to be 24 g/mole and the HCl mole fraction to be 0.15 (this is typical for most aluminized composite solid motors), the rate of ejection of HCl molecules is $dn/dt = 8.9 \times 10^{27}$ s⁻¹. The HCl concentration profile (in ppm) is calculated from

$$c = 10^6 \frac{dn/dt}{n_a u_r \pi r^2} \quad , \quad (7)$$

where n_a (m⁻³) is the atmospheric number density, u_r (m/s) is the missile velocity, and r (m) is the trail radius. For the altitude range of interest in this experiment, approximately 0.5 to 3 km, the velocity of the Titan is well approximated by

$$u_r = 2.4 \sqrt{z} \quad , \quad (8)$$

where z (m) is altitude. The atmospheric number density is approximately given by

$$n_a = 2.5 \times 10^{25} \exp\left(-\frac{z}{7.5 \times 10^3}\right) \quad , \quad (9)$$

where 7.5×10^3 m is the atmospheric scale height. The trail radius can be estimated from the rapid decrease in signal levels registered by the HCl instrument due to particulate coating of the White cell mirrors during each pass. For the first four passes through the trail the average residence time of the

aircraft was approximately 14 s; the pass-to-pass variability was approximately ± 2 s. Assuming an aircraft speed of 54 m/s (i.e., 120 mph), the effective trail radius would be $r = 376$ m. Thus, the estimated HCl trail concentrations at 500, 1000, and 3000 m is 16, 12, and 9 ppm, respectively. These estimates are in excellent agreement with the measured HCl concentrations.

6. SUMMARY

Instruments designed to measure gas phase hydrogen chloride and carbon monoxide were mounted to the bottom of a piloted plane and flown through the exhaust cloud of a Titan rocket launched in December 1995. The HCl instrument successfully measured concentrations ranging from 10 to 32 ppm over the first 10 min after launch. These HCl events were found to be temporally correlated with changes in ambient air temperature measured concurrently. In general, higher concentrations were observed at earlier times, and the measured concentration gradually diminished with time. The observed concentrations are consistent with theoretical estimates of the expected HCl concentration. Though a number of experimental difficulties were encountered, the lessons learned should result in a few simple improvements to enable better signal levels and improved signal-to-noise ratios for both the HCl and CO sensors.

7. REFERENCES

1. S. C. Richtsmeier, N. Goldstein, F. Bien, C. Schuch, J. Buckley, R. R. Bennett, and I. Wallace, "In Situ Measurement of Hydrochloric Acid in Rocket Exhaust Clouds Using a Remotely Piloted Aircraft," *J. Air & Waste Manage. Assoc.*, **45**, 981 (1995).
2. S. C. Richtsmeier, N. Goldstein, F. Bien, C. Schuch, J. Buckley, M. W. Matthew, and T. Kiesling, "1992 SPIV Flight Test Data Analysis," Spectral Sciences, Inc. Rpt. No. SSI-TR-223 (1993). Thiokol Corporation, Space Operations under Purchase Order 3GH002.
3. D. I. Sebacher, R. J. Bendura, and G. L. Gregory, "Hydrogen Chloride Measurements in the Space Shuttle Exhaust Cloud -- First Launch, April 12, 1981," *J. Spacecraft*, **19**, 366 (1982).
4. D. I. Sebacher, "Airborne nondispersive infrared monitor for atmospheric trace gases," *Rev. Sci. Instrum.*, **49**, 1520 (November 1978).
5. L. S. Bernstein, F. Bien, W. K. Cheng, and R. P. Domingue, "HCl Monitor Phase II Final Report," Spectral Sciences, Inc. Rpt. No. SSI-TR-137 (1988). Prepared for Air Force Systems Command under Contract No. F08636-86-C-0137.
6. S. C. Richtsmeier, J. Lee, F. Bien, W. K. Cheng, L. S. Bernstein, M. R. Zakin, J. Morgenstern, and R. Brousseau, "Trace Atmospheric CO Sensor (TACOS) Final Report," Spectral Sciences, Inc. Rpt. No. SSI-TR-215 (1992). Prepared for NASA under Contract No. NAS9-38491.
7. L. S. Bernstein, M. W. Matthew, and F. Bien, "Infrared Species-Specific Emission Source," U. S. Patent No. 4,780,613 (October 25, 1988).

APPENDIX A: FLOPPY DISK CONTENTS

The floppy disk contains the following files:

<i>airthcl.dat</i>	Ambient air temperature as measured by the HCl instrument.
<i>airtco.dat</i>	Ambient air temperature as measured by the CO instrument.
<i>hcl.dat</i>	HCl concentration data, 3 Hz sampling.



2350 E. El Segundo Boulevard
El Segundo, California 90245-4691
U.S.A.